AD-732 405

EDGEWOOD
ARSENAL

EDGEWOOD ARSENAL
TECHNICAL REPORT

EATR 4555

RADIATION TRANSFER BETWEEN
FLAME BURNING ZONE AND UNBURNED FUEL

by

C. Stuart Kelley, Ph.D.

October 1971

DEPARTMENT OF THE ARMY
EDGEWOOD ARSENAL
Research Laboratories
Physical Research Laboratory
Edgewood Arsenal, Maryland 21010

EDGEWOOD ARSENAL TECHNICAL REPORT

EATR 4555

RADIATION TRANSFER BETWEEN FLAME
BURNING ZONE AND UNBURNED FUEL

by

C. Stuart Kelley

Dissemination Research Department

October 1971

DEPARTMENT OF THE ARMY
EDGEWOOD ARSENAL
Research Laboratories
Physical Research Laboratory
Edgewood Arsenal, Maryland 21010

FOREWORD

Acknowledgements

2

DIGEST

The heat transferred by radiation from a flame to its unburned fuel depends upon the intensities of the flame emission spectrum, the fuel absorption spectrum, and especially on the overlap, or product, of the two spectra. The product of the two spectra was calculated point by point through the near infrared (2μ to 6μ) and was integrated over wavelength for 14 fuels, primarily hydrocarbons. In general, maximum overlap occurs in the regions of CO_2 and H_2O emission bands. Overlap values vary from 3.19×10^{-6} for methane to 0.178 for unsymmetrical dimethylhydrazine. The overlap is shown to closely approximate the total radiation intensity absorbed by the fuel, and it is demonstrated to be linearly related to the fuel regression rate. Assumptions of graybody absorption and emission are found to be poor approximations for these heat transfer processes. Methods are discussed for enhancing overlap and thereby the rate of energy release by the flame.

BLANK

CONTENTS

LIST OF FIGURES

LIST OF TABLES

RADIATION TRANSFER BETWEEN FLAME
BURNING ZONE AND UNBURNED FUEL

I. INTRODUCTION.

The heat flux emitted by a flame is transferred to a target by three possible mechanisms: conduction, convection, and radiation. The heat flux intensity from a flame, as measured by an observer, depends on the position of the observer relative to the flame. It is also dependent on flame size, flame agent configuration, wind velocity, and barriers, to name only a few of the influencing factors.

The conditions envisioned for a laboratory test for determination of emitted heat flux consist of a pool of fuel (liquid, gelled liquid, or solid), on a table of sufficient size containing few obstacles so as not to impede the air flowing radially inward to the flame. Combustion products are withdrawn vertically upwards at a velocity comparable to that of natural buoyancy. Lateral wind velocity, ambient temperature and humidity, etc., are assumed to be constant from test to test and to comprise "standard" ambient conditions.

There have been studies of the effects on flames of variations in these conditions. For example, Ryan, Penzias, and Tourin[1] and Penzias et al.[2] have investigated the effects of ambient pressure; Rein, Welker, and Sliepcevich[3] have investigated the effects of lateral wind. Lateral wind can induce flame bending, and it can also enhance the flicker that is inherent in most flames. A method of measurement has been recently described that serves to minimize the effects of flicker.[4] Given a set of standard conditions, meaningful and reproducible burning tests may be performed to measure the heat flux emitted by a fuel. These measurements and their interpretation have been reported.[5,6]

Once ignited, a fuel continues to burn by the heat transferred to it from its flame. For a liquid fuel, once the boiling point has been reached by a portion of the liquid, substantial evaporation followed by convective transport in the region (called the interconal region) between the fuel and the burning zone conveys the vapor to the ignition zone, where it is available for combustion.

This report deals with radiation transfer between a flame and its unburned fuel. In particular, it involves the physical significance of flame shape factors that occur in descriptions of

---

[1] Ryan, L. R., Penzias, G. J., and Tourin, R. H. Ohio State University. Scientific Report 1. Contract AF16(604) 6106, ARPA Order No. 6-58. An Atlas of Infrared Spectra of Flames. Part One. Infrared Spectra of Hydrocarbon Flames in the 1-5μ Region. July 1961. UNCLASSIFIED Report.

[2] Penzias, G. J., Gillman, S., Liang, E. T., and Tourin, R. H. Ohio State University. Scientific Report 3. Contract AF19(604)-6106, ARPA Order No. 6-58. An Atlas of Infrared Spectra of Flames. Part Two. Hydrocarbon-Oxygen Flames 4-15μ, Ammonia-Oxygen 1-15μ, Hydrazine-Oxygen 1-5μ, and Flames Burning at Reduced Pressures. October 1961. UNCLASSIFIED Report.

[3] Rein, R. G., Welker, J. R., and Sliepcevich, C. M. University of Oklahoma Research Institute. Ninth Quarterly Progress Report. OURI-1578-QPR-9. Contract DAAA-15-67-C-0074. Susceptibility of Potential Target Components to Defeat by Thermal Action. January 1969. UNCLASSIFIED Report.

[4] Kelley, C. S. EATR 4436. The Use of Spatially-Separated, Series-Linked Thermocouples in Flame Evaluation. August 1970. UNCLASSIFIED Report.

[5] Brown, R. E., Garfinkle, D. R., and Andersen, W. H. Shock Hydrodynamics, Inc. Final Report SHI-6245-3. Contract DAAA-15-69-C-0301. Evaluation Techniques for Flame and Incendiary Agents. June 1970. UNCLASSIFIED Report.

[6] Kelley, C. S. EATR 4492. Dependence of Heat Flux (Radiative Plus Convective) from Burning Flame Agents on the Angle from the Flame Symmetry Axis. February 1971. UNCLASSIFIED Report.

radiation transfer. The procedure is applicable to all processes involving radiation from a source to a target.

II. BACKGROUND.

A. Emission Spectra.

Two types of radiation processes are encountered in flames: incandescence, and luminescence. The former produces blackbody (or graybody) radiation, characterized by a smooth wavelength-dependent emission (see figure 1A). An increase in temperature alters the intensity versus wavelength curve, as shown in figure 1. Luminescence, on the other hand, differs substantially in its wavelength and temperature dependences. The wavelength dependence of radiation from luminescent bodies consists of emission bands, such as shown in figure 1B for emission from H_2O molecules.[7] The many bands arise from radiative transitions between discrete energy levels. Only transitions (emissions) having specific energies (hence wavelengths) are possible. The temperature dependences are somewhat difficult to generalize because they depend on the particular energy level structure of the emitter.

In any given flame, both processes contribute to radiative emission. Soot particles in the flame produce graybody radiation. Superposed on this spectrum are the luminescence spectra of the assorted radicals and neutral species of which the combustion zone is composed.

Interpretation of emission spectra is somewhat complicated. There may be a variety of combustion products in a variety of concentrations, which can also be time dependent for non-steady state processes. Emission bands from different species can overlap to further complicate the interpretation. Some identifications, however, can be made. Thus, the hydroxyl radical has an emission band at 2.8μ; carbon monoxide has vibrational emission bands at 2.8μ and 4.4μ; and there are water emission bands at 0.95μ, 1.45μ, 1.9μ, 2.7μ, 5.3μ, 5.5μ, and 6.7μ. The 1.9μ band has been found to be composed of almost 1000 fine structure lines. Carbon dioxide displays a weak emission band at 1.9μ and a vibrational band at 4.4μ, which has been found to have rotational contributions (fine structure lines) on its long wavelength side. Carbon dioxide also displays bands at 2.6μ and 15μ. Electronic transitions of C_2 occur at 1.01μ and 1.20μ.

Despite the apparent complexity of interpretation of emission spectra, some generalities may be stated. Reaction products of burning hydrocarbons consist chiefly of carbon dioxide and water. For complete combustion, these are the only reaction products. For incomplete combustion, additional products and particulates may be produced, and the resulting spectra are more complex. Nevertheless, the emission spectra from flames of hydrocarbons are quite similar.

With increasing temperature, some of the emission bands appear to shift in wavelength. One possible reason for the shift is that these bands arise from luminescent bodies; another reason is the varying amounts of the byproducts of combustion. For example, consider figure 2. Figure 2A gives the unresolved emission spectrum (solid line) at a temperature T_1. It displays a maximum at λ_1. The two peaks of which this spectrum is considered to be comprised are shown by the two dashed lines. Let the two peaks originate from two different species in the combustion zone. Raising the flame temperature to T_2, suppose the concentration of the species responsible for the low wavelength peak decreases and that of the high wavelength peak increases. The unresolved spectrum for such a situation is shown in figure 2B. If the spectrum remains unresolved, increasing the flame temperature from T_1 to T_2 appears to shift the peak of the curve from λ_1 to λ_2.

---

[7] Dickey, F. P., Gailar, N., Hoffman, J., Yarger, F., and Rogge, W. Ohio State University. Final Report, RF Project 751. Contract AF19(604)2254. A Study of the Infrared Spectra of Flames Using Phase-Discrimination Methods of Detection. July 1960. UNCLASSIFIED Report.
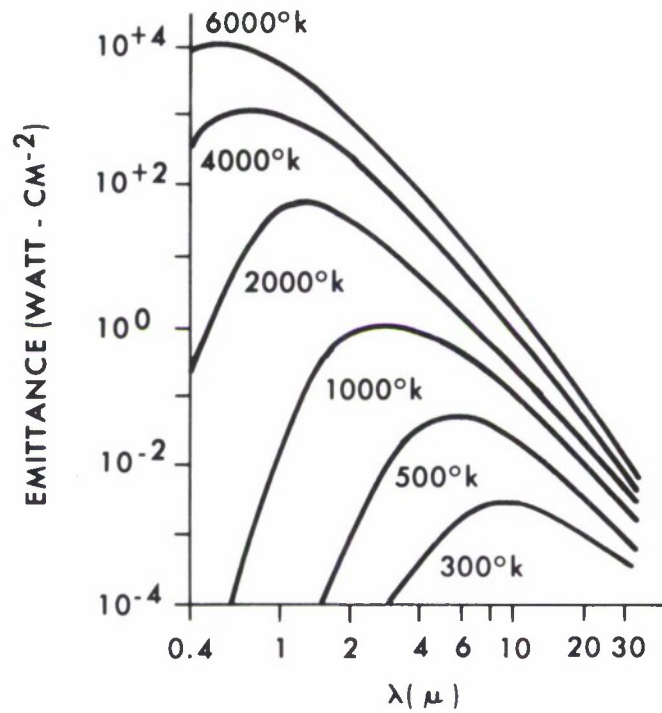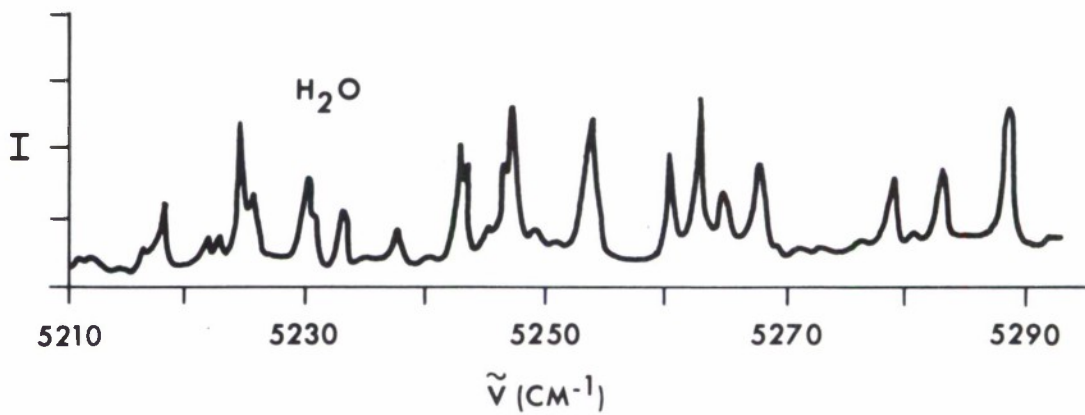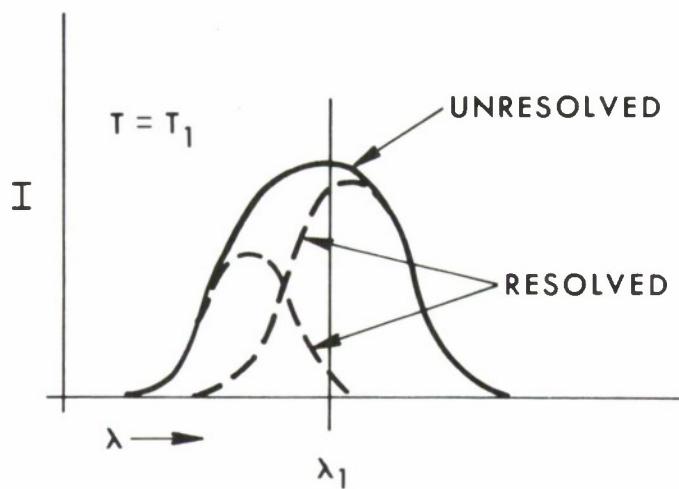
Figure 1. (A) Blackbody Emission; (B) Luminescence* of H_2O

A. Emission Doublet at Low Temperature
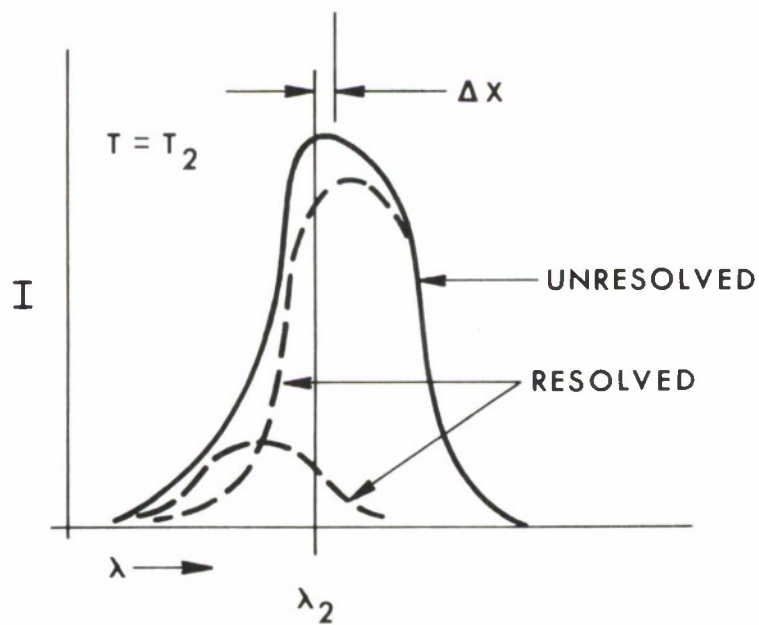
B. Emission Doublet at High Temperature

Figure 2. Possible Temperature Dependence of an Emission Doublet
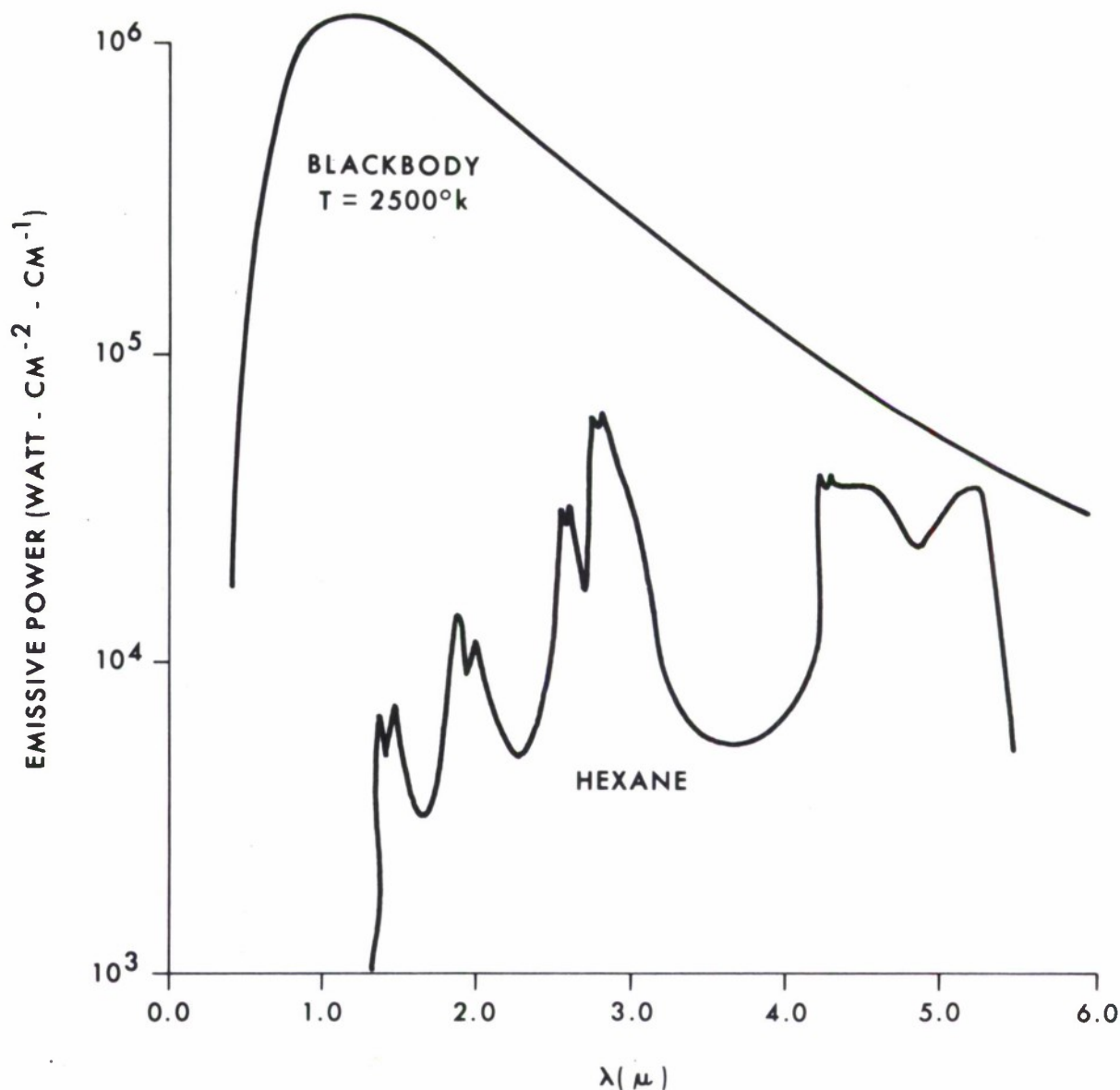
Figure 3. Absolute Emission Intensity of Hexane Flame*

*From Welker, J. R., and Sliepcevich, C. M. University of Oklahoma Research Institute. Twelfth Quarterly Progress Report. OURI-1578-APR-12. Contract DAAA-15-67-C-0074. Susceptibility of Potential Target Components to Defeat by Thermal Action. September 1969. UNCLASSIFIED Report.

The actual intensity of the emission of one fuel (specifically hexane) compared with that of a blackbody radiator at 2500°K is shown in figure 3.[8] The intensity of radiation from the flame is considerably less than that from the blackbody radiator, and it peaks at a longer wavelength. This indicates that the flame temperature is considerably lower than 2500°K. This is also true for the emission spectra of other fuels.

[8]Welker, J. R., and Sliepcevich, C. M. University of Oklahoma Research Institute. Twelfth Quarterly Progress Report, OURI-1578-QPR-12. Contract DAAA-15-67-C-0074. Susceptibility of Potential Target Components to Defeat by Thermal Action. September 1969. UNCLASSIFIED Report.

11

Emission spectra from various parts of a flame were measured and found to vary as a function of the position in the flame.[9] Spectra were taken of a variety of fuels and from selected areas of the flame. The data for an acetone flame are reproduced here as figure 4. Spectra were taken at the coordinates (y, z), with y and z measured in inches. The distance upward from the center of the flame base, along the symmetry axis of the flame, is z. The distance from the center of the flame, perpendicular to the symmetry axis, is y. Not only do the intensities of the bands change with position, they also change with respect to each other. This reflects the changes in concentrations and temperatures of the various species responsible for the emission bands with a change of position in the flame.

Emission spectra of flames from various mixtures of kerosene and oxygen have been measured,[1] and it was found that a small variation in the stoichiometry from unity (0.827 to 1.204) did not significantly alter the emission spectrum. The emission from a flame, however, is highly dependent on the pressure of the surrounding atmosphere.[2] The emission substantially decreased with decreasing pressure.

Previous investigators[10,11] have characterized the radiation from a flame by an average emissivity. That is, the flames were considered to be graybody radiators. Four fuels have been ranked qualitatively according to the intensity of radiation returned to the fuel surface from its flame: benzene > gasoline > kerosene > ethanol.[11] An ethanol flame, for example, is of relatively low intensity (low average emissivity), whereas a benzene flame is comparatively intense (high average emissivity). The basis for this ranking was an estimate of average flame emissivities over a narrow spectral region.

So far, discussion has centered primarily on the infrared spectra of flames. Flames, of course, also emit radiation in the visible and ultraviolet spectra. A summary of such spectra is available.[12]

B.   Transfer of Radiation.

Radiation emitted by the flame zone and the convective column above the flame is diminished by two factors: the inverse square dependence of intensity on distance, and attenuation by gases and other material. Both processes occur, regardless of whether the transfer is to the unburned fuel or to a target within or outside the flame.

Consider the case in which radiation from both the flame and its convective column is transferred to a target that is distant from the fuel. The radiation is attenuated (in addition to the inverse square dependence) in its passage through air primarily by absorption bands of CO_2 and H_2O, which lie in the spectral regions of the flame emission bands. Absorption spectra of CO_2 and H_2O in the wavelength region of interest are shown in figures 5 and 6. Figure 7 gives the absorption spectrum of air. The H_2O and CO_2 absorption bands may be identified readily.

---

[9]Hood, J. D. A Method for the Determination of the Radiative Properties of Flames. Ph.D. Thesis, University of Oklahoma. 1966.

[10]Rasbash, D. J., Rogowski, Z. W., and Stark, G. W. V. Properties of Fires of Liquids. Fuel *35*, 94 (1956).

[11]Carpenter, G. E., Andersen, W. H., Garfinkle, D. R., and Brown, R. E. Shock Hydrodynamics, Inc. First Quarterly Progress Report SHI-6245-1. Contract DAAA-15-69-C-0301. Evaluation Techniques for Flame and Incendiary Agents. May 1969. UNCLASSIFIED Report.

[12]Lewis, B., and von Elbe, G. Combustion, Flames and Explosions of Gases. Academic Press, Inc., New York, New York. 1961.
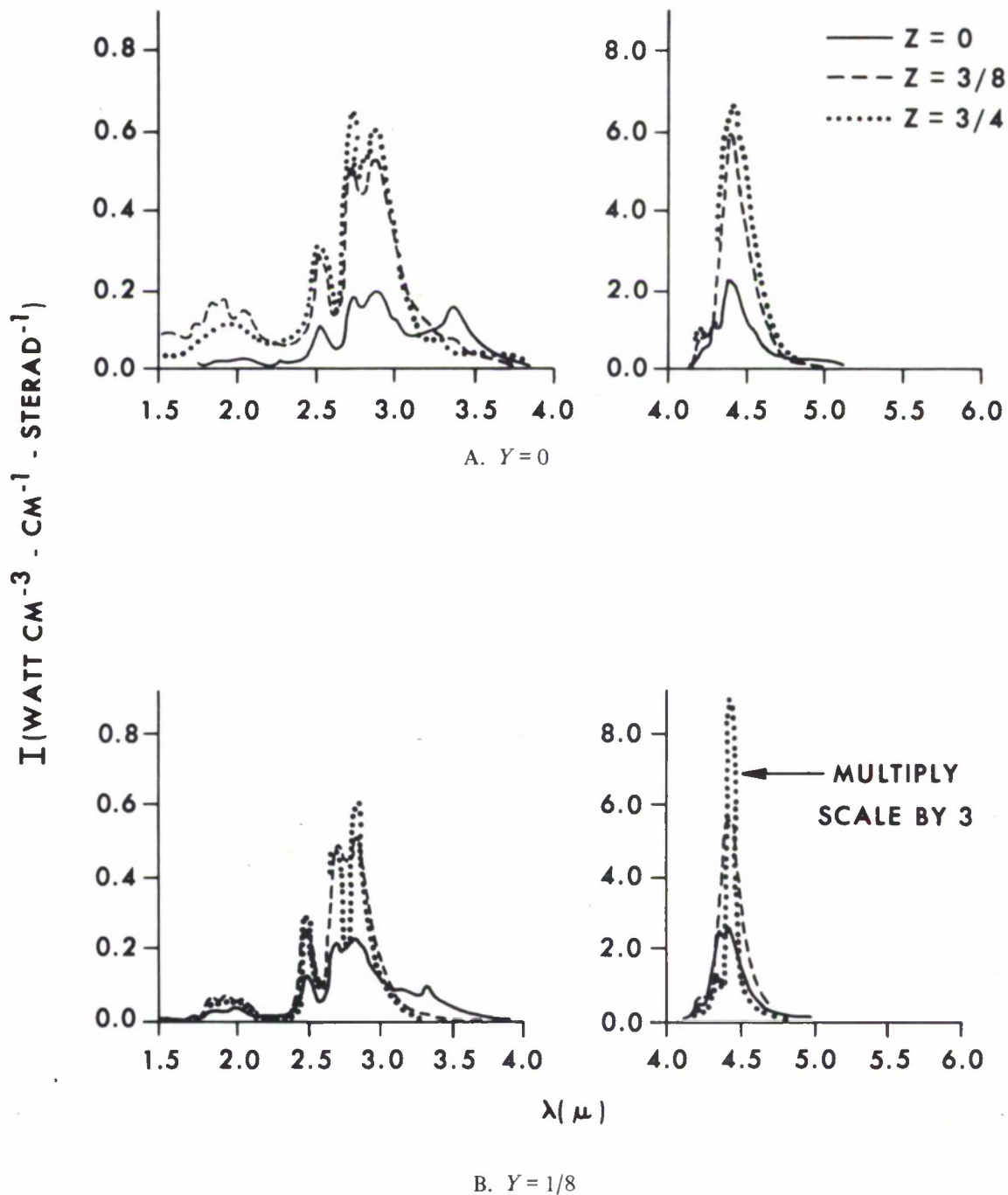
Figure 4. Flame Emission From Acetone Flame*

*From Hood, J. D. A Method for the Determination of the Radiative Properties of Flames. Ph.D. Thesis. University of Oklahoma. 1966.

13
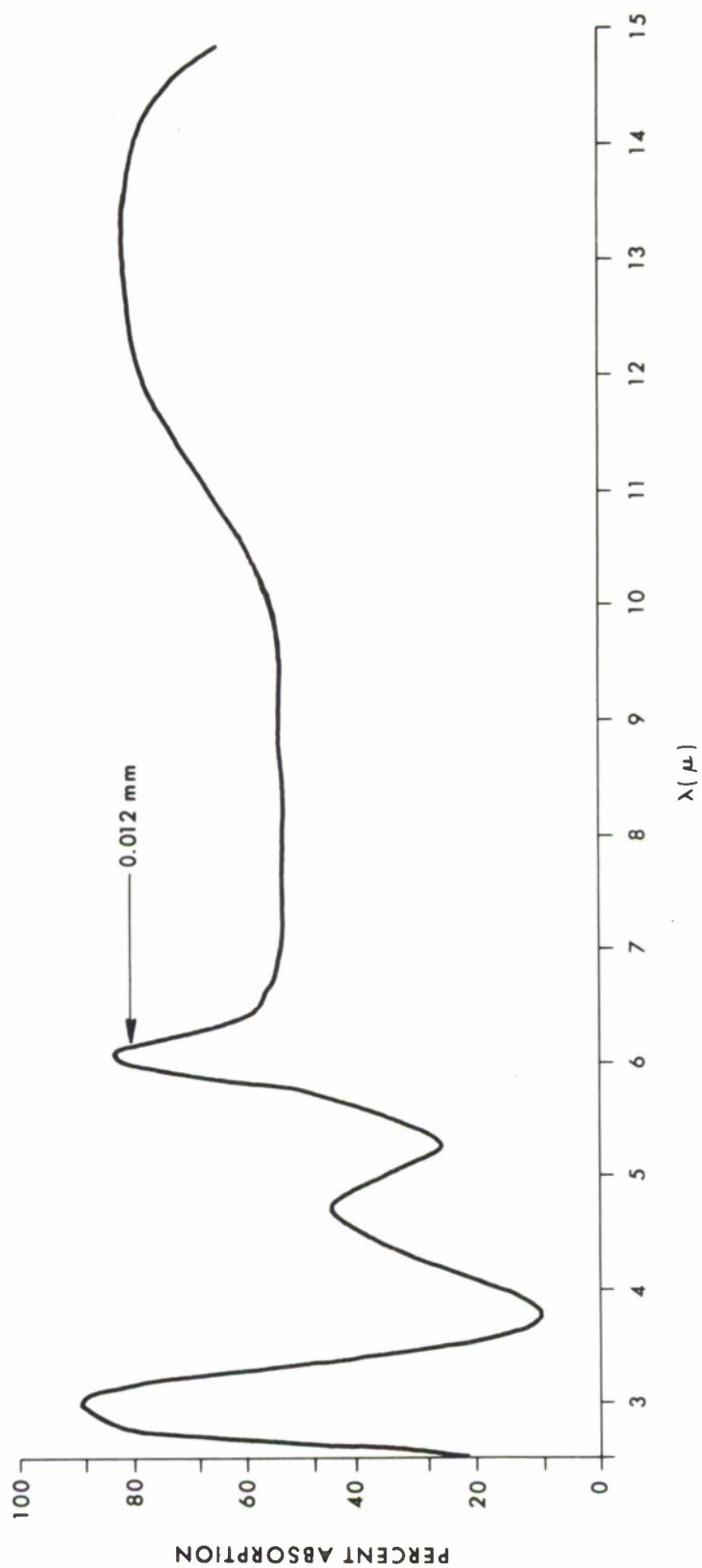
Figure 5. Absorption Spectrum of Water

14
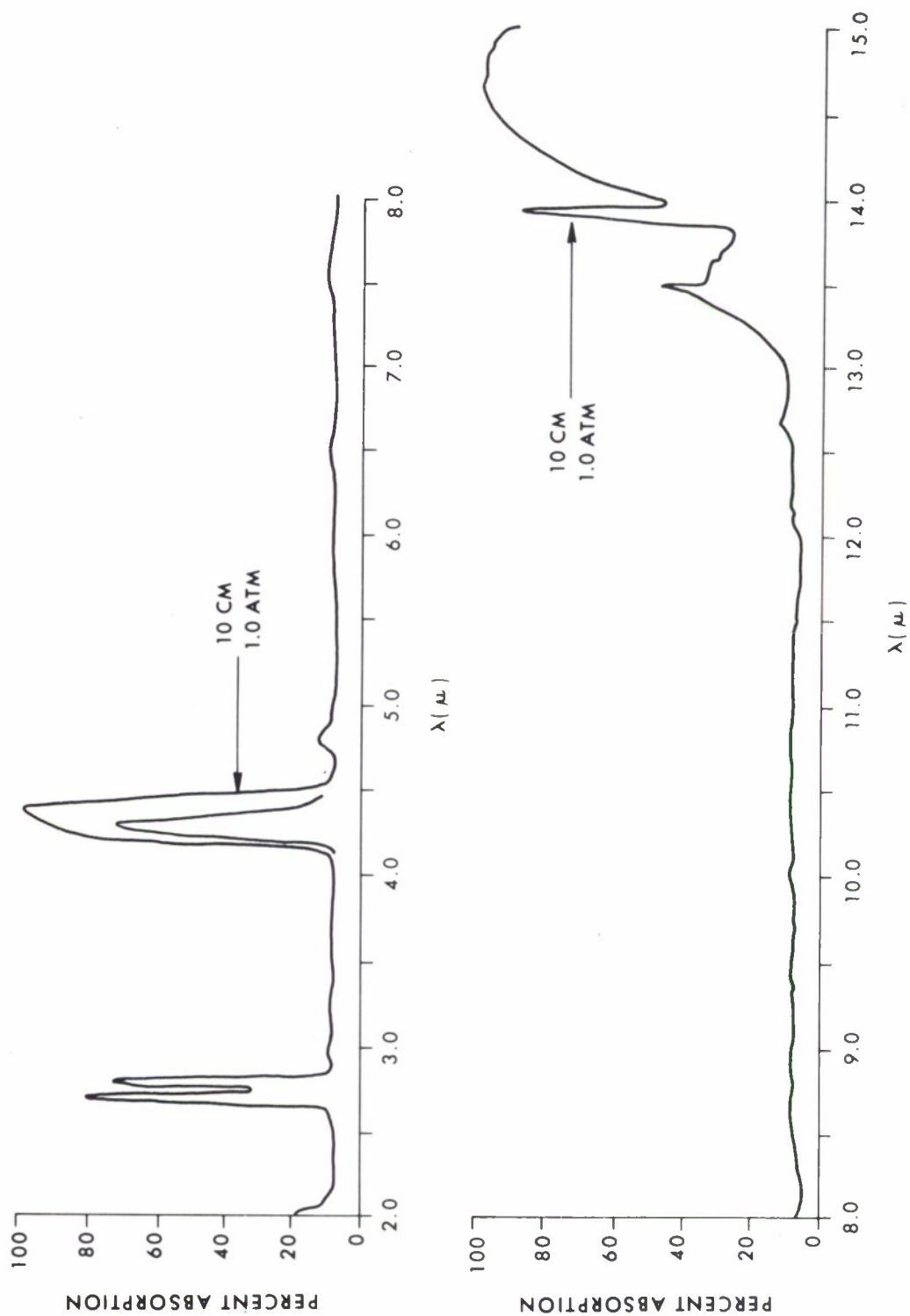
Figure 6. Absorption Spectrum of Carbon Dioxide*

*From Colthup, N. B., Daley, L. H., and Wiberly, S. E. Introduction to Infrared and Raman Spectroscopy. Academic Press, Inc., New York, New York. 1964.

15
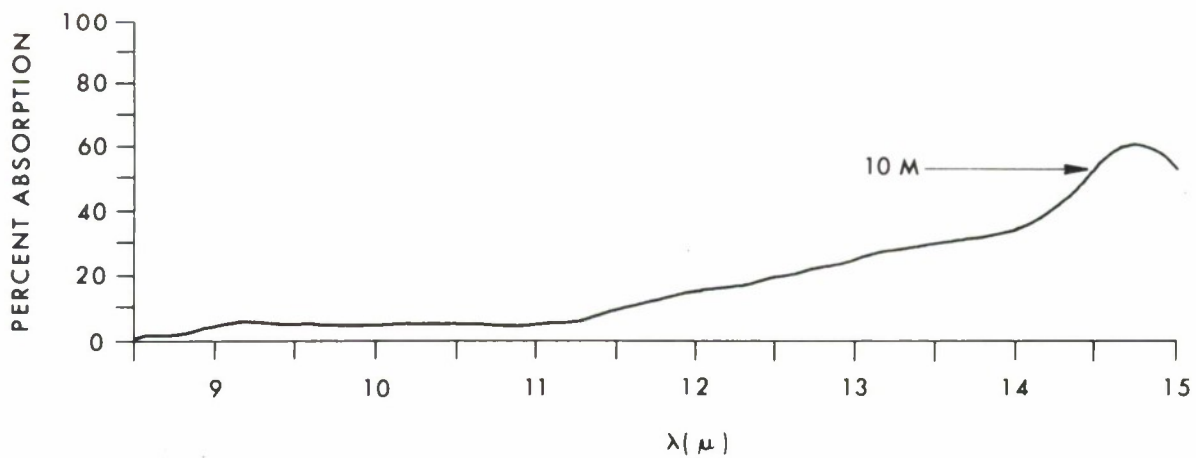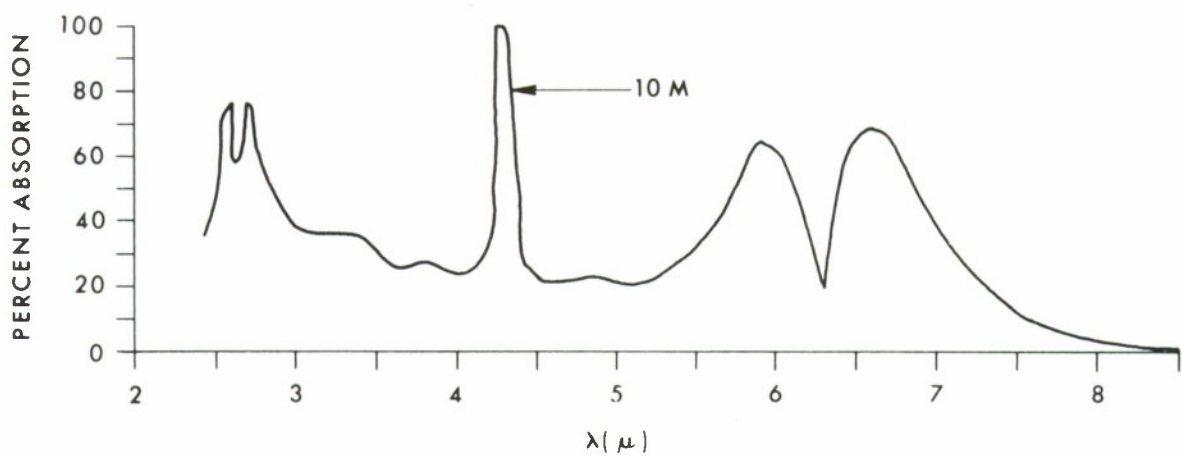
Figure 7. Absorption Spectrum of Air (Sea Level, 25°C, 30% Relative Humidity)

For the case of heat transfer to the unburned fuel, radiation from the flame is attenuated by interconal gases. Radiation from the convective column is attenuated in its passage through the column, the flame, and the interconal gases.

The identities and concentrations of interconal gases vary as a function of height above the fuel and also with horizontal distance from the flame symmetry axis to the flame boundary. Thus, just above the pool one would expect a layer of vaporized fuel. With increasing height, one encounters progressively higher concentrations of intermediate and final reaction products. The same progression is encountered with increasing distance from (and normal to) the flame symmetry axis toward the flame boundary (at constant height).

C.   Absorption Spectra.

Radiation incident upon a surface is either reflected, absorbed, or transmitted; the determining factor for heat transfer to an object is the absorption spectrum of that object. Some generalizations can be made for radiation feedback from a flame to its unburned fuel.

Most of the fuels considered here are hydrocarbons and therefore have common spectral characteristics. This is most easily appreciated by consideration of the absorption spectra of the liquid fuels. In the absorption spectrum of hexane (figure B-8 of appendix B), the band at 3.5μ characterizes the carbon-hydrogen bond, and the band at 6.8μ characterizes CH_2 and CH_3 resonances. Correlation of infrared spectra with the structure of the absorbing species has been extensively developed, and the origins of specific bands can be identified.[13]

The same criterion that has been used to rank fuels according to intensity of radiation returned to the unburned fuel (namely, average emissivity, see section IIA) has been used to establish a ranking by the average absorption coefficient of unburned fuel and of the interconal gases. For example, three fuels have been ranked qualitatively according to the average absorption coefficients of their liquids: kerosene > gasoline > benzene.[14] Thus, the assumption has been made of graybody absorbers as well as emitters.

The intensity of the radiation returned to the unburned fuel comprises only a part of the process of radiation transfer. Absorption by the unburned fuel comprises the remainder. For example, high radiation intensity from the flame, unless accompanied by absorption within the fuel, will not significantly transfer heat to (warm) the liquid. For a solid fuel containing microscopic impurities, transition intensities for optical transitions have been derived,[15] from which absorption and emission spectra may be calculated.

The wavelength dependences of both the radiative emission from the flame and the optical absorption of the fuel are also important. Little warming takes place if absorption bands of the fuel do not occur in the same wavelength regions as the radiative emission bands from the flame. On this basis, it is expected that the fuels having the most efficient radiative transfer are those for which: (1) the flame emission bands are relatively intense; (2) the optical absorption bands of the unburned fuel are intense; and (3) the absorption bands of the fuel occur in the same wavelength regions as the flame emission bands. Neglecting attenuation of radiation by interconal gases (most

[13]Colthup, N. B., Daley, L. H., and Wiberly, S. E. Introduction to Infrared and Raman Spectroscopy. Academic Press, Inc., New York, New York. 1964.

[14]Brown, R. E., Andersen, W. H., Garfinkle, D. R., and Zernow, L. Shock Hydrodynamics, Inc. Annual Summary Report SHI-6005-4. Contract DAAA-15-67-C-0172. Evaluation Techniques for Flame and Incendiary Agent. p 46. July 1968. UNCLASSIFIED Report.

[15]Kelley, C. S. EATR 4426. A Simplified Expression for Oscillator Strengths of Transitions Between Different Quadratic Modes of a Configuration Coordinate Model. August 1970. UNCLASSIFIED Report.

accurate for small diameter pools), a measure of the radiation transfer is the overlap of the absorption spectrum of the unburned fuel and the emission spectrum of the flame.

Consider the effect of subsurface absorption of radiation that is incident upon, and normal to, the upper surface of a fuel. The fuel is characterized by a finite depth, h, and a wavelength-dependent absorption coefficient, $\alpha(\lambda)$.

With a large value of αh, and consequently a relatively large heat storage in the bulk of the fuel, subsurface vaporization can occur. This has, in fact, been observed.[10] The size of the bubbles increased with the flame intensity. For example, benzene (which has a relatively luminous flame) produced large bubbles, whereas kerosene (relatively nonluminous) produced small bubbles. No bubbling was observed in ethanol (nonluminous flame) pools. During bubbling heat transferred by conduction into the bulk from the upper heated layers of the liquid was impeded, and less heat was transferred from the liquid to its substrate. Convective currents in the bulk of the liquid increase the conductive transfer of heat to the substrate. Intense radiation can cause superheating of the bulk liquid, and surface temperatures of a few degrees in excess of the boiling point have been observed.[16] On the other hand, low bubbling, which enhances conduction to the substrate, decreases the heat available for emission from the flame.

For large values of α, heating primarily occurs at the fuel surface, and subsequent boiling removes this heated layer. For small values of α, bulk heating takes place. Although the net heat transfer is greater for large values of α, this heat is not available for transfer to the substrate because surface evaporation withdraws heat from the fuel. So, more efficient heating of the bulk (and, consequently, the largest amount of heat available for conductive transfer to the substrate) occurs for small values of α.

Absorption of radiation by the vaporizing gases just above the surface of the fuel also decreases the radiation intensity returned to the fuel. The temperature of such a vapor will exceed that of the vapor present in a nonluminous flame.

III. THEORY.

The transfer of heat at steady state from a flame to the surface of its unburned fuel has been represented by the following relation,[17] which has been modified[18] to include the effect of partial reflection of radiation at the fuel surface. It is presented here in the modified form.

$$q = \tfrac{1}{4}\pi d^2 \left\{ K[(T_f - T_b)/d] + U(T_f - T_b) + \sigma F(T_f^4 - T_b^4)[1 - e^{-\gamma d}](1 - r) \right\} \tag{1}$$

The heat transfer rate, q (in, say, calorie-second^{-1}) at the surface of the fuel consists of three terms. The first term on the right of equation (1) represents conduction effects. The diameter of the pool of the liquid is d, and the conductive coefficient is K. The flame temperature is T_f, and T_b represents the temperature of the surface of the fuel. The second term represents convection processes, and U is the coefficient of convection. The third term represents radiative processes. The flame is considered to be a graybody radiator, and σ is the Stefan-Boltzmann constant. The term $(1 - e^{-\gamma d})$ represents the absorption of radiation by gases between the flame and the unburned fuel. The absorption coefficient of these gases is γ, which is wavelength dependent. The factor $(1 - r)$ is

[16] Magnus, G. Tests on Combustion Velocity of Liquid Fuels and Temperature Distribution in Flames and Beneath Surface of the Burning Liquid. Int'l Symposium on the Use of Models in Fire Research. Nat'l Acad. Sci.–NRC Publ. 786, 76. 1961.

[17] Hottel, H. C. Review of 'Certain Laws Governing Diffusive Burning of Liquids'. Fire Research Abstracts and Reviews *1*, 41 (1959).

[18] Brown, R. E., Andersen, W. H., Garfinkle, D. R., and Zernow, L. *Op. cit.*, p 52.

that fraction of the incident radiation not reflected by the surface of the fuel. The flame shape factor F for radiation transfer from flame to fuel varies with flame size and shape.

Dividing the left side of equation (1) by the surface area of the pool ($\frac{1}{4}\pi d^2$) and by the volumetric heat of vaporization ($\rho_f \Delta H_v$) gives the fuel regression rate. The density of the fuel is ρ_f, and the heat of vaporization is ΔH_v. In this form, shown as equation (2), the regression rate, dz/dt, is a function of the pan diameter. The vertical coordinate z is measured downward from the initial upper surface of the fuel.

$$dz/dt = (\tfrac{1}{4}\pi d^2 \rho_f \Delta H_v)^{-1} q \tag{2}$$

$$dz/dt = (\rho_f \Delta H_v)^{-1} \left\{ K[(T_f - T_b)/d] + U(T_f - T_b) + \sigma F(T_f^4 - T_b^4)[1 - e^{-\gamma d}](1 - r) \right\} \tag{3}$$

Equation (3), as it stands, is only an approximation. Even so, the form of the radiation term is somewhat in error. Consider graybody radiation from a flame. It is of the form $\sigma \epsilon_f T_f^4$, where ϵ_f is the emissivity of the radiator. This intensity is then modified by a flame shape factor, F_f, to account for the specific geometry of the radiator and absorber. In addition, of the intensity $\sigma \epsilon_f T_f^4 F_f$, only the fraction $(1 - e^{-\gamma d})$ reaches the fuel surface, and then only the fraction $(1 - r)$ of that is transmitted into the fuel. Thus, the radiation that penetrates the surface is $\sigma \epsilon_f T_f^4 F_f (1 - e^{-\gamma d})(1 - r)$. If the surface is also treated as a graybody, the intensity $\sigma \epsilon_b T_b^4 F_b (1 - r)$ is radiated from the fuel surface. The net radiation intensity is

$$\sigma \epsilon_f T_f^4 F_f (1 - e^{-\gamma d})(1 - r) - \sigma \epsilon_b T_b^4 F_b (1 - r) \tag{4}$$

Replacing the erroneous radiation term in equation (3) gives

$$dz/dt = (\rho_f \Delta H_v)^{-1} \left\{ K[T_f - T_b)/d] + U(T_f - T_b) + \sigma(1 - r)[\epsilon_f T_f^4 F_f (1 - e^{-\gamma d}) - \epsilon_b T_b^4 F_b] \right\} \tag{5}$$

Heat absorption rate, fuel vaporization rate, and regression rate are all heat-transfer controlled, and all relate to the same phenomenon—the transfer of heat from the combustion zone to the unburned fuel.

The contribution to the heat absorption rate (and, consequently, to the burning rate) by convection has been studied, and several articles on the subject have been published.[10,*]

The conductive contribution to the heat absorption rate would be expected to be small because of the small coefficient of thermal conductivity for gases. This is true for larger flames, as may be seen by reference to equation (5). The d^{-1} dependence of the conduction term indicates the importance of this term at small values of d. The radiation term dominates for large d values. The convection term is, to a first approximation, independent of d. This analysis of the relative importance of the terms in equation (5) as a function of d is not complete. For example, the dependences of F_f and F_b on pool size are not considered, nor is the fact that the radiation term dominates in sooty flames.

Consider a pool of large diameter, where the radiation term is dominant. Then the regression rate may be written as

$$dz/dt = V \cong A(1 - e^{-\gamma d}) \tag{6}$$

---

*See, for example, references 2, 5, 8, and 9 of reference 10.

where $A = (\rho_f \Delta H_v)^{-1} \sigma (1 - r) \epsilon_f T_f^4 F_f$ is taken as independent of d. The approximation introduced by neglecting the term in T_b^4 is, in general, quite good. It will be discussed in more detail later. For two different pool diameters, d_1 and d_2,

$$V_1/V_2 = \frac{1 - e^{-\gamma d_1}}{1 - e^{-\gamma d_2}} \tag{7}$$

Even though F_f and F_b are dependent on pool diameter, evidence for the validity of equation (7) has been found experimentally.[19]

It has been shown elsewhere[20] that the regression rate can be empirically approximated by

$$dz/dt \simeq 1.267 \times 10^{-4} (\Delta H_c/\Delta H_v)(1 - e^{-\gamma d}) \tag{8}$$

where γ is the absorption coefficient of the flame, and ΔH_c is the heat of combustion. Thus, the regression rate increases with an increase in the product of $\Delta H_c/\Delta H_v$ and $(1 - e^{-\gamma d})$. The factors by themselves, however, may not be directly proportional to dz/dt. That is, $\Delta H_c/\Delta H_v$ is not strictly proportional to dz/dt because γ cannot be held constant from flame to flame.

The flame emissivity has been related to the flame absorption coefficient,[21]

$$\epsilon = 1 - e^{-\gamma d} \tag{9}$$

consequently

$$dz/dt \simeq 1.267 \times 10^{-4} (\Delta H_c/\Delta H_v)\epsilon \tag{10}$$

The present work considers small-scale flames, supported above cylindrical fuels (in pools), and investigates the transfer of radiation from the flame to the fuel. Because of the small pool size, the volume of unburned fuel vapor between the flame and the pool is small. With d small in equation (5), the factor $(1 - e^{-\gamma d}) \simeq 1$, and the radiative heat transfer rate

$$q_r = (\rho_f \Delta H_v) \tfrac{1}{4}\pi d^2 \, dz/dt \tag{11}$$

$$= \tfrac{1}{4}\pi d^2 \sigma (1 - r)[\epsilon_f T_f^4 F_f (1 - e^{-\gamma d}) - \epsilon_b T_b^4 F_b] \tag{12}$$

is approximated by

$$q_r \simeq \tfrac{1}{4}\pi d^2 \sigma (1 - r)[\epsilon_f T_f^4 F_f - \epsilon_b T_b^4 F_b] \tag{13}$$

Equation (13) represents q_r with the additional assumption that radiation returned to the pool is either absorbed by the pool at the surface or reflected away. Equations (12) and (13) do not, therefore, allow for warming of the bulk of the fuel by radiation absorbed beneath the surface.

---

[19] Burgess, D. S., Grumer, J., and Wolfhard, W. G. Burning Rates of Liquid Fuels in Large and Small Open Trays. Fire Res. Abstr. Rev. 2, 10 (1960).

[20] Burgess, D. S., Strasser, A., and Grumer, J. Diffusive Burning of Liquid Fuels in Open Trays. Fire Res. Abstr. Rev. 3(3), 91 (1961).

[21] Atallah, S., and Allan, D. S. Safe Separation Distances from Liquid Fuel Fires. Fire Technol. 7, 47 (1971).

20

It should be noted that in equation (13) the flame temperature is considerably higher than the temperature of the fuel. Also, in general, $\epsilon_f \cong \epsilon_b \equiv \epsilon$, and $0.8 \leqslant \epsilon \leqslant 1.0$.[22] The high emissivity of the flame is caused primarily by incandescence of particles in the combustion zone. Even for $T_f = 4T_b$, the error incurred by the approximation $T_f^4 - T_b^4 \cong T_f^4$ is only 0.5%. Typically, $T_f \cong 1000°K$ for the flames considered here. Taking the largest value of T_b, namely the boiling point of the fuel, $T_b < 400°K$, and $T_f^4/T_b^4 > 39$, the square bracketed expression in equation (13) may be closely approximated by $\epsilon T_f^4 F_f$. Defining $\epsilon F_f = F$,

$$q_r \cong \tfrac{1}{4}\pi d^2 \, \sigma F(1 - r)T_f^4 \tag{14}$$

Consider now the effect of subsurface absorption of radiation that is incident upon, and normal to, the upper surface of a fuel. The fuel is characterized by a finite depth h, and a wavelength-dependent absorption coefficient $\alpha(\lambda)$.

The absorption of radiation by the fuel is dependent upon both the wavelength of the incident radiation and the distance z (as measured downward) into the fuel. The radiation intensity $I_r = (\tfrac{1}{4}\pi d^2)^{-1} q_r$ (in say, calorie-centimeter^{-2}-second^{-1}) at a depth z is given by

$$I_r(\lambda, z) = I_{0_r}(\lambda)(1 - r)e^{-\alpha(\lambda)z} \tag{15}$$

where $I_{0_r}(\lambda)$ is the wavelength-dependent radiation intensity incident upon the upper surface of the fuel. In general, $r = r(\lambda)$.[23] The intensity I_a absorbed by the fuel is $I_{0_r} - I_r$, or

$$I_a(\lambda, z) = I_{0_r}(\lambda)\left\{1 - [1 - r(\lambda)]e^{-\alpha(\lambda)z}\right\} \tag{16}$$

The total intensity I_{at} absorbed by the fuel is the integral of I_a over wavelength, divided by the wavelength span $(\lambda_{max} - \lambda_{min})$ over which absorption occurs:

$$I_{at} = (\lambda_{max} - \lambda_{min})^{-1} \int_{\lambda_{min}}^{\lambda_{max}} I_{0_r}(\lambda)\left\{1 - [1 - r(\lambda)]e^{-\alpha(\lambda)z}\right\}d\lambda \tag{17}$$

The integrand of equation (17) approaches rI_{0_r} (always less than I_{0_r}) as αh approaches zero and increases smoothly to a maximum of I_{0_r} as αh approaches infinity. Therefore, to increase the radiative heat absorbed, either α or h (or both) should be increased.

The absorption coefficient for a particular fuel is an invariant physical property. With a given volume, the fuel will absorb more heat if the pool is of small diameter and deep. Decreasing the pool diameter, however, reduces the intensity of the radiation from the flame, so that a compromise must be struck for optimal results. Increasing the depth of the pool increases the amount of heat available for conductive transfer to the substrate.

Consider the relation between the overlap, O_ν, of the emission and absorption spectra and the intensity I_{at} absorbed by the bulk of the fuel. In calculation of the overlap, the normalized emission intensity is

$$f_\epsilon(\lambda) = I_{0_r}(\lambda)/I_0' \tag{18}$$

[22] Belason, B., Castle, G., Crowley, D., and D'Avanzo, L. A Fire Simulation Facility for Materials Response Testing. Fire Technol. 6, 179 (1970).

[23] Kelley, C. S. Optical Absorption of Divalent Chromium in Zinc Sulfide. Appendix A. Ph.D. Thesis, University of Delaware. June 1970.

where I_0' is the intensity of a reference peak (the 4.5μ band of hexane, for example). The absorption fraction

$$f_\alpha(\lambda) = [I_{0_r} - I_r(z')]/I_{0_r} = 1 - e^{-\alpha(\lambda)z'} \qquad (19)$$

where z' will be chosen to be 0.100 mm (see section IV). The overlap

$$O_v = (\lambda_{max} - \lambda_{min})^{-1} \int_{\lambda_{min}}^{\lambda_{max}} f_\alpha(\lambda) f_\epsilon(\lambda) d\lambda \qquad (20)$$

becomes

$$O_v = (\lambda_{max} - \lambda_{min})^{-1} (I_0')^{-1} \int_{\lambda_{min}}^{\lambda_{max}} I_{0_r}(\lambda)[1 - e^{-\alpha(\lambda)z'}] d\lambda \qquad (21)$$

In this calculation, the surface reflectivity $r(\lambda)$ has not been included. The overlap defined by equation (21), however, can be related to the radiation intensity transferred to the fuel, equation (17). From differentiation of equations (17) and (21),

$$\frac{dI_{at}/d\lambda}{dO_v/d\lambda} = \frac{I_0' \{1 - [1 - r(\lambda)] e^{-\alpha(\lambda)z}\}}{1 - \epsilon^{-\alpha(\lambda)z}} \qquad (22)$$

or

$$I_{at} = I_0' \int_{\lambda_{min}}^{\lambda_{max}} \left(1 - \frac{r(\lambda)}{1 - e^{\alpha(\lambda)}}\right) (dO_v/d\lambda) d\lambda \qquad (23)$$

or

$$I_{at} = I_0' O_v \qquad (24)$$

if $r(\lambda) = 0$. If, in addition, $I_0' = 1$, $I_{at} = O_v$. These conditions are met provided that: (1) the emission intensities are normalized, and (2) the intensity reflected from the fuel surface is small compared to the intensity transmitted. The first condition is met by normalization of the emission spectra.

The Fresnel equation for reflection at the surface of a semi-infinite dielectric slab is

$$r = \left(\frac{n-1}{n+1}\right)^2 \qquad (25)$$

The refractive index n for benzene[24] is 1.5, so that $r = 0.04$. Thus, the intensity reflected away from the surface is 24 times smaller than the intensity transmitted. In fact, for $n \leqslant 2, r \leqslant 11\%$. For

[24]Handbook of Chemistry and Physics. 40th Ed. ed C. D. Hodgman. Chemical Rubber Publishing Company, Cleveland, Ohio. 1959.

the hydrocarbons considered here, $n \leq 1.5$. Then the intensity absorbed by the bulk of the fuel is accurately given by

$$I_{at} \simeq O_v \tag{26}$$

Thus, the total intensity (normalized) absorbed by the fuel is closely approximated by the overlap. The overlap, as one would anticipate, closely represents the intensity of radiation absorbed by the fuel.

Heat is transferred to a pool (of diameter d) at the rate $\frac{1}{4}\pi d^2 I_{at}$. This heat first warms and then evaporates the fuel. Once the boiling point has been reached, no further warming occurs, and all heat serves to evaporate the fuel. The rate of change of the fuel mass is $\frac{1}{4}\pi d^2 \rho_f(dz/dt)$. The rate of heat loss is the product of the mass evaporation rate and the heat of vaporization: $\frac{1}{4}\pi d^2 \Delta H_v \rho_f(dz/dt)$. For steady state conditions, the heat from radiation equals that lost from evaporation. Equating the two:

$$dz/dt = (\rho_f \Delta H_v)^{-1} I_{at} \tag{27}$$

Using equation (24) and the condition for normalized emission spectra ($I_0' = 1$),

$$dz/dt \simeq (\rho_f \Delta H_v)^{-1} O_v \tag{28}$$

That is, given the density and heat of vaporization of a fuel, the regression rate can be calculated from the overlap. Equation (28) may be rearranged as

$$O_v \simeq (\rho_f \Delta H_v)dz/dt \tag{29}$$

The units of the overlap for this relation are those of heat flux (for example, calorie-centimeter^{-2}-second^{-1}). To convert this overlap to the unitless overlap used throughout this report, equation (29) is to be divided by 0.72 cal-cm^{-2}-sec^{-1}. This is the intensity under the 4.5μ emission band of hexane (see figure 3) that was chosen to have the normalized, unitless intensity of 1.0. Thus, equation (29) becomes

$$O_v \simeq 1.39(\rho_f \Delta H_v)dz/dt \tag{30}$$

where the units of ρ_f are gram-centimeter^{-3}, ΔH_v is in calorie-gram^{-1}, dz/dt in centimeter-second^{-1} and O_v is unitless.

Although equation (10) is empirical, it can be combined with equation (30) to give

$$O_v \simeq 1.76 \times 10^{-4} \rho_f \Delta H_c \epsilon \tag{31}$$

or, by equation (9),

$$O_v \simeq 1.76 \times 10^{-4} \rho_f \Delta H_c (1 - e^{-\gamma d}) \tag{32}$$

In both equations 31 and 32, the overlap is unitless.

IV. PROCEDURE.

The specific fuels to be considered in this section are listed in appendix A, together with some of their properties. The information was obtained from several sources.[11,14,24,25]

---

[25]Chemical Engineers' Handbook. ed J. H. Perry. 4th Ed. McGraw-Hill Book Company, New York, New York. 1961.

All optical absorption spectra were obtained from the same reference[26] except for the spectra of triethylaluminum (TEA),[27] carbon dioxide,[28] carbon monoxide (CO),[28] unsymmetrical dimethlhydrazine (UDMH),[27] methylhydrazine (MMH),[27] and carbonyl sulfide (COS).[29] The thickness of the neat (undiluted) sample was not kept constant from fuel to fuel. To facilitate comparison of the spectra, they were normalized to the same sample thickness (0.100 mm). The spectra obtained from gases were additionally normalized to 1 atm pressure. The non-normalized absorption spectra are presented in appendix B. Sample thicknesses are listed on the figures. The absorption spectra of gases list the pressures of the gases and sample thicknesses.

Flame emission spectra are presented in appendix C. These spectra were obtained from several references. The spectra for acetone and cyclohexane were obtained from the same source.[30] This reference also gave spectra spanning 2μ to 5μ for methanol. The spectra for benzene, Napalm Test Solvent (NTS) and the 2μ to 6μ region of hexane all came from the same source.[31] The spectra for ammonia and hydrazine came from one reference.[2] Emission spectra of methane and propane are from a common source.[32] Both the emission spectra of methylhydrazine and unsymmetrical dimethylhydrazine are taken from the same reference.[33] Emission spectra for carbon monoxide and carbonyl sulfide came from one source.[34] These spectra were normalized by comparison of spectra of one fuel from all references. The 4.5μ band of the hexane spectrum was common to all references and was used as the basis for normalization.

For convenience, the absorption intensity was taken as that fraction $f_\alpha(\lambda)$ of the incident radiation that is absorbed by a sample of 0.100-mm thickness. The maximum intensity of the 4.5μ emission band of hexane was normalized to 1.0. The fraction $f_\epsilon(\lambda)$ is that fraction of this maximum intensity. Thus, the overlap is unitless, being measured as the integral over wavelength of the product of $f_\alpha(\lambda)$ and $f_\epsilon(\lambda)$ (see equation 20).

Some of the spectra did not completely span one of the spectral regions considered (2μ to 6μ, 2μ to 13μ, or 2μ to 15μ). These spectra, therefore, were extrapolated over small wavelength spans. These extrapolations appear as dashed lines in the figures.

[26] Catalog of the Infrared Spectra of the American Petroleum Institute. Research Project 44. Petroleum Research Laboratory, Texas A&M, College Station, Texas. 1970.

[27] Sadtler Standard Spectra, Sadtler Research Laboratories, Philadelphia, Pennsylvania.

[28] Pierson, R. H., Fletcher, A. N., and Gantz, E. St. C. Catalog of Infrared Spectra for Qualitative Analysis of Gases. Anal. Chem. *28*, 1218-1239 (1956).

[29] Andrews, D. A., Hurtubise, F. G., and Krassig, H. The Presence of Monothiocarbonate Substituents in Cellulose Xanthates. Can J. Chem. *38*, 1381-1398 (1960).

[30] Welker, J. R., and Sliepcevich, C. M. University of Oklahoma Research Institute. Final Report, OUR1-1604-FR. Grant DA-AMC-035-95(A). October 1968. UNCLASSIFIED Report.

[31] Kahrs, J., and Burgess, D. CRDL Special Publication 6-1. Field Calorimetry/Chemical Studies. Proceedings of the Third Flame-Incendiary Conference. August 1965. UNCLASSIFIED Report.

[32] Bell, E. E., Burnside, P. B., Cermak, W. C., and Dam, C. F. Ohio State University Research Foundation. Final Report. Contract AF 30-(602)-1047. A Study of Infrared Emission from Flame. Part 1. June 1955. UNCLASSIFIED Report.

[33] Penzias, G. J. The Warner and Swasey Company. Contract NONR 3657 (00), ARPA Order No. 237-62. An Atlas of Infrared Spectra of Flames. Part Four. Additional Nitrogenous Liquid Fuels and Oxidizers. October 1964. UNCLASSIFIED Report.

[34] Bell, E. E., Burnside, P. B., Dickey, F. P., Kopczynski, S. L., and Rowntree, R. F. The Ohio State University Research Foundation. Final Report. Contract AF 30(602)-1047. A Study of Infrared Emission from Flames. September 1956. UNCLASSIFIED Report.

Two different methods were used to compute the overlap. The first is essentially an estimate; the second is exact. The first estimate of the overlap was obtained by finding the product of the average absorption fraction $\langle f_\alpha \rangle$ over a spectral region and average emission fraction $\langle f_\epsilon \rangle$ over the same region. That is,

$$\langle f_\alpha \rangle = (\lambda_{max} - \lambda_{min})^{-1} \int_{\lambda_{min}}^{\lambda_{max}} f_\alpha \, d\lambda \tag{33}$$

$$\langle f_\epsilon \rangle = (\lambda_{max} - \lambda_{min})^{-1} \int_{\lambda_{min}}^{\lambda_{max}} f_\epsilon \, d\lambda \tag{34}$$

and the average overlap is

$$\langle O_\nu \rangle = \langle f_\alpha \rangle \, \langle f_\epsilon \rangle \tag{35}$$

This overlap is, therefore, obtained essentially through graybody approximations. The three spectral regions (2μ to 6μ, 2μ to 13μ, and 2μ to 15μ) were chosen primarily because of the emission spectra. The spectra spanned one, two, or all three regions, depending on the fuel (see appendix C).

Values of $\langle f_\alpha \rangle$ and $\langle f_\epsilon \rangle$ are listed in tables I and II. They were obtained by planimetry directly from the figures. The tables list agents in order of decreasing $\langle f_\alpha \rangle$ and $\langle f_\epsilon \rangle$ as calculated over 2μ to 6μ. A ranking of fuels in order of $\langle f_\epsilon \rangle$ corresponds to a ranking by flame intensity. Average overlap values were computed from tables I and II and are listed in table III. Table III lists fuels by decreasing average overlap values as calculated over 2μ to 6μ, 2μ to 13μ, and 2μ to 15μ. These average overlap values vary depending on the wavelength span considered. The most accurate overlap values are those for the widest wavelength span. In the 2μ to 15μ region, however, fewer overlap values could be computed than in the 2μ to 6μ region. Therefore, a comparison of the largest number of fuels is for the rather short 2μ to 6μ region. The small average overlap for fuels below cyclohexane in table III occurs because their absorption spectra were obtained from gaseous samples rather than liquids. Because the gas phase is normally employed for these fuels, however, average overlap values are given for this phase. It is to be emphasized that the average overlap values in table III were obtained through graybody approximations.

The exact overlap O_ν was calculated also. The product of the wavelength-dependent absorption fraction $f_\alpha(\lambda)$ and the wavelength-dependent emission fraction $f_\epsilon(\lambda)$ was calculated point by point throughout the wavelength region under consideration. The calculation amounted to evaluation of equation (20). The product of f_α and f_ϵ as a function of wavelength for the various fuels is presented in the figures of appendix D. From these figures, it appears that most of the overlap occurs in the 4.5μ and the 2.5μ regions.

Results of the calculation of the exact overlap are presented in table IV for the same three spectral regions considered above. Fuels are listed in order of decreasing overlap in the table. These exact overlap values for 2μ to 6μ span a wide range—from 0.178 for UDMH to 3.19×10^{-6} for methane. The average overlap values in table III differ substantially from the exact values in table IV, as does the ordering of the fuels by overlap. It appears, therefore, that the graybody approximations used in computing the average overlap values are not accurate.

The average absorption fraction, $\langle f_\alpha \rangle$, for each of the fuels listed in table I was obtained by use of equation (33). It represents that fraction of an incident wavelength-dependent (or

Table I. Average Absorption Fractions

Fuel	Average absorption fraction[a] (f_α) over		
	2μ-6μ	2μ-13μ	2μ-15μ
UDMH	4.27×10^{-1}	7.68×10^{-1}	7.19×10^{-1}
MMH	3.81×10^{-1}	6.27×10^{-1}	6.40×10^{-1}
NTS	3.16×10^{-1}	3.27×10^{-1}	3.42×10^{-1}
TEA	2.22×10^{-1}	4.14×10^{-1}	4.46×10^{-1}
Hexane	1.97×10^{-1}	2.32×10^{-1}	2.43×10^{-1}
Heptane	1.87×10^{-1}	2.41×10^{-1}	2.48×10^{-1}
Benzene	1.61×10^{-1}	2.71×10^{-1}	3.03×10^{-1}
Methanol[b]	1.55×10^{-1}	2.07×10^{-1}	—
Cyclohexane	5.84×10^{-2}	6.25×10^{-2}	5.52×10^{-2}
Isooctane	5.5×10^{-2}	1.63×10^{-1}	1.73×10^{-1}
Acetone	2.37×10^{-4}	2.85×10^{-4}	2.5×10^{-4}
COS	1.87×10^{-4}	9.95×10^{-5}	9.84×10^{-5}
Propane	1.68×10^{-4}	1.78×10^{-4}	1.74×10^{-4}
CO	9.00×10^{-5}	3.28×10^{-5}	2.76×10^{-5}
Methane	5.53×10^{-5}	2.21×10^{-5}	1.90×10^{-5}
Hydrazine	1.66×10^{-6}	7.35×10^{-6}	7.5×10^{-6}
Ammonia	2.78×10^{-7}	1.19×10^{-6}	1.14×10^{-6}

[a]Normalized to 0.100-mm thickness, in units of fraction of intensity absorbed in that thickness at a pressure of 1.00 atm.

[b]The sample thickness quoted in the reference of the spectrum is a factor of 10 too small. This is corrected here.

independent) radiative flux that is absorbed by the unburned fuel. A somewhat different interpretation of an average absorption fraction[30] is that fraction of the radiative flux emitted by the flame that is absorbed by the unburned fuel:

$$\langle f_\alpha' \rangle = O_v / \langle f_\epsilon \rangle = \int_{\lambda_{min}}^{\lambda_{max}} f_\alpha(\lambda) f_\epsilon(\lambda) d\lambda \bigg/ \int_{\lambda_{min}}^{\lambda_{max}} f_\epsilon(\lambda) d\lambda \tag{36}$$

Thus, of the maximum radiative flux available for absorption (essentially $\langle f_\epsilon \rangle$), only a fraction (essentially O_v) is absorbed. Then, $\langle f_\alpha' \rangle$ is a measure of how effectively a fuel absorbs radiation from its own flame.

Accordingly, $\langle f_\alpha' \rangle$ for each of 14 fuels was computed. The results are presented in table V. The fuels are listed in order of decreasing $\langle f_\alpha' \rangle$, as computed over 2μ to 6μ. The values span a wide range, from 6.82×10^{-1} for UDMH to 2.55×10^{-5} for methane.

V. INTERPRETATION.

It was anticipated that the exact overlap values could be related to other fuel properties through the equations developed in section III. For example, equation (30) relates overlap to ρ_f, ΔH_v, and dz/dt.

Table II. Average Emission Fractions

Fuel	Average emission fraction* (f_ϵ) over		
	$2\mu\text{-}6\mu$	$2\mu\text{-}13\mu$	$2\mu\text{-}15\mu$
Methanol	5.37×10^{-1}	3.53×10^{-1}	—
Hexane	4.91×10^{-1}	3.76×10^{-1}	4.41×10^{-1}
Cyclohexane	3.09×10^{-1}	—	—
MMH	2.70×10^{-1}	2.65×10^{-1}	3.28×10^{-1}
Benzene	2.61×10^{-1}	—	—
UDMH	2.61×10^{-1}	2.92×10^{-2}	3.46×10^{-1}
Acetone	2.59×10^{-1}	—	—
NTS	1.80×10^{-1}	—	—
Ammonia	1.79×10^{-1}	2.53×10^{-1}	2.70×10^{-1}
CO	1.69×10^{-1}	6.15×10^{-2}	5.19×10^{-2}
Methane	1.25×10^{-1}	4.46×10^{-2}	3.83×10^{-2}
Propane	1.08×10^{-1}	3.95×10^{-2}	3.35×10^{-2}
Hydrazine	1.06×10^{-1}	1.57×10^{-1}	1.86×10^{-1}
COS	3.55×10^{-2}	2.67×10^{-2}	2.30×10^{-2}

*Normalized so that the intensity of the 4.5μ hexane band maximum is 1.0.

Table III. Average Overlap

Fuel	Average overlap $\langle O_v \rangle = \langle f_\alpha \rangle \langle f_\epsilon \rangle$, over		
	$2\mu\text{-}6\mu$	$2\mu\text{-}13\mu$	$2\mu\text{-}15\mu$
UDMH	1.11×10^{-1}	2.25×10^{-1}	2.49×10^{-1}
MMH	1.03×10^{-1}	1.66×10^{-1}	2.10×10^{-1}
Hexane	9.48×10^{-2}	8.73×10^{-2}	1.07×10^{-1}
Methanol	8.33×10^{-2}	7.30×10^{-2}	—
NTS	5.69×10^{-2}	—	—
Benzene	4.21×10^{-2}	—	—
Cyclohexane	1.80×10^{-2}	—	—
Propane	1.82×10^{-4}	7.04×10^{-6}	5.84×10^{-6}
Acetone	6.14×10^{-5}	—	—
CO	1.52×10^{-5}	2.02×10^{-6}	1.43×10^{-6}
Methane	6.92×10^{-6}	1.21×10^{-6}	7.28×10^{-7}
COS	6.64×10^{-6}	2.66×10^{-7}	2.26×10^{-6}
Hydrazine	1.76×10^{-7}	1.16×10^{-6}	1.39×10^{-6}
Ammonia	4.98×10^{-8}	3.00×10^{-7}	3.08×10^{-7}

Table IV. Exact Overlap

Fuel	Exact overlap*, O_ν, over		
	$2\mu\text{-}6\mu$	$2\mu\text{-}13\mu$	$2\mu\text{-}15\mu$
UDMH	1.78×10^{-1}	1.81×10^{-1}	2.08×10^{-1}
Benzene	1.49×10^{-1}	—	—
MMH	9.43×10^{-2}	1.77×10^{-1}	2.31×10^{-1}
Cyclohexane	8.85×10^{-2}	—	—
Hexane	3.37×10^{-2}	3.99×10^{-2}	4.87×10^{-2}
Methanol	2.89×10^{-2}	2.69×10^{-2}	—
NTS	2.02×10^{-2}	—	—
Hydrazine	3.87×10^{-4}	8.70×10^{-4}	1.15×10^{-3}
COS	2.25×10^{-4}	8.17×10^{-5}	6.93×10^{-5}
Ammonia	6.38×10^{-5}	1.30×10^{-4}	1.34×10^{-4}
CO	2.56×10^{-5}	9.29×10^{-6}	7.88×10^{-6}
Acetone	2.56×10^{-5}	—	—
Propane	1.48×10^{-5}	5.66×10^{-6}	4.81×10^{-6}
Methane	3.19×10^{-6}	1.15×10^{-6}	9.79×10^{-7}

*Unitless, see text.

Table V. Absorption Fraction, $\langle f_\alpha' \rangle$

Fuel	Absorption fraction, $\langle f_\alpha' \rangle$, over		
	$2\mu\text{-}6\mu$	$2\mu\text{-}13\mu$	$2\mu\text{-}15\mu$
UDMH	6.82×10^{-1}	6.19×10^{-1}	6.03×10^{-1}
Benzene	5.71×10^{-1}	—	—
MMH	3.49×10^{-1}	6.68×10^{-1}	7.05×10^{-1}
Cyclohexane	2.86×10^{-1}	—	—
NTS	1.12×10^{-1}	—	—
Hexane	6.86×10^{-2}	1.06×10^{-1}	1.10×10^{-1}
Methanol	5.38×10^{-2}	7.63×10^{-2}	—
COS	6.33×10^{-3}	3.06×10^{-3}	3.01×10^{-3}
Hydrazine	3.65×10^{-3}	5.53×10^{-3}	6.18×10^{-3}
Ammonia	3.56×10^{-4}	5.14×10^{-4}	4.96×10^{-4}
CO	1.51×10^{-4}	1.51×10^{-4}	1.52×10^{-4}
Propane	1.37×10^{-4}	1.43×10^{-4}	1.43×10^{-4}
Acetone	9.88×10^{-5}	—	—
Methane	2.55×10^{-5}	2.58×10^{-5}	2.56×10^{-5}

Table VI. Comparison of O_v to T_f and Equation 30

Fuel	T_f	dz/dt (cm/sec)	O_v (eq 30)	Exact overlap (2μ-6μ)
	°C			
Benzene	2266	6.4×10^{-3}*	7.38×10^{-1}	1.49×10^{-1}
Cyclohexane	2269	2.1×10^{-3}	1.95×10^{-1}	8.85×10^{-2}
Hexane	2258	2.3×10^{-3}	1.84×10^{-1}	3.37×10^{-2}
Methanol	–	1.7×10^{-3}	4.87×10^{-1}	2.89×10^{-2}
NTS	–	1.7×10^{-3}	1.41×10^{-1}	2.02×10^{-2}
Ammonia	≤1850	–	–	6.38×10^{-5}

*Average of the two values in appendix A.

The fuels were ranked by overlap values (computed for 2μ to 6μ) and compared to rankings by the fuel properties listed in appendix A. Relevant fuel properties are listed in table VI along with exact overlap values. It appears that dz/dt and T_f increase with increasing overlap.

A weak dependence of the flame temperature on overlap would be expected for the following reasons. With increasing overlap, the pool regression rate increases, which increases the rate of vapor evolution. Increased vapor pressure above the fuel produces an expansion of the flame, with a corresponding increase in the flame volume and surface area. Because of absorption by the flame, the radiation it emits depends primarily on the surface area of the flame. The radiation retained (absorbed) by the flame, however, is characterized by an exponential dependence $(I = I_0 [1 - exp(-\gamma d)])$ on a "flame radius," d. Thus, with increasing overlap, the flame absorbs at a rate faster than the surface emits (d^2 dependence), producing a net flame temperature increase.

A more dominant effect, though, is the variation of the heat of reaction from fuel to fuel. The variation of flame temperature from fuel to fuel is quite closely related to the heat of reaction of the agent, which is distributed among the reaction products. This is, in fact, the method used to determine theoretical flame temperatures. It is the concentration of reaction products that defines the flame temperature. Thus, a fuel with a high heat of reaction and a low concentration of reaction products would be anticipated to have a high flame temperature. The effect of overlap on flame temperature, therefore, is considered to be secondary.

Table VI lists values of the overlap calculated from equation (30) for all fuels for which values of ρ_f, ΔH_v, and dz/dt were listed in appendix A. The calculated overlap values increase with increasing exact overlap and are roughly five times too large.

One factor has been disregarded in these overlap calculations—absorption of radiation by interconal gases. As stated earlier, this approximation is best for small flames. Wavelength-dependent absorption coefficients have been measured for laboratory-scale flames.[30,35] The experiments, however, measured the absorption of both the interconal gases and the flame itself. These spectra are available for acetone, cyclohexane, benzene, ethanol, hexane, and natural gas and span about 2μ to 6μ.[30] They could not be readily incorporated into the overlap calculations

---

[35]Klaubert, E. C. Block Engineering, Inc. Final Technical Report. Contract DA-18-035-AMC-262(A). Field Calorimetry/IR Instrumentation. December 1965. UNCLASSIFIED Report.

because: (1) the spectra include flame absorption, which does not occur in the heat transfer process considered here; and (2) radiation from the flame tip travels a greater distance to the pool than does radiation from near the flame base—to incorporate this, it would be necessary to specify the dimensions of a particular flame, resulting in a loss of generality.

Nevertheless, to obtain an estimate of the magnitude of this effect, consider the specific case of a 10-cm diameter pool of burning acetone. The intensity of the flame radiation returned to the fuel is diminished by the factor $1 - exp(-\gamma x)$, where γ is the absorption coefficient for interconal gases, and x represents an average distance of the flame from the fuel surface. For a pool of diameter 10 cm, the flame height[21] is about 40 cm, and $x \simeq 20$ cm is representative. From Welker and Sliepcevich,[30] an average γ for an acetone flame is 0.026 cm^{-1}, and $1 - exp(-\gamma x) \simeq 0.4$. Thus, the computed overlap values may be a factor of 2 too large. Taking this reduction into consideration, the overlap values computed from equation (30) are roughly within a factor of 2 of the exact overlap values (see table VI). It appears, therefore, that even at small pool diameters, absorption by interconal gases is not negligible and may considerably diminish the intensity of radiation fed back to the fuel.

From the figures of appendix D, it can be seen that the regions of maximum overlap for the fuels occur near 4.5μ and 2.5μ. The 3.5μ, 6μ and 7μ regions are next in importance.

From equation (10), dz/dt is empirically related to $\Delta H_c/\Delta H_v$ and $\epsilon = 1 - e^{-\gamma d}$. Because dz/dt is related to the overlap, it would be expected that the overlap would increase with increasing $\Delta H_c/\Delta H_v$ and ϵ. Atallah and Allan[21] list values of γ for a variety of fuels, as obtained from other references.[10,20] These values of γ are given here in table VII. From these values of γ, and using $d = 10$ cm (typical for the flames considered here), overlap values were computed from equation (32) using appropriate values of the flame properties (listed in appendix A). These computed overlap values are also given in table VII, along with the exact overlap (for 2μ to 6μ). The computed values are roughly seven times too large. This factor may be reduced somewhat due to absorption by interconal gases. Nevertheless, equation (30) is a somewhat better approximation to the exact overlap than is equation (32).

VI. CONCLUSIONS.

Heat transfer from a flame to its unburned fuel by all three transfer processes (convection, radiation, and conduction) is considered. The contribution by each mechanism is discussed for different sizes and shapes of the fuel. The radiative transfer process is discussed in detail for flame sizes in which it predominates. The effects of incandescence, luminescence, flame temperature and shape, absorption of radiation by interconal gases, surface reflectivity, and absorption in the bulk of the fuel are discussed. The relation between the heat transfer rate and the burning rate is shown. Criteria are established for effective transfer of heat from the flame to its unburned fuel. The roles of the absorption and emission coefficients in the heat transfer process are

Table VII. Comparison of O_v and Equation 32

Fuel	γ(cm^{-1})*	O_v, from eq 32	Exact O_v (2μ-6μ)
Benzene	0.026	5.86×10^{-1}	1.49×10^{-1}
Hexane	0.019	2.31×10^{-1}	3.37×10^{-2}
Methanol	0.046	2.68×10^{-1}	2.89×10^{-2}
UDMH	0.025	—	1.78×10^{-1}

*From Atallah, S., and Allan, D. S. Safe Separation Distances from Liquid Fuel Fires. Fire Technology Vol. 7, 47 (1971).

described. The radiation intensity is discussed as a function of position in the flame, as are the dependences on mixture ratios of fuel to oxidizer, and the pressure of the surrounding atmosphere.

Average absorption coefficients over 2μ to 6μ, 2μ to 13μ, and 2μ to 15μ are determined for 17 fuels. The average emission intensities are evaluated for 14 fuels over 2μ to 6μ, 10 fuels over 2μ to 13μ, and 9 fuels over 2μ to 15μ. A ranking of fuels according to their average emission intensities is equivalent to ranking them by the intensity of the radiation they emit. Thus, in order of decreasing average emission intensity, as obtained over 2μ to 6μ, the fuels are: methanol, hexane, cyclohexane, methylhydrazine, benzene, unsymmetrical dimethylhydrazine, acetone, Napalm Test Solvent, ammonia, carbon monoxide, methane, propane, hydrazine, and carbonyl sulfide.

Average overlap values, the product of the average absorption coefficient, and the average emission fraction, are computed over 2μ to 6μ for 14 fuels, 2μ to 13μ for 10 fuels, and 2μ to 15μ for 9 fuels. The exact overlap values are computed for 14 fuels by obtaining the product of the absorption coefficient and the emission intensity point by point throughout the spectrum, and integrating over each of the wavelength regions mentioned above. In decreasing order or importance, the regions of maximum overlap occur near 4.5μ, 2.5μ, 3.5μ, 6μ and 7μ. In order of decreasing exact overlap for the 2μ to 6μ region, the fuels are: unsymmetrical dimethylhydrazine, benzene, methylhydrazine, cyclohexane, hexane, methanol, Napalm Test Solvent, hydrazine, carbonyl sulfide, ammonia, carbon monoxide, acetone, propane, and methane. The average overlap values do not agree with the exact overlap values. They are, however, accurate to within an order of magnitude. The ranking of fuels by average overlap does not agree with the ranking by exact overlap values. It appears that the graybody approximations heretofore used in the calculation of radiation transfer are rather poor, and that the specific absorption and emission spectra must be taken into consideration.

That fraction $\langle f_\alpha ' \rangle$, of the flame intensity that is absorbed by the fuel is the exact overlap divided by the average emission intensity. In order of decreasing $\langle f_\alpha ' \rangle$ for the 2μ to 6μ region, the fuels are: unsymmetrical dimethylhydrazine, benzene, methylhydrazine, cyclohexane, Napalm Test Solvent, hexane, methanol, carbonyl sulfide, hydrazine, ammonia, carbon monoxide, propane, acetone, and methane.

The overlap values and their calculation are important in heat transfer processes because it is by this mechanism that radiative heat is transferred from a flame to a target. In the present situation, the overlap values are a measure of the transfer of heat from a flame to its unburned fuel. If the flame shape and temperature were invariant from fuel to fuel, then overlap would be the predominant factor in the radiative heat transfer process. As such, it would be an underlying factor responsible for the variation of flame properties from fuel to fuel.

The exact overlap is shown to be closely related to the total radiation intensity absorbed by the bulk of the fuel. They are related through the surface reflectivity, r, of the fuel. For small values of r (as is the present case), the total radiation intensity absorbed by the bulk of the fuel is closely approximated by the exact overlap values. From a comparison of the derived expressions for the overlap and the measured values, it appears that absorption by interconal gases is not negligible, even for relatively small diameter pools.

The emission spectra of hydrocarbons are primarily a result of emission by carbon dioxide and water vapor (reaction products of compute combustion), whose most intense bands lie near 2μ and 4.5μ. To increase overlap, the absorption spectra could be modified to provide additional absorption bands in these two regions. This can be accomplished, perhaps, by appropriate additives.

31
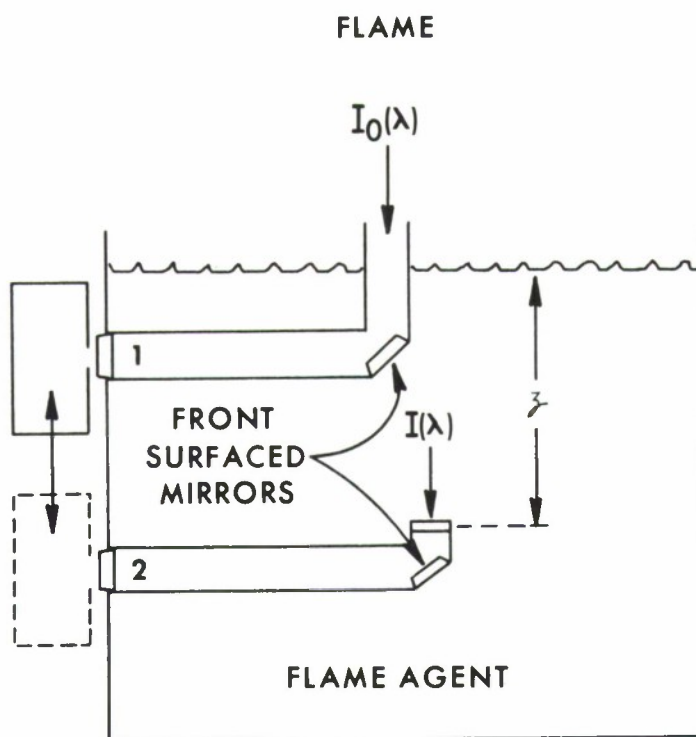
FLAME

Figure 8. Proposed Experimental Apparatus

VII. RECOMMENDATIONS.

It is recommended that the investigation of radiation heat transfer between a flame and its unburned fuel be continued on an experimental basis. The experimental setup in figure 8 is suggested. Of the radiation $I_0(\lambda)$ incident upon the surface of the fuel, a fraction—preferably sampled from the center of the surface of the agent—is transmitted, without substantial loss, to the entrance slit of a spectrophotometer (at position 1). The spectrophotometer should be capable of spanning about 1μ to 15μ. A second, similar, light tube transmits the intensity $I(\lambda)$, at a known depth z, to position 2. The spectrophotometer is then lowered to that position to measure $I(\lambda)$. This process provides a means of measuring the intensity $I_0(\lambda)$ of radiation incident at the surface of the fuel. From $I_0(\lambda) - I(\lambda)$, the intensity absorbed by the fuel can be found. This method allows for absorption by interconal gases and could be extended to measure overlap from flames of any desired size.

LITERATURE CITED

1. Ryan, L. R., Penzias, G. J., and Tourin, R. H. Ohio State University. Scientific Report 1. Contract AF19(604)-6106, ARPA Order No. 6-58. An Atlas of Infrared Spectra of Flames. Part One. Infrared Spectra of Hydrocarbon Flames in the $1-5\mu$ Region. July 1961. UNCLASSIFIED Report.

2. Penzias, G. J., Gillman, S., Liang, E. T., and Tourin, R. H. Ohio State University. Scientific Report 3. Contract AF19(604)-6106, ARPA Order No. 6-58. An Atlas of Infrared Spectra of Flames. Part Two. Hydrocarbon-Oxygen Flames $4-15\mu$, Ammonia-Oxygen $1-15\mu$, Hydrazine-Oxygen $1-5\mu$, and Flames Burning at Reduced Pressures. October 1961. UNCLASSIFIED Report.

3. Rein, R. G., Welker, J. R., and Sliepcevich, C. M. University of Oklahoma Research Institute. Ninth Quarterly Progress Report. OURI-1578-QPR-9. Contract DAAA-15-67-C-0074. Susceptibility of Potential Target Components to Defeat by Thermal Action. January 1969. UNCLASSIFIED Report.

4. Kelley, C. S. EATR 4436. The Use of Spatially-Separated, Series-Linked Thermocouples in Flame Evaluation. August 1970. UNCLASSIFIED Report.

5. Brown, R. E., Garfinkle, D. R., and Andersen, W. H. Shock Hydrodynamics, Inc. Final Report SHI-6245-3. Contract DAAA-15-69-C-0301. Evaluation Techniques for Flame and Incendiary Agents. June 1970. UNCLASSIFIED Report.

6. Kelley, C. S. EATR 4492. Dependence of Heat Flux (Radiative Plus Convective) from Burning Flame Agents on the Angle from the Flame Symmetry Axis. February 1971. UNCLASSIFIED Report.

7. Dickey, F. P., Gailar, N., Hoffman, J., Yarger, F., and Rogge, W. Ohio State University. Final Report, RF Project 751. Contract AF19(604)2254. A Study of the Infrared Spectra of Flames Using Phase-Discrimination Methods of Detection. July 1960. UNCLASSIFIED Report.

8. Welker, J. R., and Sliepcevich, C. M. University of Oklahoma Research Institute. Twelfth Quarterly Progress Report, OURI-1578-QPR-12. Contract DAAA-15-67-C-0074. Susceptibility of Potential Target Components to Defeat by Thermal Action. September 1969. UNCLASSIFIED Report.

9. Hood, J. D. A Method for the Determination of the Radiative Properties of Flames. Ph.D. Thesis, University of Oklahoma. 1966.

10. Rasbash, D. J., Rogowski, Z. W., and Stark, G. W. V. Properties of Fires of Liquids. Fuel 35, 94 (1956).

11. Carpenter, G. E., Andersen, W. H., Garfinkle, D. R., and Brown, R. E. Shock Hydrodynamics, Inc. First Quarterly Progress Report SHI-6245-1. Contract DAAA-15-69-C-0301. Evaluation Techniques for Flame and Incendiary Agents. May 1969. UNCLASSIFIED Report.

12. Lewis, B., and von Elbe, G. Combustion, Flames and Explosions of Gases. Academic Press, Inc., New York, New York. 1961.

13. Colthup, N. B., Daley, L. H., and Wiberly, S. E. Introduction to Infrared and Raman Spectroscopy. Academic Press, Inc., New York, New York. 1964.

14. Brown, R. E., Andersen, W. H., Garfinkle, D. R., and Zernow, L. Shock Hydrodynamics, Inc. Annual Summary Report SHI-6005-4. Contract DAAA-15-67-C-0172. Evaluation Techniques for Flame and Incendiary Agent. p 46. July 1968. UNCLASSIFIED Report.

15. Kelley, C. S. EATR 4426. A Simplified Expression for Oscillator Strengths of Transitions Between Different Quadratic Modes of a Configuration Coordinate Model. August 1970. UNCLASSIFIED Report.

16. Magnus, G. Tests on Combustion Velocity of Liquid Fuels and Temperature Distribution in Flames and Beneath Surface of the Burning Liquid. Int'l Symposium on the Use of Models in Fire Research. Nat'l. Acad. Sci.—NRC Publ. 786, 76. 1961.

17. Hottel, H. C. Review of 'Certain Laws Governing Diffusive Burning of Liquids'. Fire Research Abstracts and Reviews *1*, 41 (1959).

18. Brown, R. E., Andersen, W. H., Garfinkle, D. R., and Zernow, L. *Op. cit.,* p 52.

19. Burgess, D. S., Grumer, J., and Wolfhard, W. G. Burning Rates of Liquid Fuels in Large and Small Open Trays. Fire Res. Abstr. Rev. *2,* 10 (1960).

20. Burgess, D. S., Strasser, A., and Grumer, J. Diffusive Burning of Liquid Fuels in Open Trays. Fire Res. Abstr. Rev. *3*(3), 91 (1961).

21. Atallah, S., and Allan, D. S. Safe Separation Distances from Liquid Fuel Fires. Fire Technol. *7,* 47 (1971).

22. Belason, B., Castle, G., Crowley, D., and D'Avanzo, L. A Fire Simulation Facility for Materials Response Testing. Fire Technol. *6,* 179 (1970).

23. Kelley, C. S. Optical Absorption of Divalent Chromium in Zinc Sulfide. Appendix A. Ph.D. Thesis, University of Delaware. June 1970.

24. Handbook of Chemistry and Physics. 40th Ed. ed C. D. Hodgman. Chemical Rubber Publishing Company, Cleveland, Ohio. 1959.

25. Chemical Engineers' Handbook. ed J. H. Perry. 4th Ed. McGraw-Hill Book Company, New York, New York. 1961.

26. Catalog of the Infrared Spectra of the American Petroleum Institute. Research Project 44. Petroleum Research Laboratory, Texas A&M, College Station, Texas. 1970.

27. Sadtler Standard Spectra, Sadtler Research Laboratories, Philadelphia, Pennsylvania.

28. Pierson, R. H., Fletcher, A. N., and Gantz, E. St. C. Catalog of Infrared Spectra for Qualitative Analysis of Gases. Anal. Chem. *28,* 1218-1239 (1956).

29. Andrews, D. A., Hurtubise, F. G., and Krassig, H. The Presence of Monothiocarbonate Substituents in Cellulose Xanthates. Can. J. Chem. *38,* 1381-1398 (1960).

30. Welker, J. R., and Sliepcevich, C. M. University of Oklahoma Research Institute. Final Report, OURI-1604-FR. Grant DA-AMC-035-95(A). October 1968. UNCLASSFIED Report.

31. Kahrs, J., and Burgess, D. CRDL Special Publication 6-1. Field Calorimetry/ Chemical Studies. Proceedings of the Third Flame-Incendiary Conference. August 1965. UNCLASSIFIED Report.

32. Bell, E. E., Burnside, P. B., Cermak, W. C., and Dam, C. F. Ohio State University Research Foundation. Final Report. Contract AF 30 (602)-1047. A Study of Infrared Emission from Flame. Part I. June 1955. UNCLASSIFIED Report.

33. Penzias, G. J. The Warner and Swasey Company. Contract NONR 3657 (00), ARPA Order No. 237-62. An Atlas of Infrared Spectra of Flames. Part Four. Additional Nitrogenous Liquid Fuels and Oxidizers. October 1964. UNCLASSIFIED Report.

34. Bell, E. E., Burnside, P. B., Dickey, F. P., Kopczynski, S. L., and Rowntree, R. F. The Ohio State University Research Foundation. Final Report. Contract AF 30(602)-1047. A Study of Infrared Emission from Flames. September 1956. UNCLASSIFIED Report.

35. Klaubert, E. C. Block Engineering, Inc. Final Technical Report. Contract DA-18-035-AMC-262(A). Field Calorimetry/IR Instrumentation. December 1965. UNCLASSIFIED Report.

BLANK

APPENDIXES

BLANK

APPENDIX A

PROPERTIES OF FUELS

The following tables list various properties of fuels. They include those properties that may be of interest to a researcher working with flame investigations. The information was culled from several references (see section IV of text).

Table A-I. Molecular Weights and Melting and Boiling Points of Fuels

Common name	Approved name	Formula	Mole wt	mp	bp
			gm	°C	
Methanol	Methanol	CH_3OH	32.0	−97.8	64.65
Hexane	Hexane	C_6H_{14}	86.2	94.3	69.0
Cyclohexane	Cyclohexane	$(CH_2)_6$	82.1	6.5	81.4
Benzene	Benzene	C_6H_6	78.1	5.51	80.1
Octane	Octane	$CH_3(CH_2)_6CH_3$	114.2	−56.5	125.8
Acetone	2-propanone	CH_3COCH_3	58.1	−95	56.5
Ammonia	Ammonia	NH_3	17.0	−77.7	−33.35
Hydrazine	Hydrazine	$(NH_2)_2$	32.0	1.4	113.5
Heptane	Heptane	$CH_3(CH_2)_5CH_3$	100.2	90.5	98.427
Isooctane	2,2,4-Trimethyl pentane	$(CH_3)_3CCH_2CH(CH_3)_2$	114.2	−107.4	99.3
TEA	Triethylaluminum	$Al_2(C_2H_5)_6$	228.3	−45.5	186.6
NTS	Napalm Test Solvent	a	93.2[b]	−	−
CO	Carbon monoxide	CO	28.0	−207	−190
Propane	Propane	$CH_3CH_2CH_3$	44.1	−189.9	−42.17
Methane	Methane	CH_4	16.0	−184	−161.5
UDMH	1,2-Dimethyl hydrazine	$CH_3(NH_2)_2CH_3$	62.1	−	81
MMH	Methylhydrazine	CH_3NHNH_2	46.1	<−80	87.5
COS	Carbonyl sulfide	COS	60.1	−138	−50.2

[a]Percentages by weight of constituents: 57% heptane, 20% cyclohexane, 18% benzene, 5% 2,2,4-trimethyl pentane.
[b]Estimated from percentages of constituents.

Table A-II. Density, Surface Tension, Specific Heat, and Thermal Conductivity of Fuels

Common name	Density	Surface tension	Specific heat at 20°	Thermal conductivity (for a temp gradient of $1°C\ cm^{-1}$ at $20°C$, in units of 10^{-4})
	$gm\text{-}cm^{-3}$	$dyne\text{-}cm^{-1}$	$cal\text{-}gm^{-1}\text{-}°C^{-1}$	$cal\text{-}cm^{-2}\text{-}sec^{-1}$
Methanol	0.7961	22.61	0.600	4.832
Hexane	0.6603	18.43	0.660	3.287
Cyclohexane	0.7791	25.5	—	3.5
Benzene	0.8790	28.85	0.406	3.780
Octane	0.7036	21.8	0.578	3.469
Acetone	0.792	23.70	0.528	4.543
Ammonia	0.7710	23.4 (11.1°C)	0.5232	1.198
Hydrazine	1.011	91.5 (25°C)	—	—
Heptane	0.6838	—	0.490	3.354
Isooctane	0.6918	—	—	—
TEA	0.8324	—	—	—
NTS	0.7384*	—	—	—
CO	1.250	—	0.248	5.58
Propane	2.0096	—	0.576 (0°C)	0.359
Methane	0.7168	—	0.544	7.23
UDMH	0.8274	31.6	—	—
COS	2.721	—	—	—

*Estimated from percentages of constituents.

40

Table A-lll. Vapor Pressure, Heats of Combustion and Vaporization,
and Regression Rates of Fuels

Common name	Temp where vapor pressure is 100mm Hg	Heat of combustion ΔH_c	Heat of vaporization ΔH_v	Regression rate, dz/dt
	$°C$	$Kcal\text{-}gm^{-1}$	$cal\text{-}gm^{-1}$	$cm\text{-}sec^{-1}$
Methanol	21.2	5.17	262.8	1.7×10^{-3}
Hexane	15.8	11.5	87.3	2.3×10^{-3}
Cyclohexane	25.5	11.1	85.4	2.1×10^{-3}
Benzene	26.1	12.6	94.3	$\begin{cases} 4.8 \times 10^{-3} \text{ [a]} \\ 8.0 \times 10^{-3} \text{ [b]} \end{cases}$
Octane	65.7	11.11	80.0	–
Acetone	7.7	7.38	124.5	–
Ammonia	−68.4	–	327.1 (at bp)	–
Heptane	41.8	11.5	75.4	–
Isooctane	58.3	–	64.9	–
TEA	139	10.2	~65	2×10^{-3} [c]
NTS	–	–	80.3[d]	1.7×10^{-3}
CO	−205.7	–	50.4	–
Propane	−79.6	11.1	83.4	–
Methane	−181.4	11.95	138	–
COS	−85.9	–	–	–

[a]Pan diameter = 15.2 cm. *From* Brown, R. E., Andersen, W. H., Garfinkle, D. R., and Zernow, L. Shock Hydrodynamics, Inc. Annual Summary Report SHl-6005-4. Contract DAAA-15-67-C-0172. Evaluation Techniques for Flame and Incendiary Agent. p 46. July 1968. UNCLASSIFIED Report.

[b]Pan diameter = 30 cm. *From* Rasbash, D. J., Rogowski, Z. W., and Stark, G. W. V. Properties of Fires of Liquids. Fuel *35*, 94 (1956).

[c]Pan 6 by 2 inches. *From* Brown, Andersen, Garfinkle, and Zernow, op. cit.

[d]Estimated from percentages of constituents.

Table A-IV. Flame Temperature, $\Delta H_c/\Delta H_v$, Heat of Reaction,
and Stoichiometrie Mixture of Fuels

Common name	Temp T_f	$\Delta H_c/\Delta H_v$	Heat of reaction at 25°C	Stoiehiometrie mixture
	°C		Kcal-mole^{-1}	vol %
Methanol	—	19.7	173.65	12.28
Hexane	2258	132	995.01	2.16
Cyclohexane	2269	130	936.88	2.27
Benzene	2266	133	780.98	2.71
Octane	2003	139	1307.53	1.65
Acetone	—	59.2	427.79	4.97
Ammonia	$\gtrsim$1850	—	—	21.81
Heptane	—	153	1151.27	1.87
Isooctane	—	—	—	1.65
TEA	—	~160	2345	—
NTS	—	—	1049.55*	—
CO	—	—	—	29.50
Propane	—	133	49.3	4.02
Methane	—	86.8	193	9.47

*Estimated from percentages of constituents, taking heat of reaction of isooctane as that of octane.

Table A-V. Flammability Limits, Spontaneous Ignition Temperature, Adiabatie Flame
Temperature, and Flame Speed of Fuels

Common name	Flammability limits		Spontaneous ignition temp	Adiabatie flame temp at U_f	Max flame speed U_f
	Lean	Rieh			
	% stoichiometric		°C		cm-sec^{-1}
Methanol	48	408	469	—	49
Hexane	51	400	261	2221	40
Cyelohexane	48	401	270	—	40
Benzene	43	336	592	2288	40
Oetane	51	425	240	—	—
Acetone	59	233	561	2105	46
Ammonia	—	—	651	—	—
Heptane	53	450	247	2196	40
Isooetane	48	360	447	2216	34
CO	34	676	609	—	40
Propane	51	283	504	2232	40
Methane	46	164	632	2219	34

APPENDIX B

ABSORPTION SPECTRA OF FUELS

The non-normalized absorption spectra presented on the following pages were taken from a variety of sources. These references and the procedure for normalization are discussed in section IV of the text.
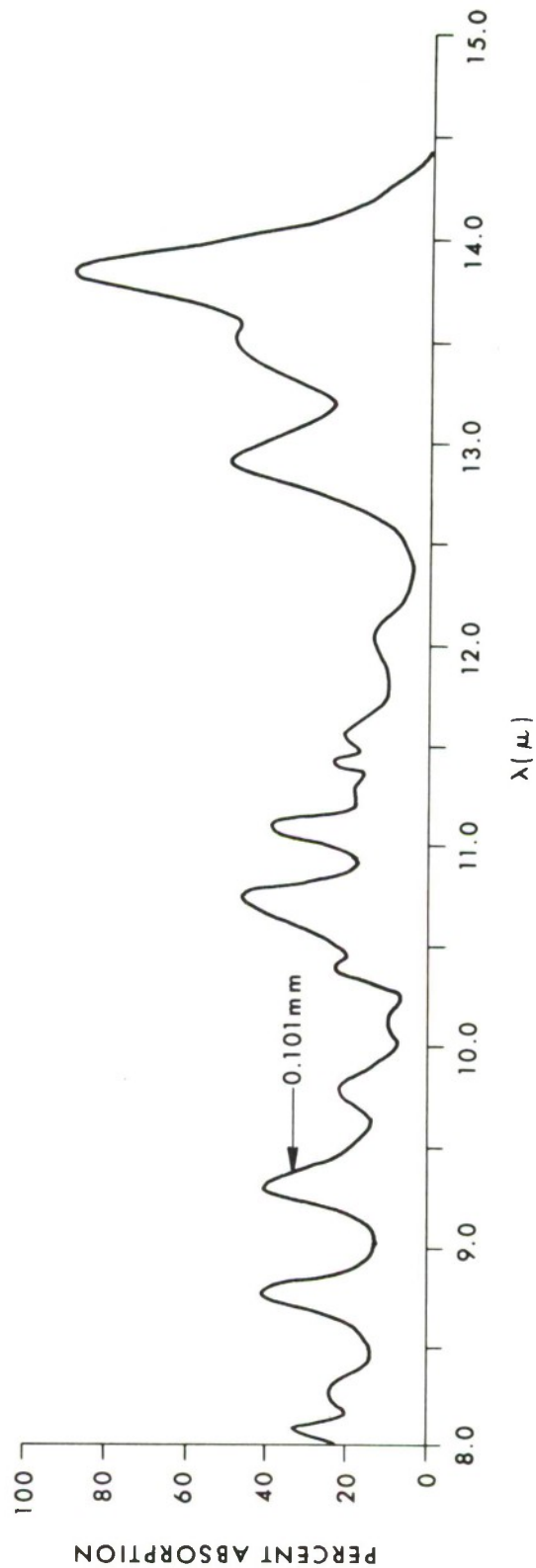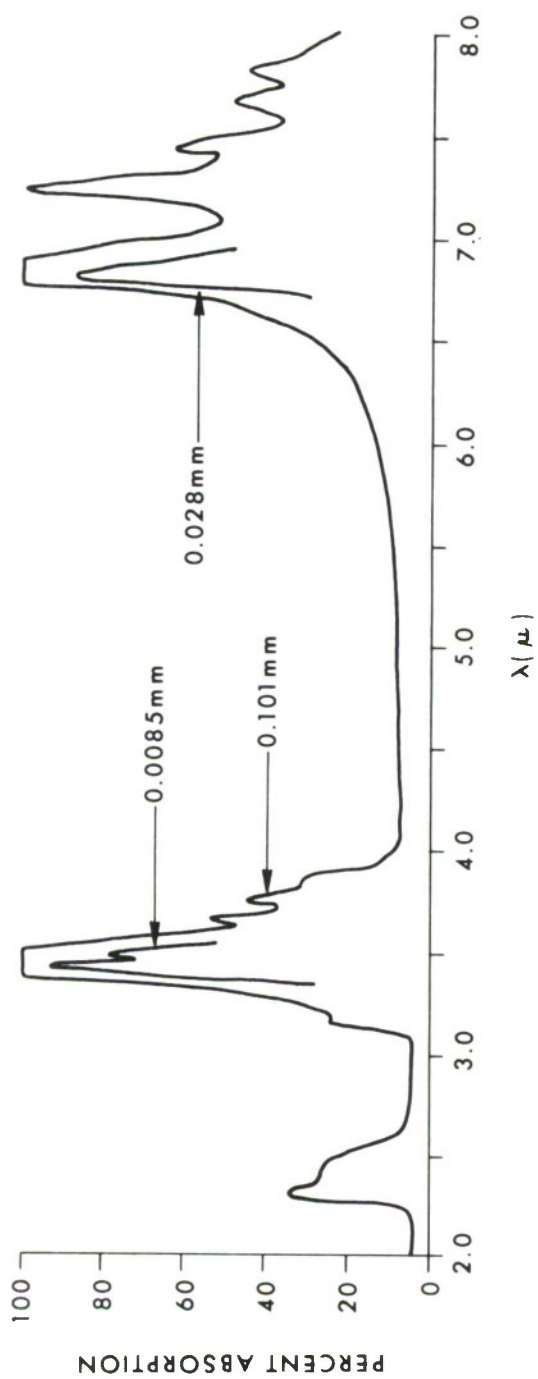
Figure B-1. Absorption Spectrum of Heptane*

Figure B-2. Absorption Spectrum of Isooctane*

*Ibid.
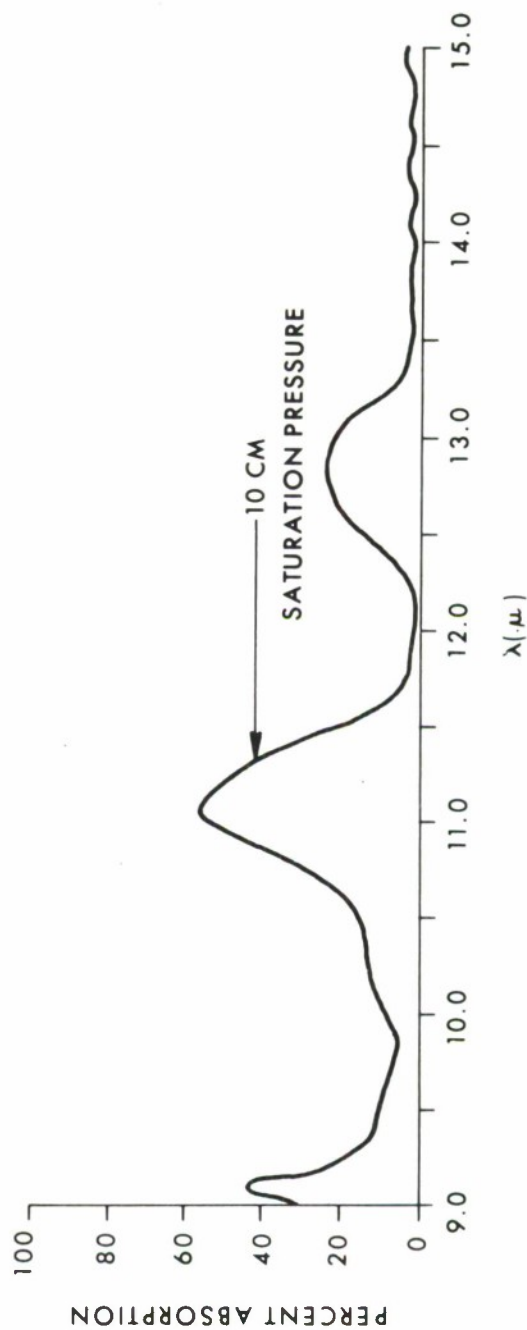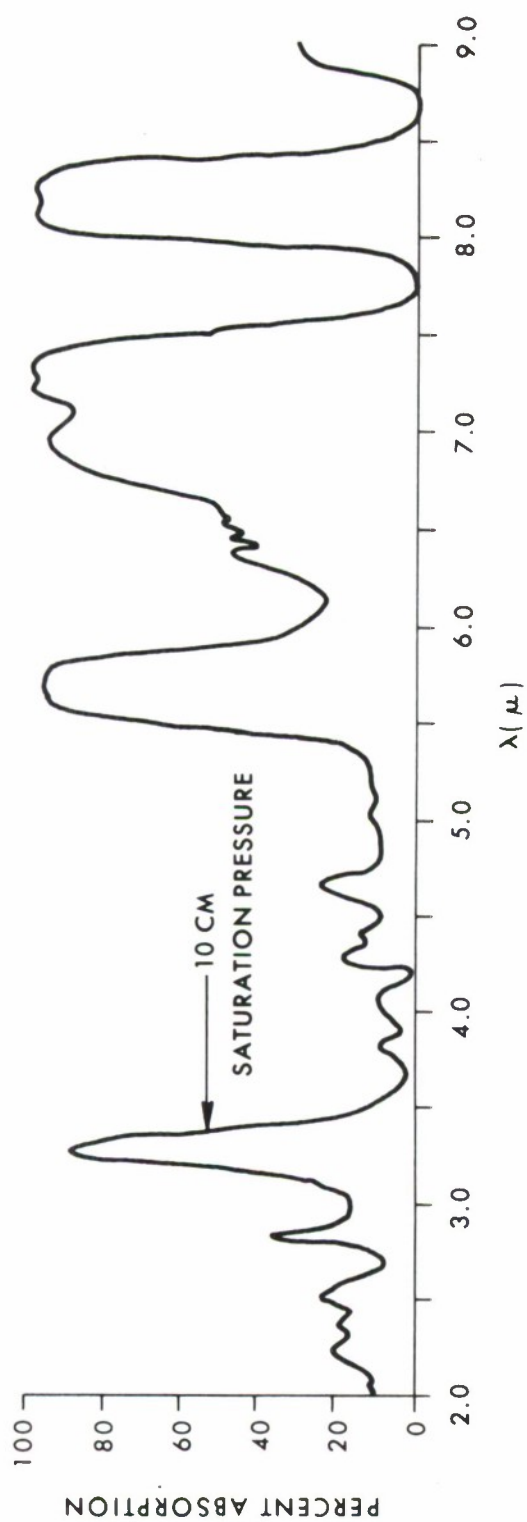
Figure B-3. Absorption Spectrum of Acetone*

*Ibid.
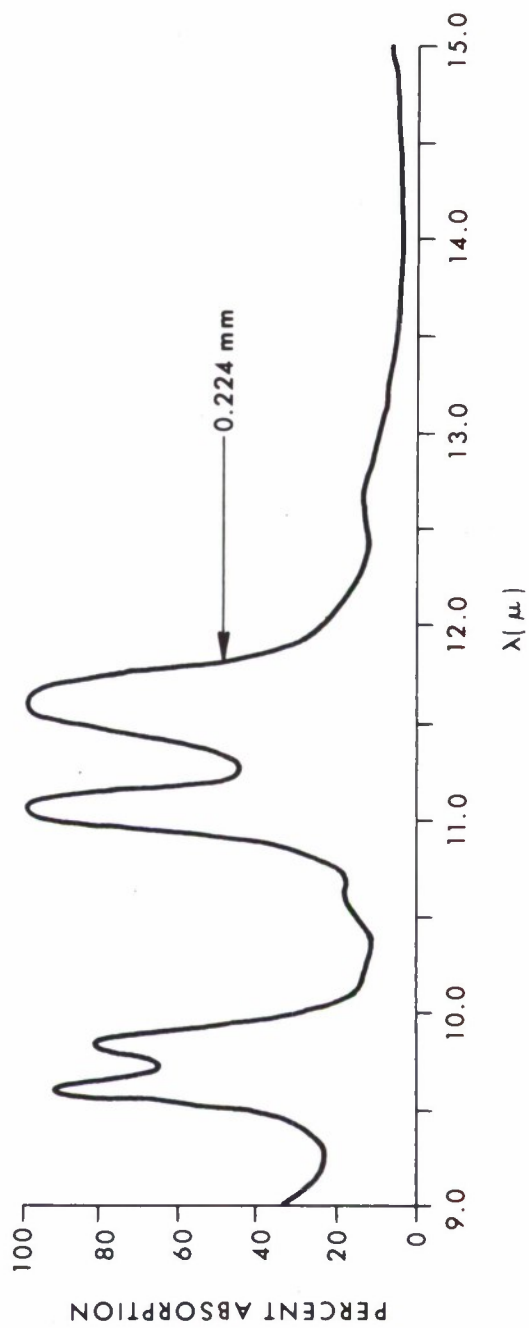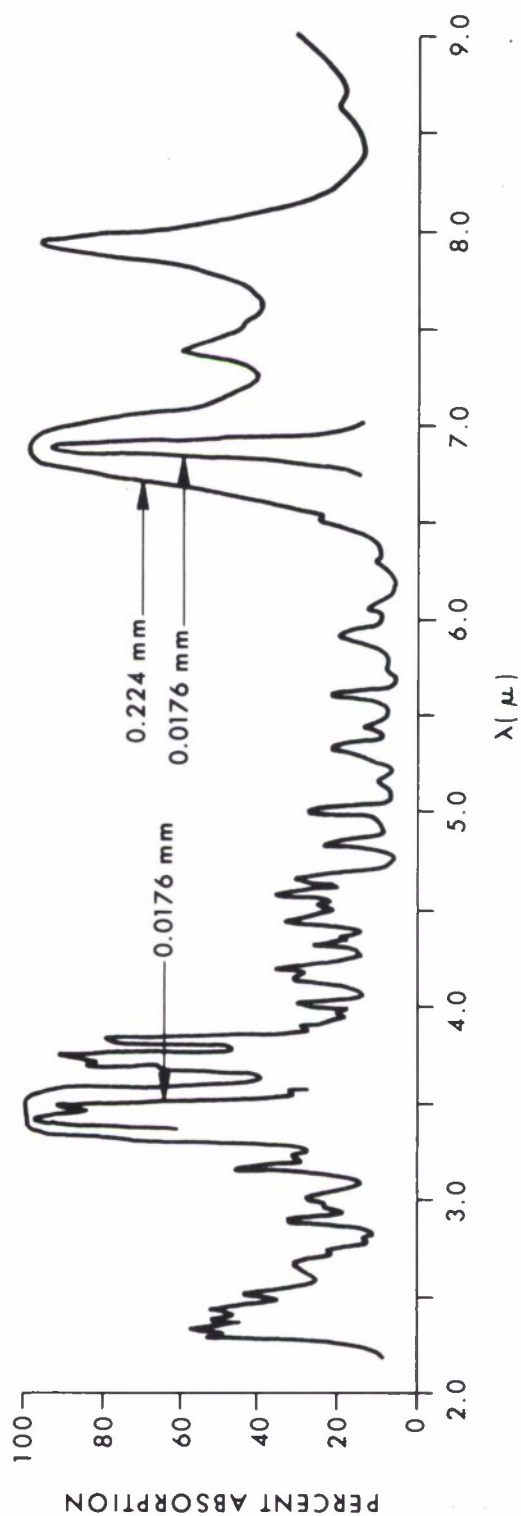
Figure B-4. Absorption Spectrum of Cyclohexane*

*Ibid.
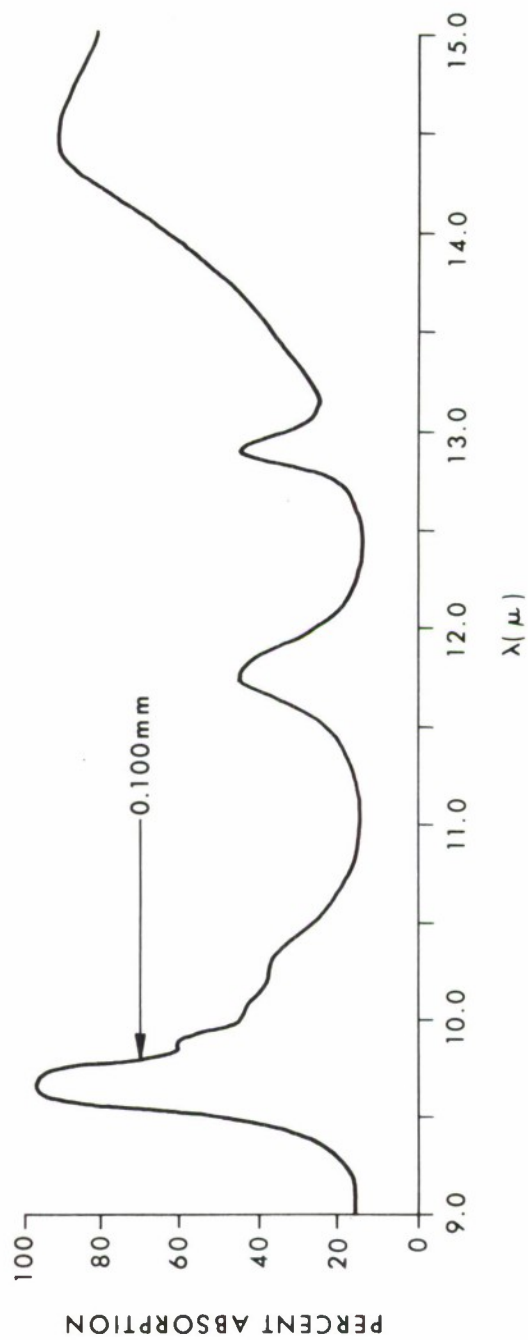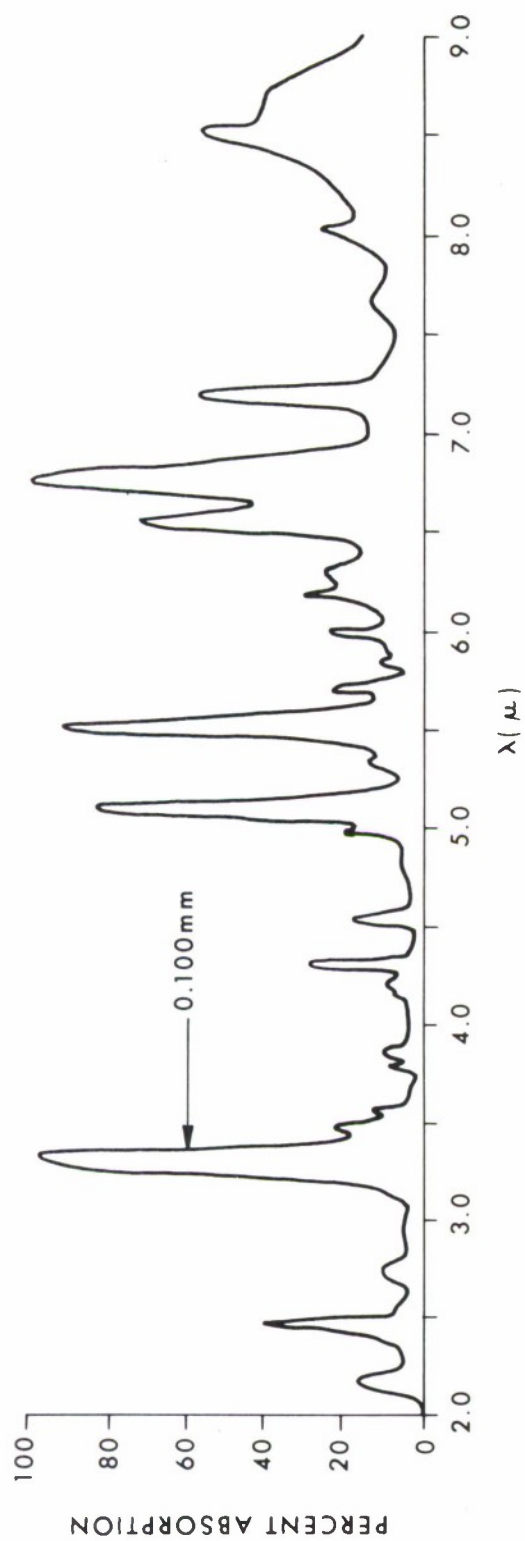
Figure B-5. Absorption Spectrum of Benzene*

*Ibid.
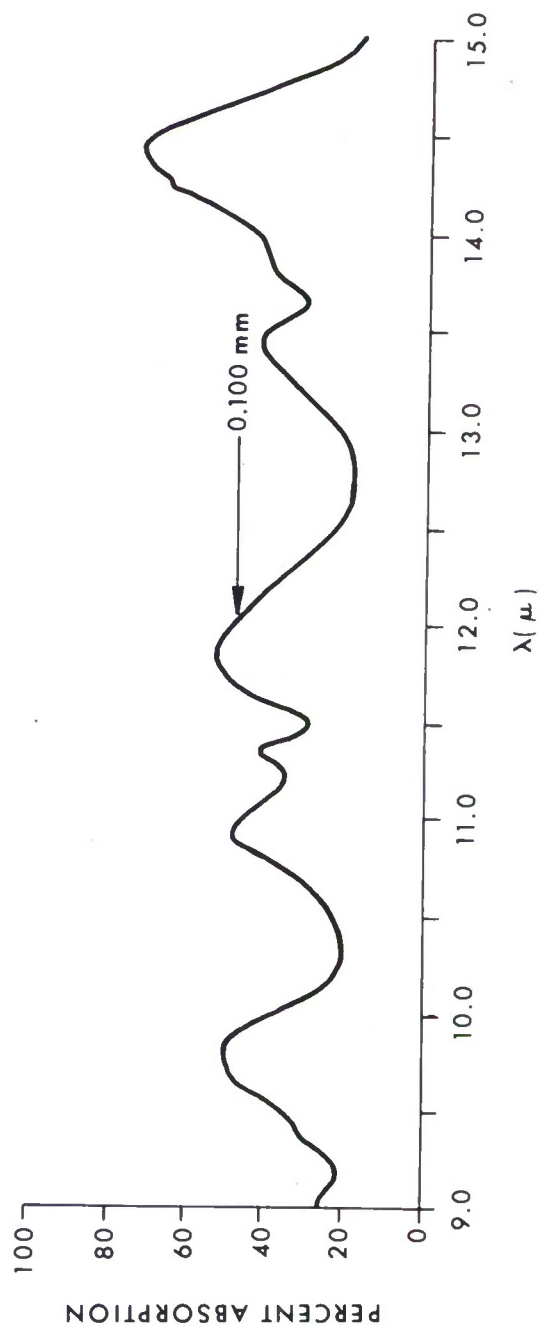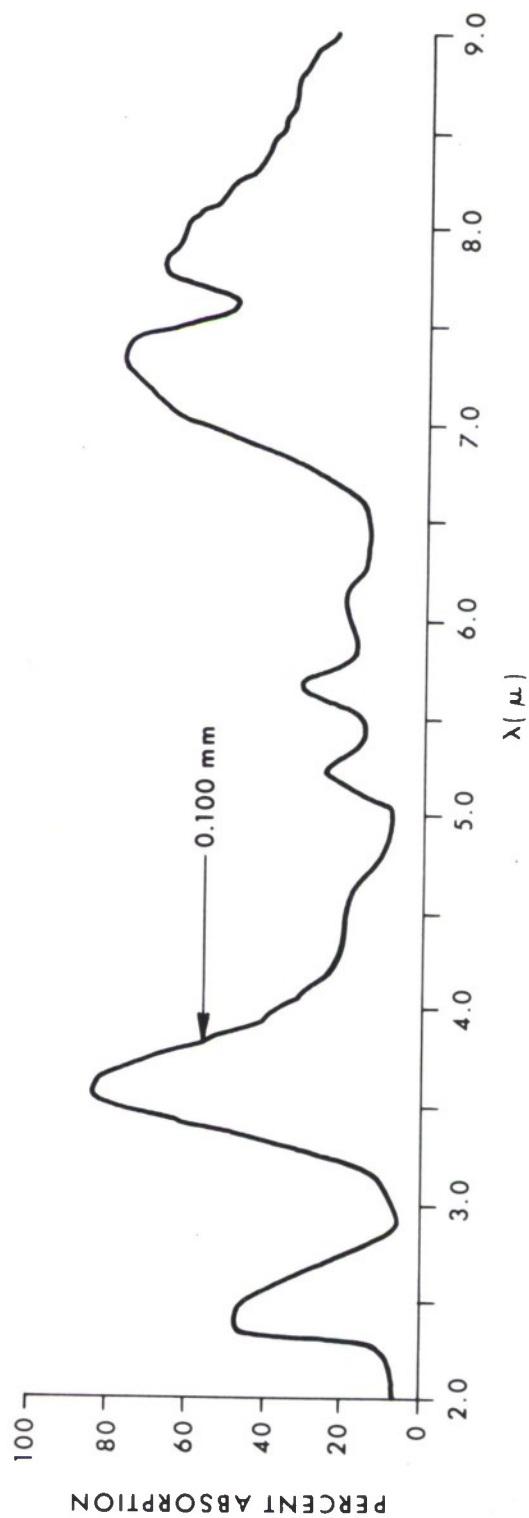
Figure B-6. Absorption Spectrum of Napalm Test Solvent

Appendix B

49
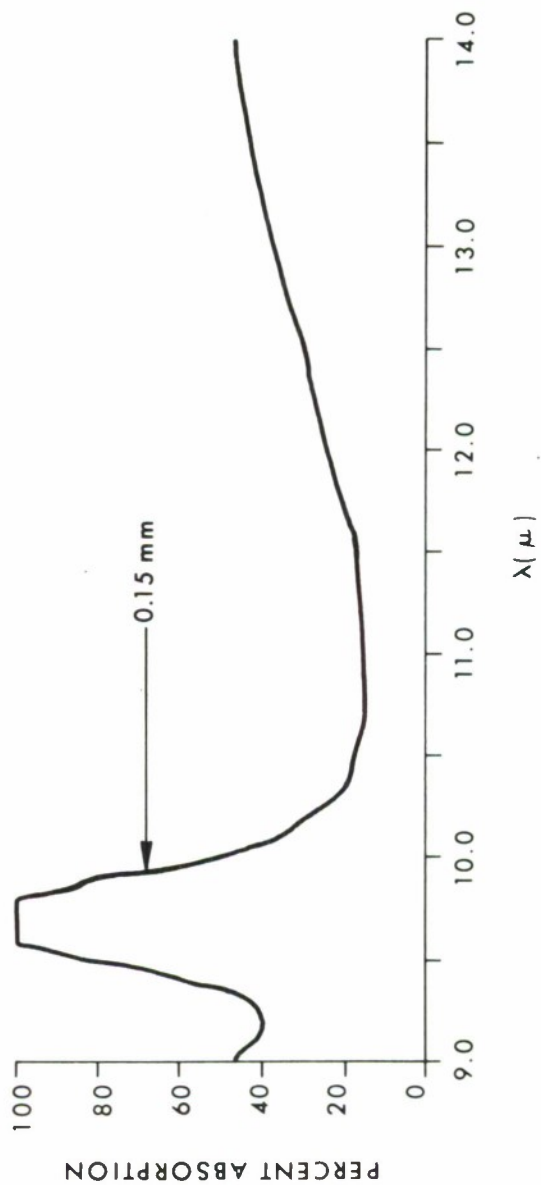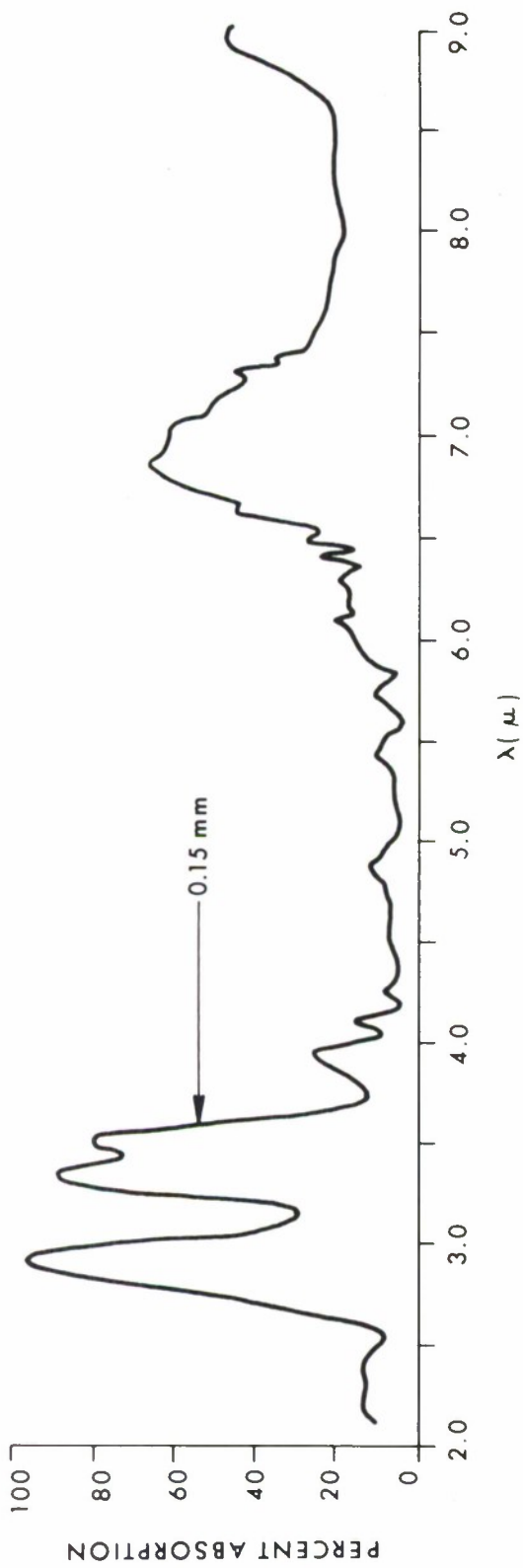
Figure B-7. Absorption Spectrum of Methanol*

*Ibid.
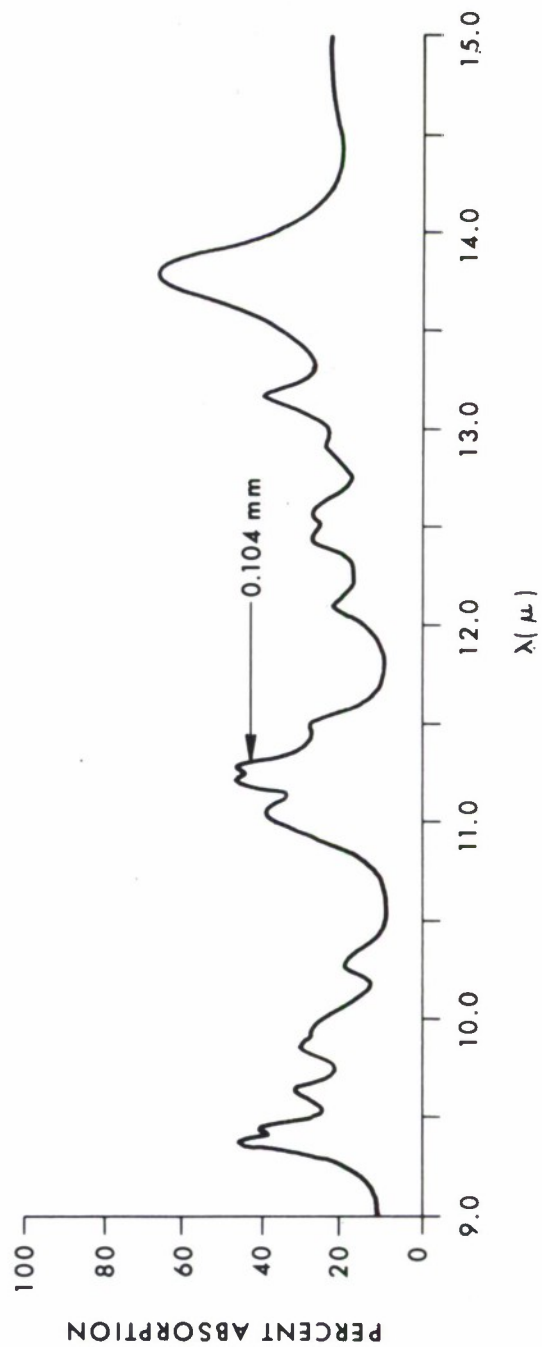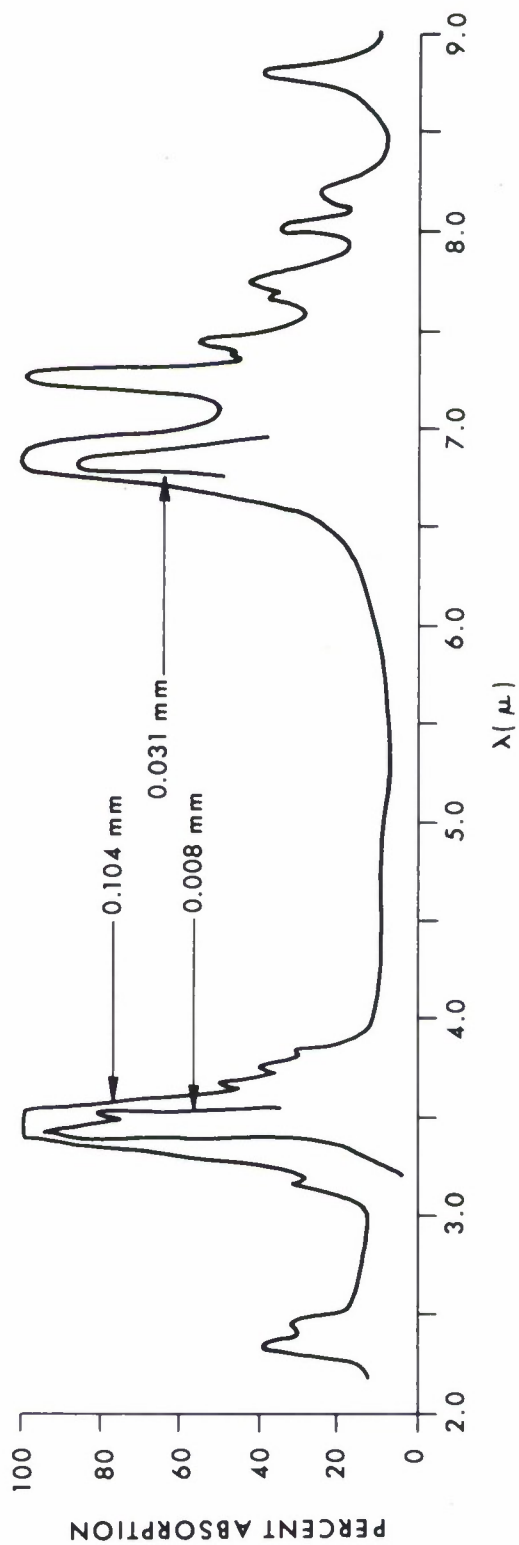
Figure B-8. Absorption Spectrum of Hexane*

*Ibid.

Appendix B

51
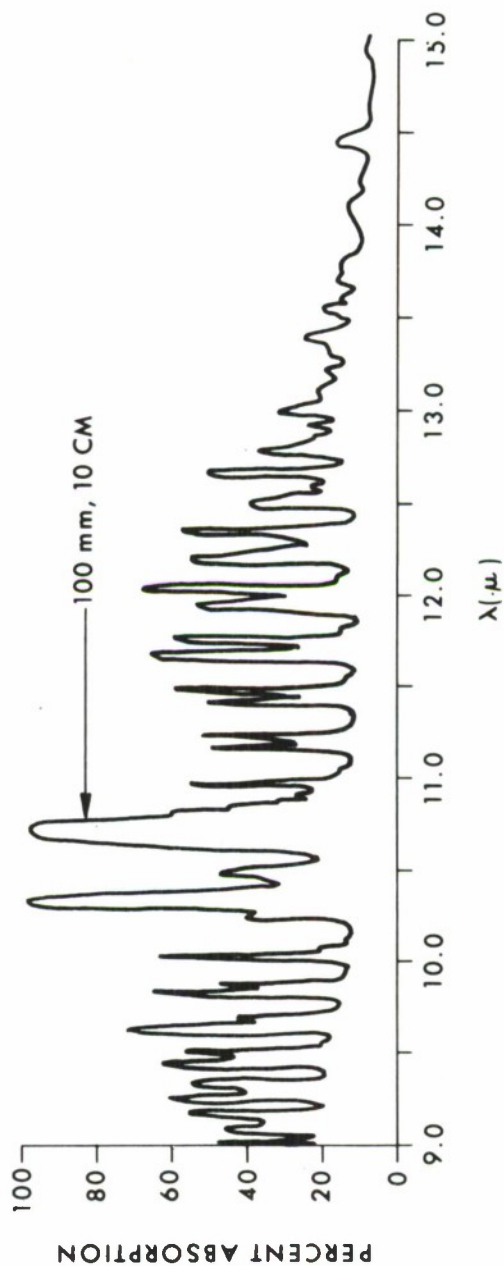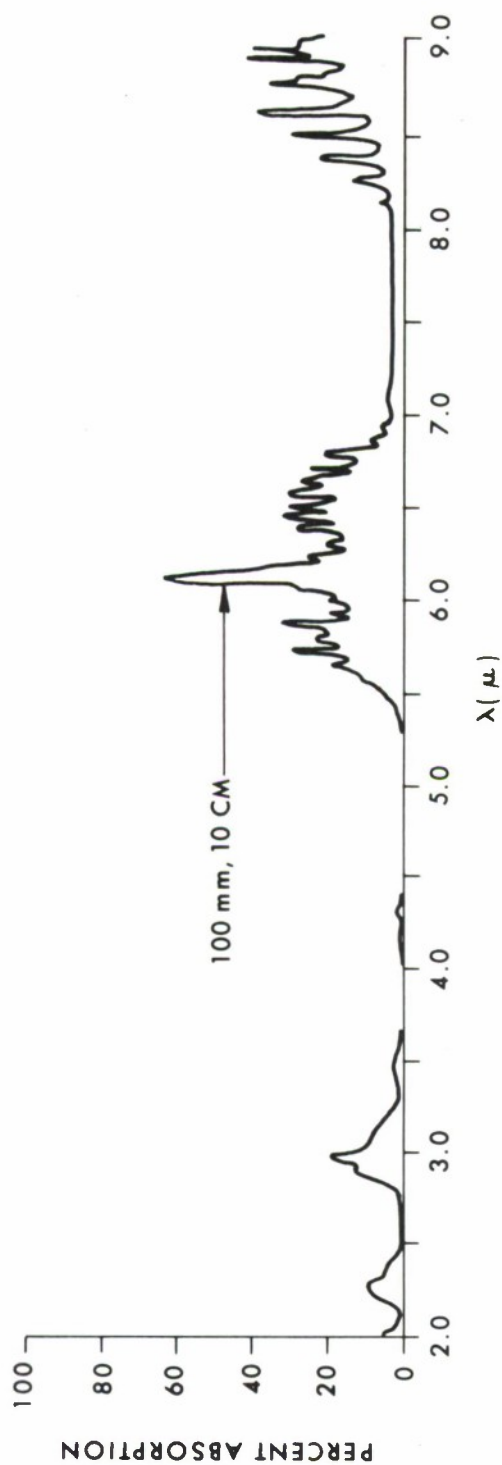
Figure B-9. Absorption Spectrum of Ammonia*

*Ibid.
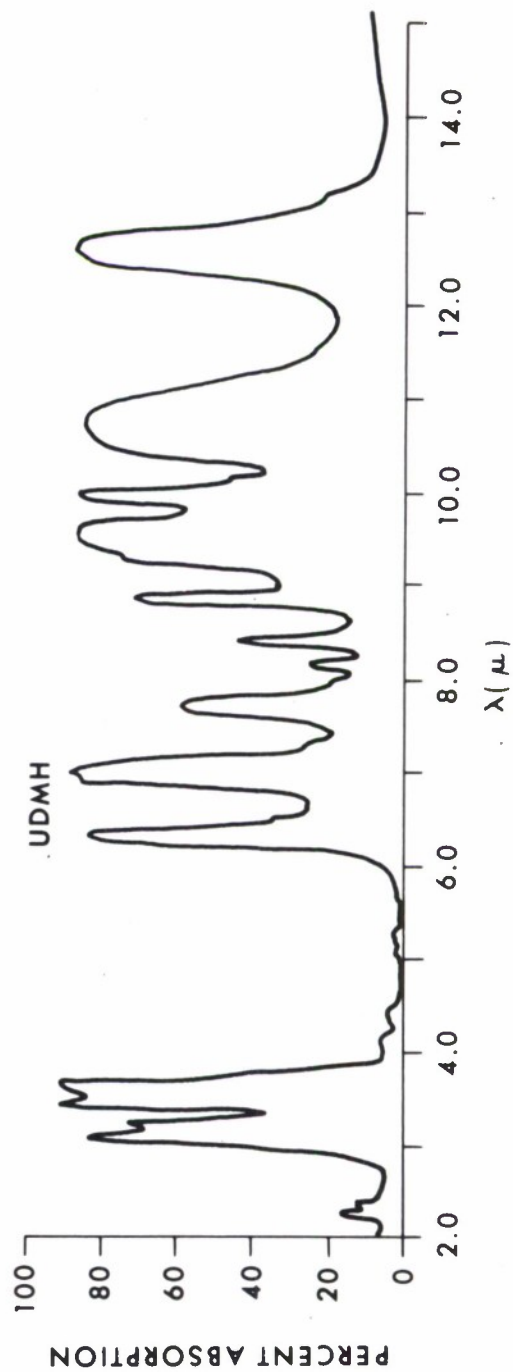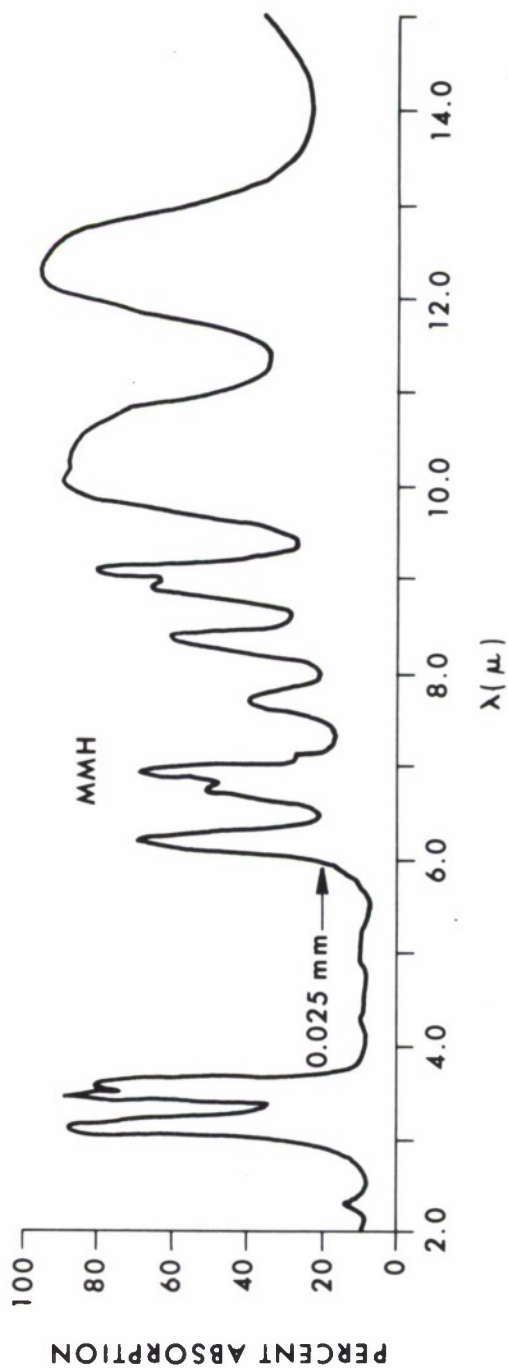
Figure B-10. Absorption Spectra of MMH and UDMH*

*From Pierson, R. H., Fletcher, A. N., and Gantz, E. St. C. Catalog of Infrared Spectra for Qualitative Analysis of Gases. Anal. Chem. 28, 1218-1239 (1956).
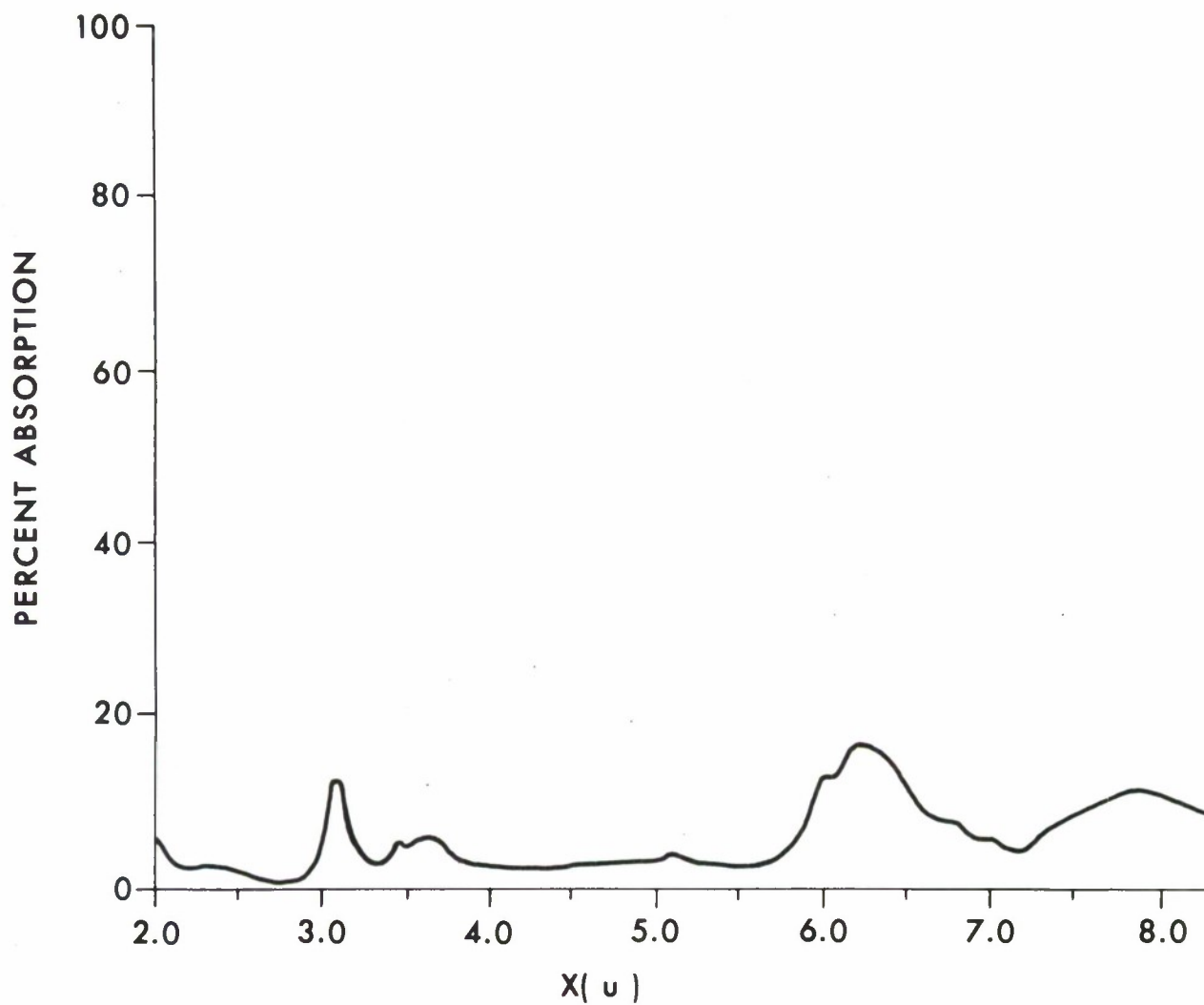
Figure B-11. Absorption Spectrum of Hydrazine*

Ibid.

15 mm, 10CM
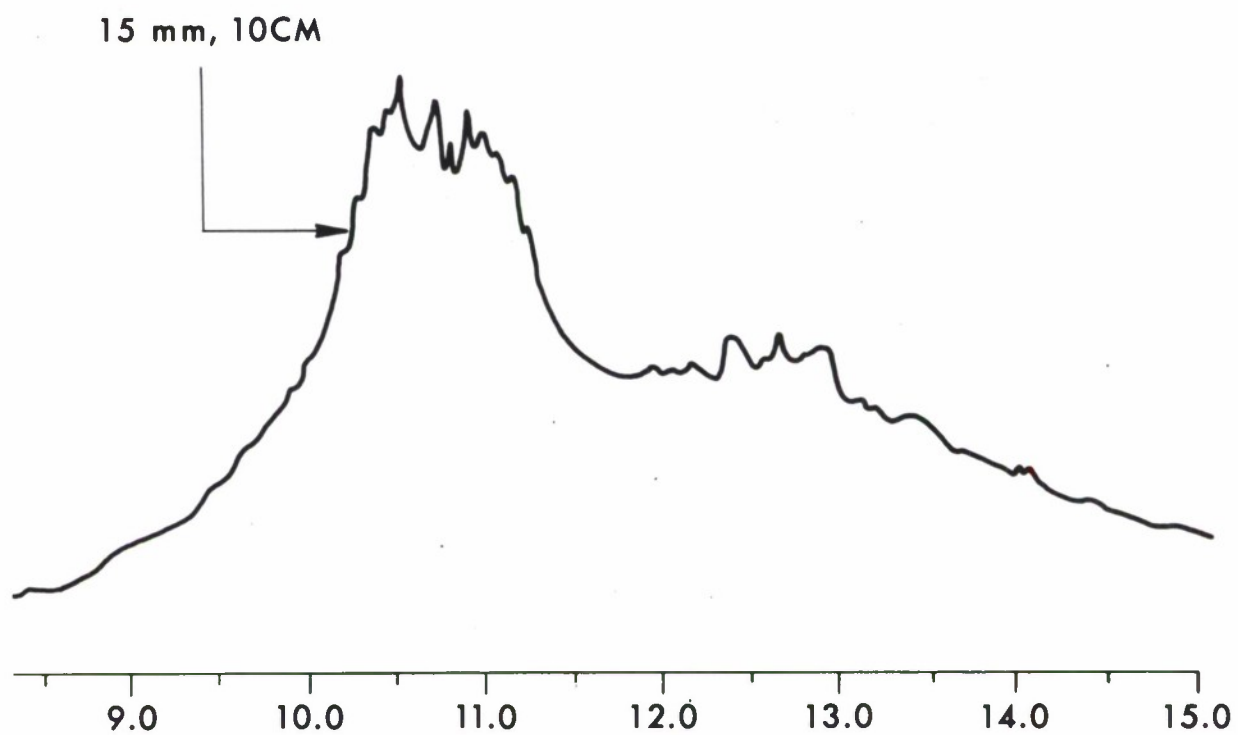
Figure B-11. Continued
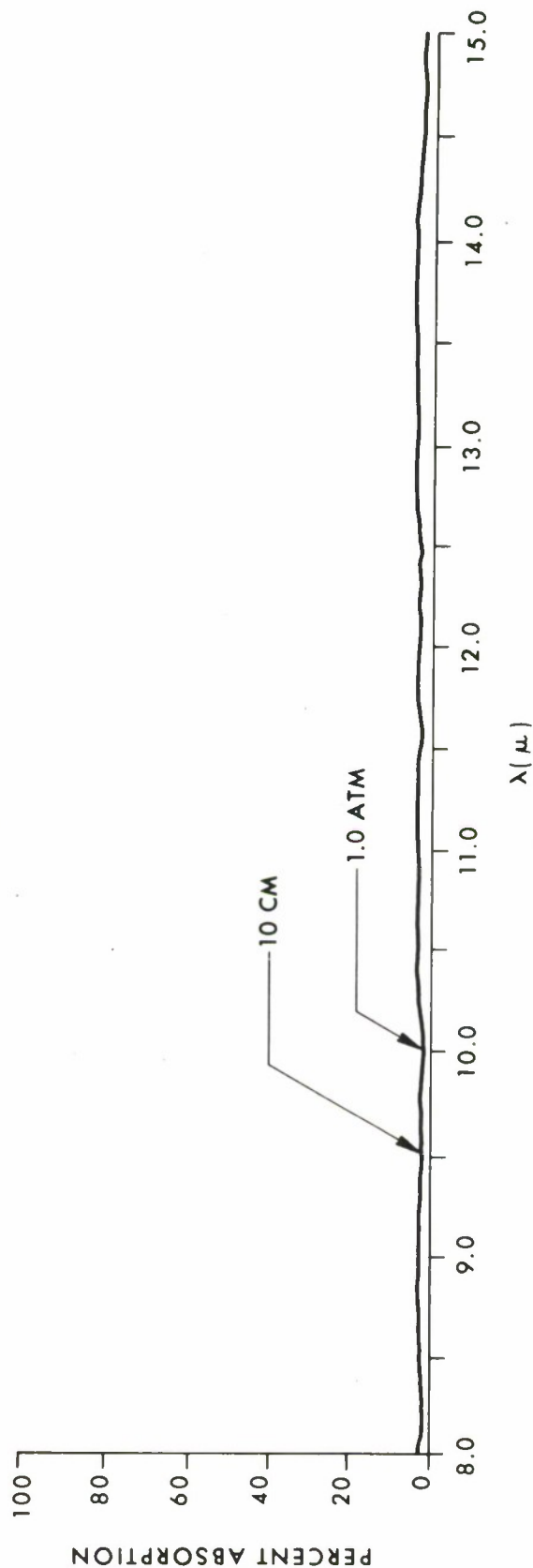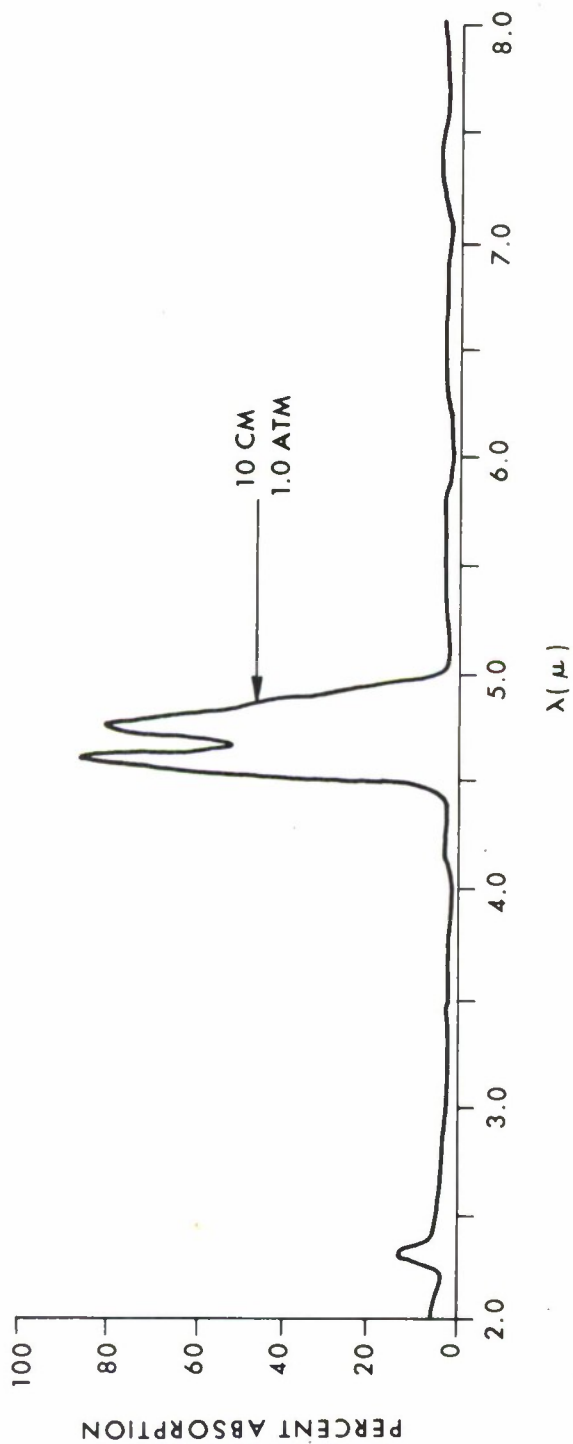
Figure B-12. Absorption Spectrum of Carbon Monoxide*

*From Colthup, N. B., Daley, L. H., and Wiberly, S. E. Introduction to Infrared and Raman Spectroscopy. Academic Press, Inc., New York, New York. 1964.
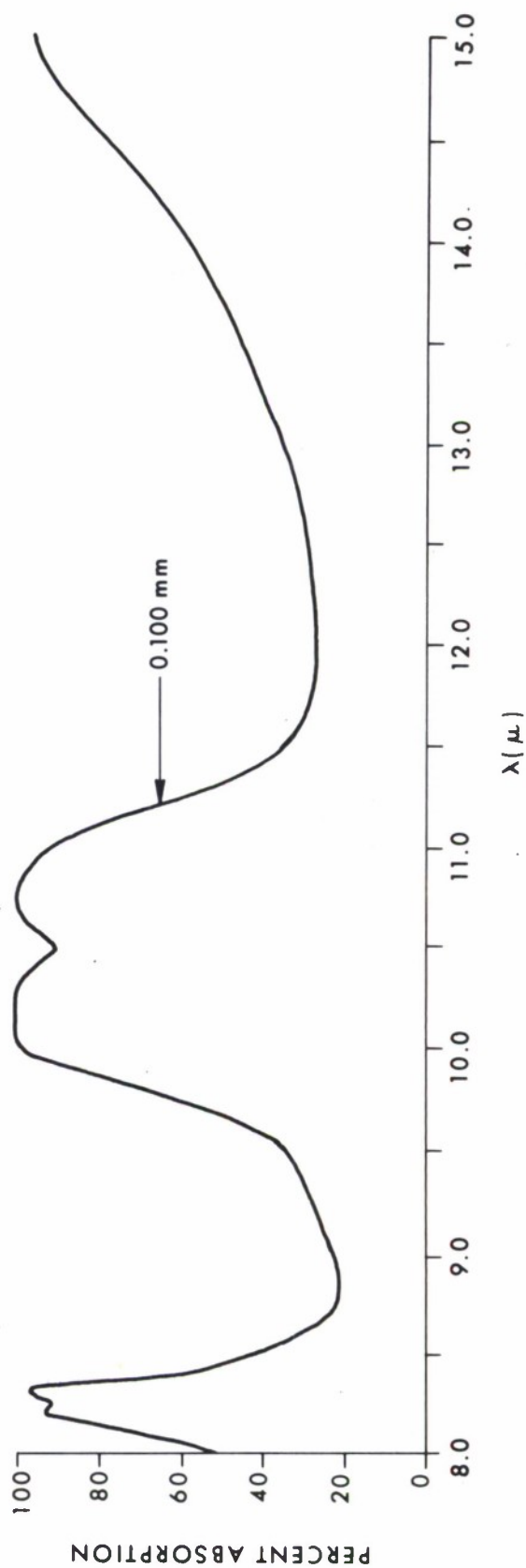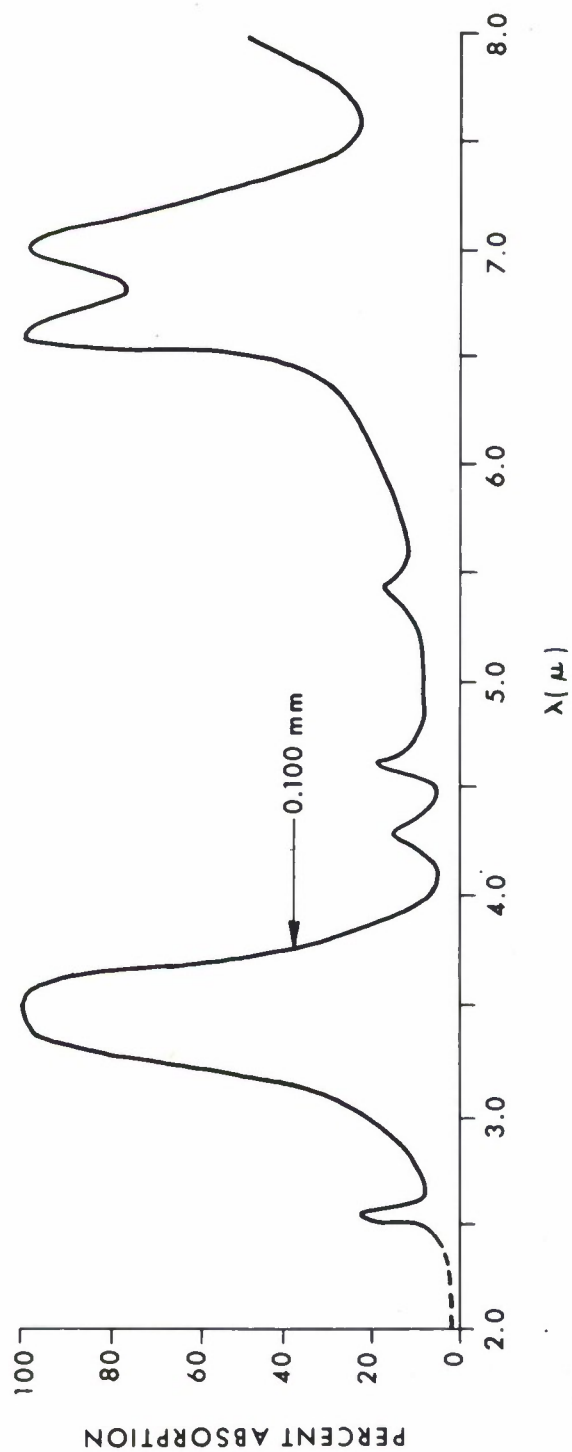
Figure B-13. Absorption Spectrum of Triethylaluminum*

*From Pierson, Fletcher, and Gantz, op cit.

Appendix B

57
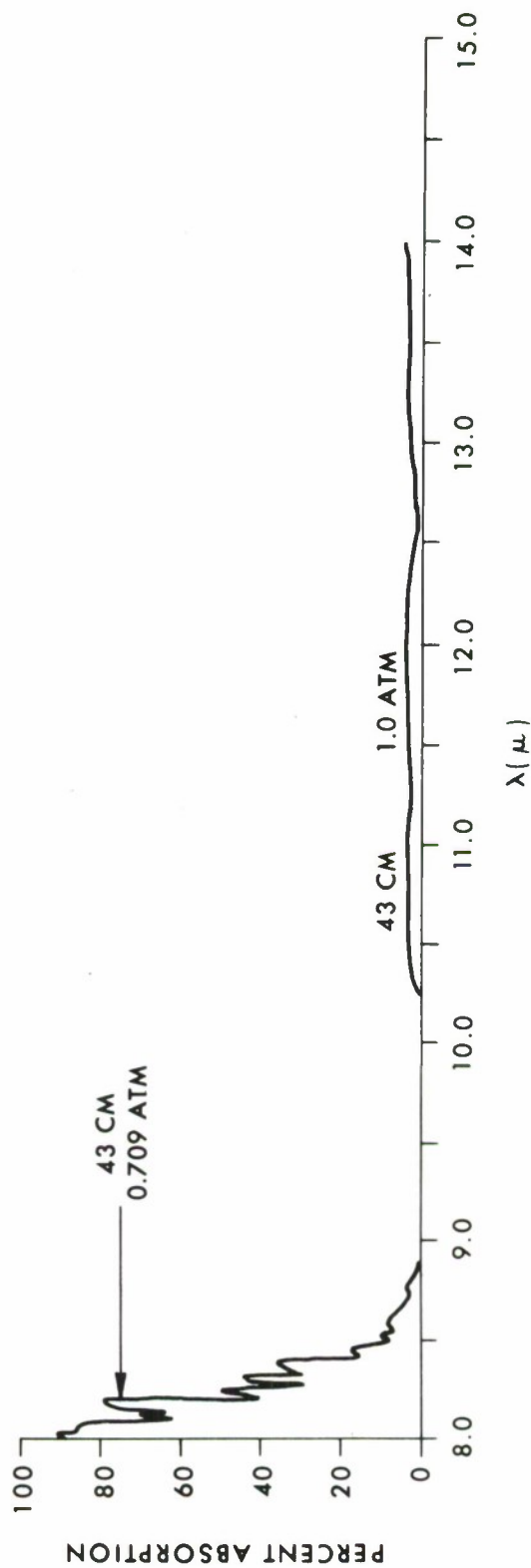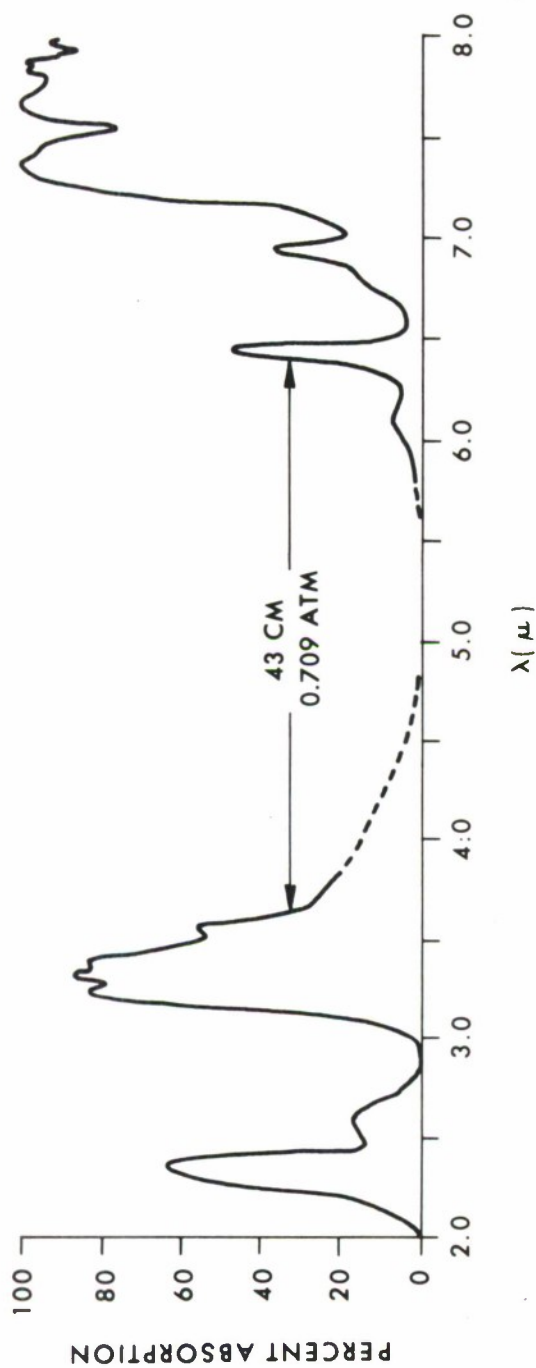
Figure B-14. Absorption Spectrum of Methane*

*From Sadtler Standard Spectra, Sadtler Research Laboratories, Philadelphia, Pennsylvania.
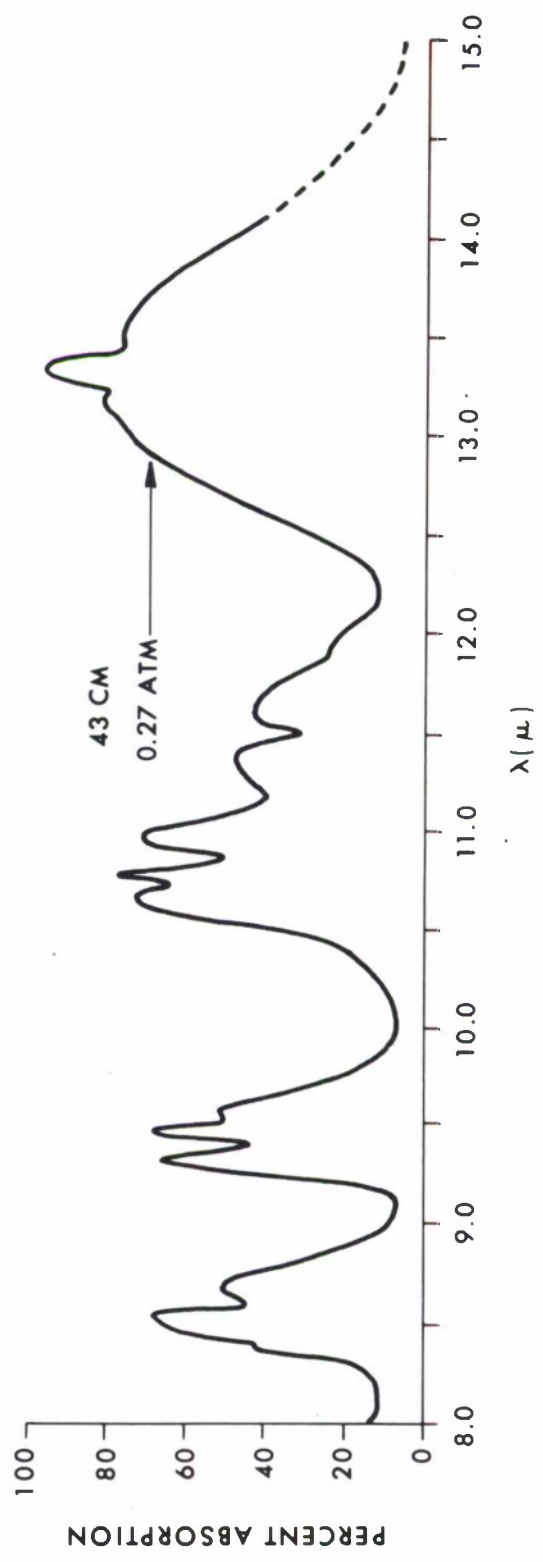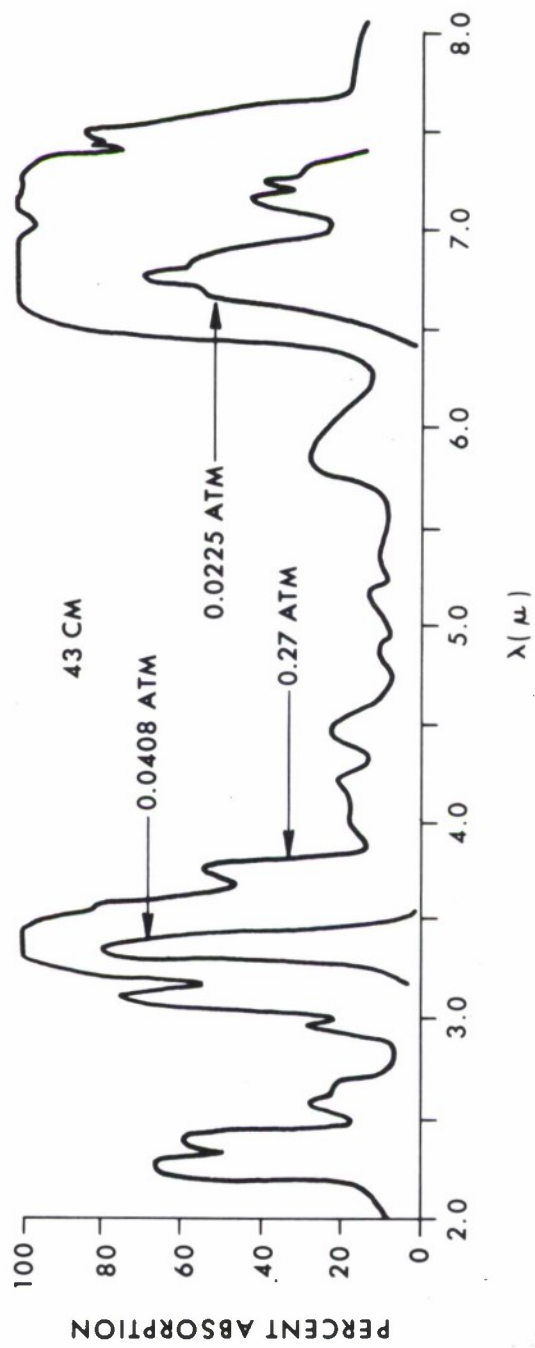
Figure B-15. Absorption Spectrum of Propane*

*Ibid.
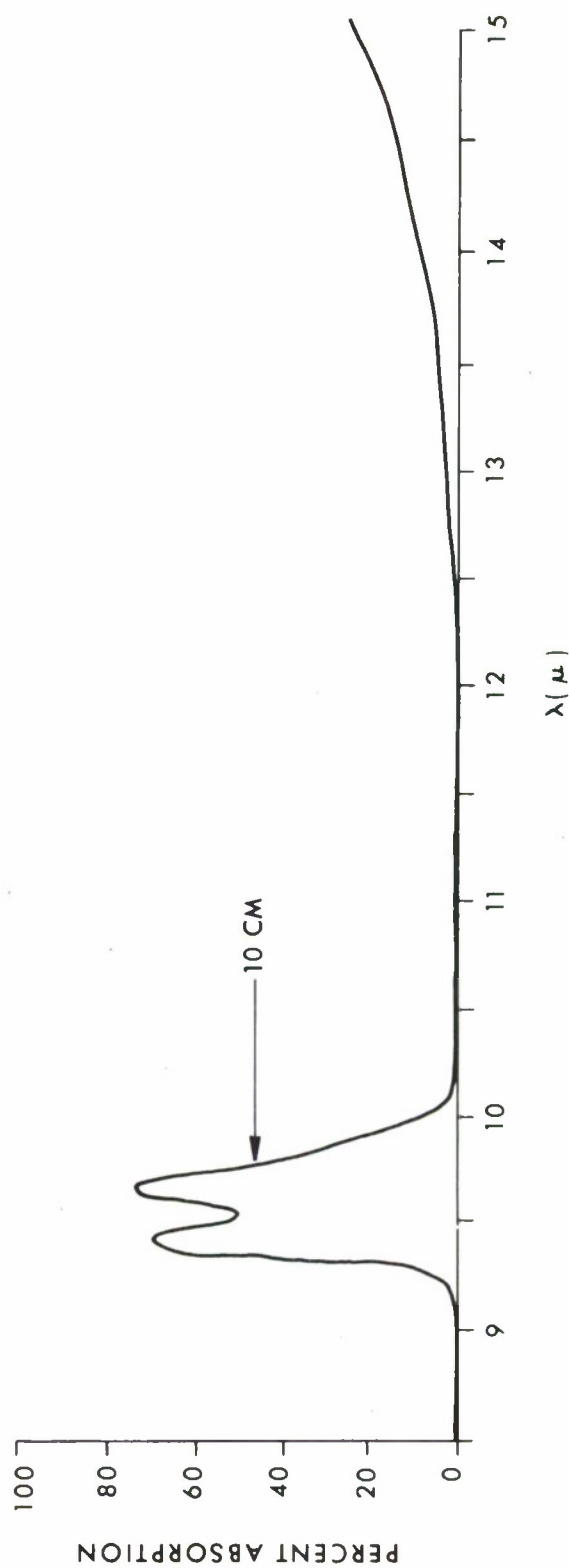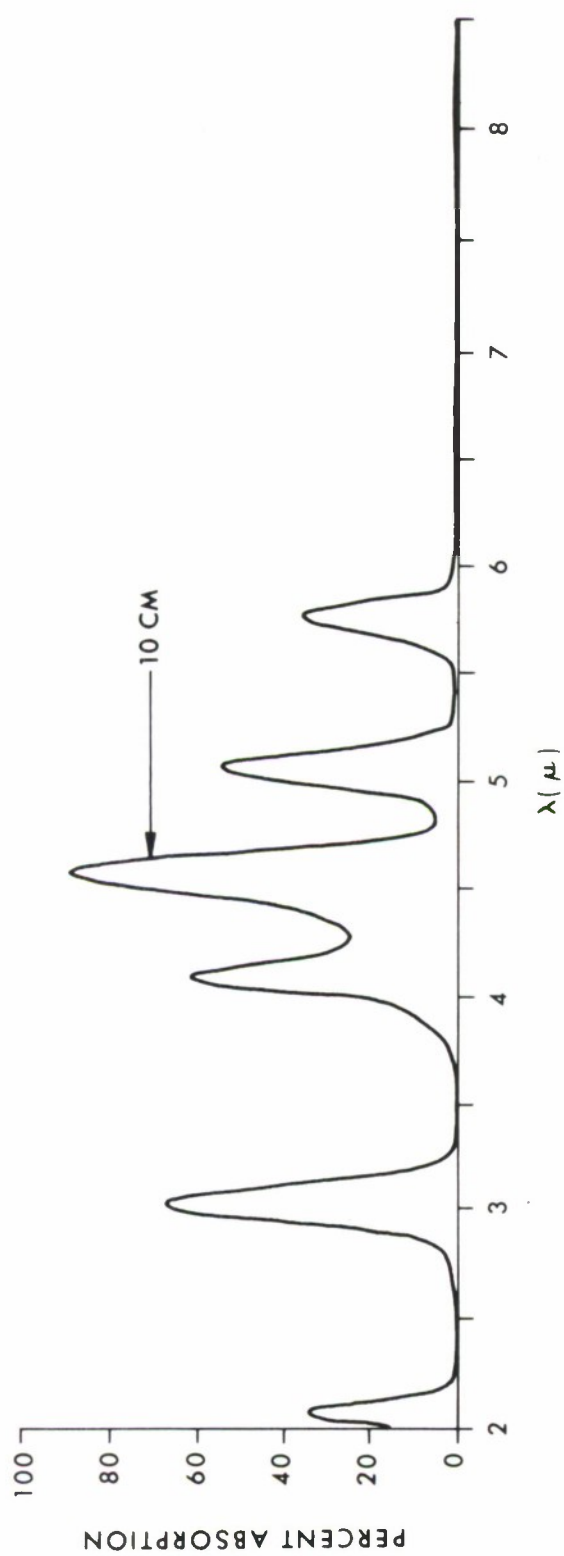
Figure B-16. Absorption Spectrum of Carbonyl Sulfide*

*From Andrews, D. A., Hurtubise, F. G., and Krassig, H. The Presence of Monothiocarbonate Substituents in Cellulose Xanthates. Can. J. Chem. 38, 1381-1398 (1960).

APPENDIX C

FLAME EMISSION SPECTRA OF FUELS

Emission spectra of flames from various fuels are given on the following pages. The spectra were obtained from a variety of references and are normalized. The references and the procedure for normalization are described in section IV of the text.

Because the primary reaction products of burning hydrocarbons are water, carbon dioxide, and carbon monoxide, the emission spectra of hydrocarbon fuels have common characteristics.
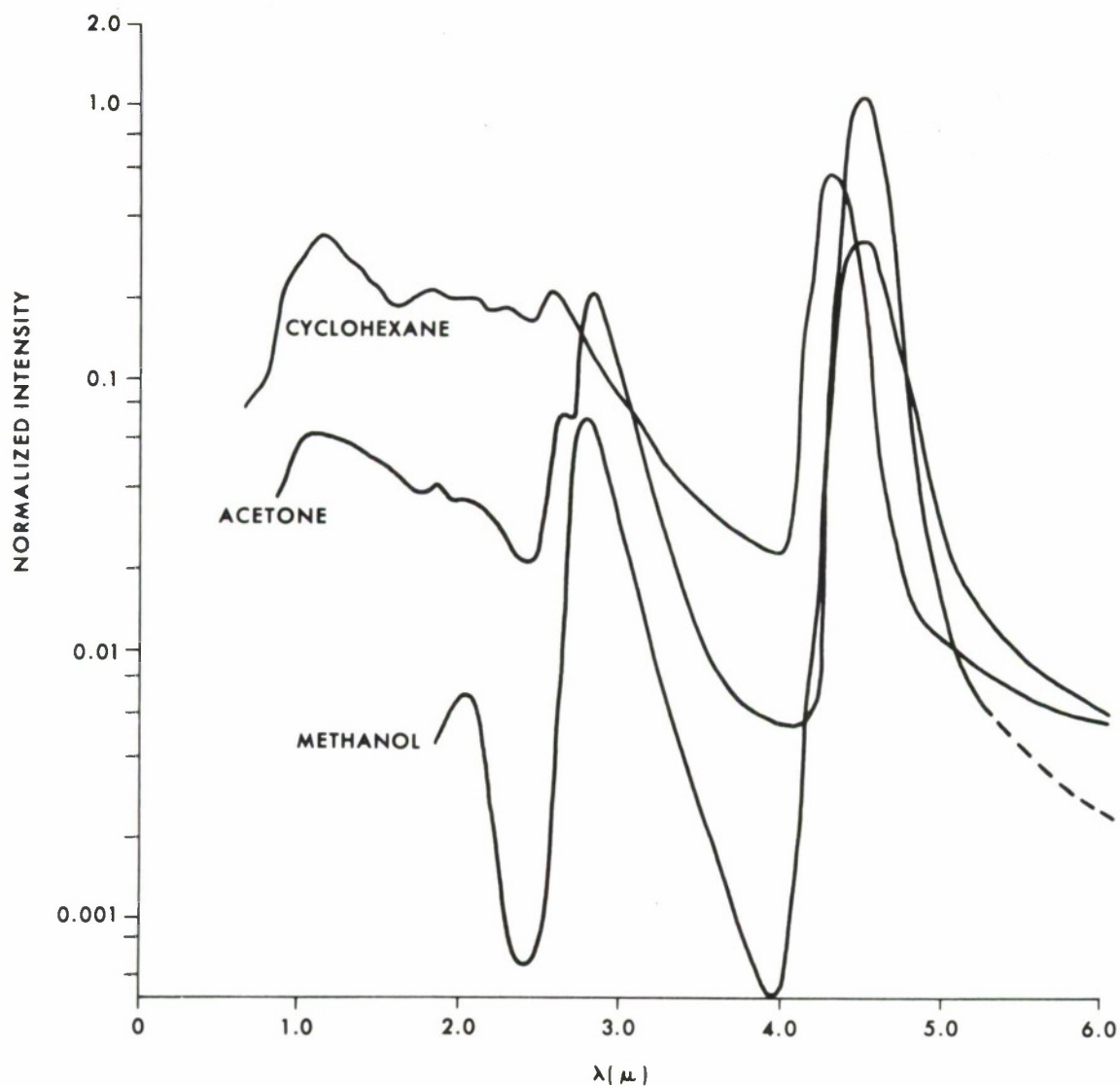
Figure C-1. Emission of Acetone, Cyclohexane, and Methanol Flames*
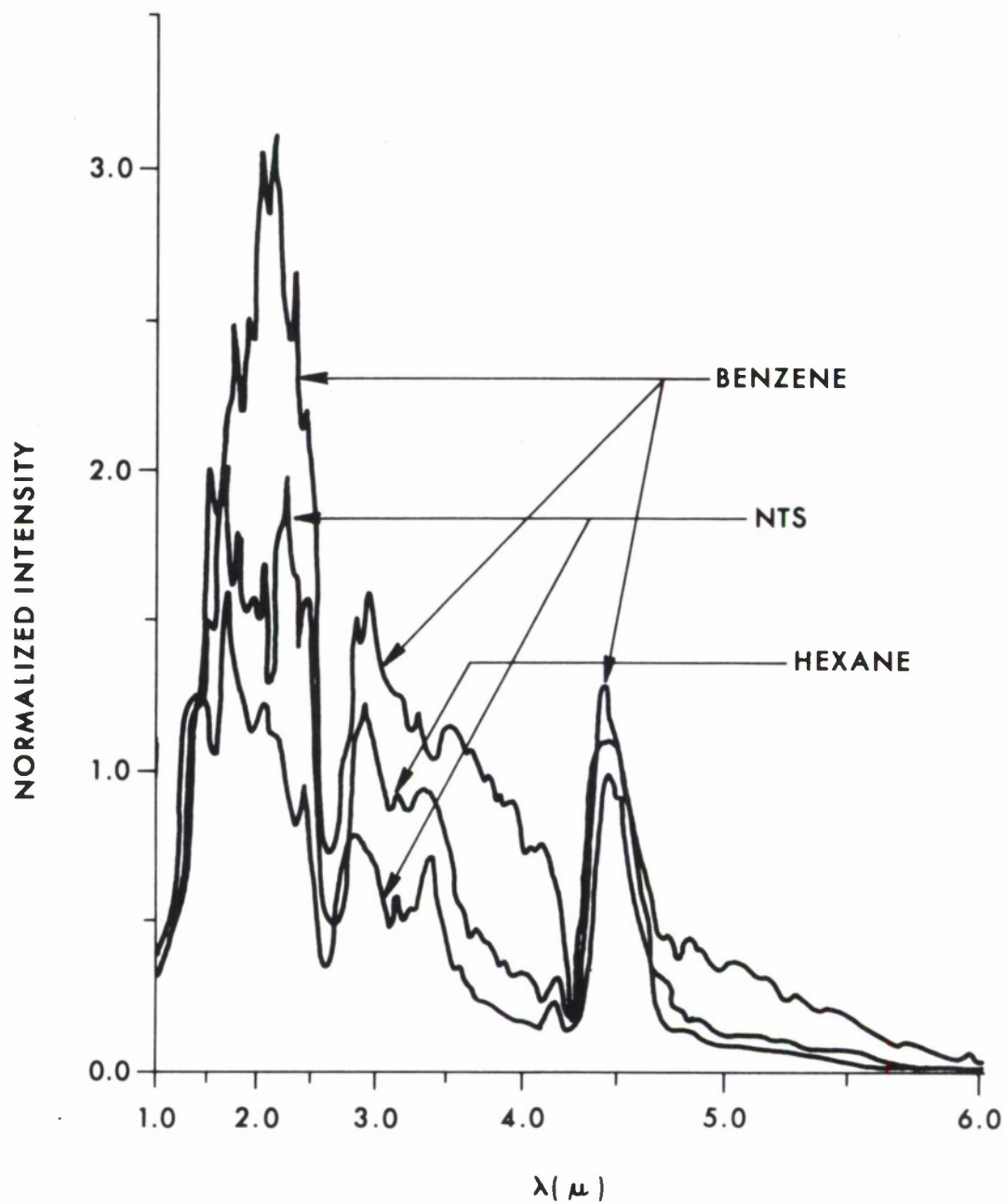
Figure C-2. 2μ to 6μ Flame Emission Spectra of Benzene, Hexane, and Napalm Test Solvent*

*From Kahrs, J., and Burgess, D. CRDL Special Publication 6-1. Field Calorimetry/Chemical Studies. Proceedings of the Third Flame-Incendiary Conference. August 1965. UNCLASSIFIED Report.
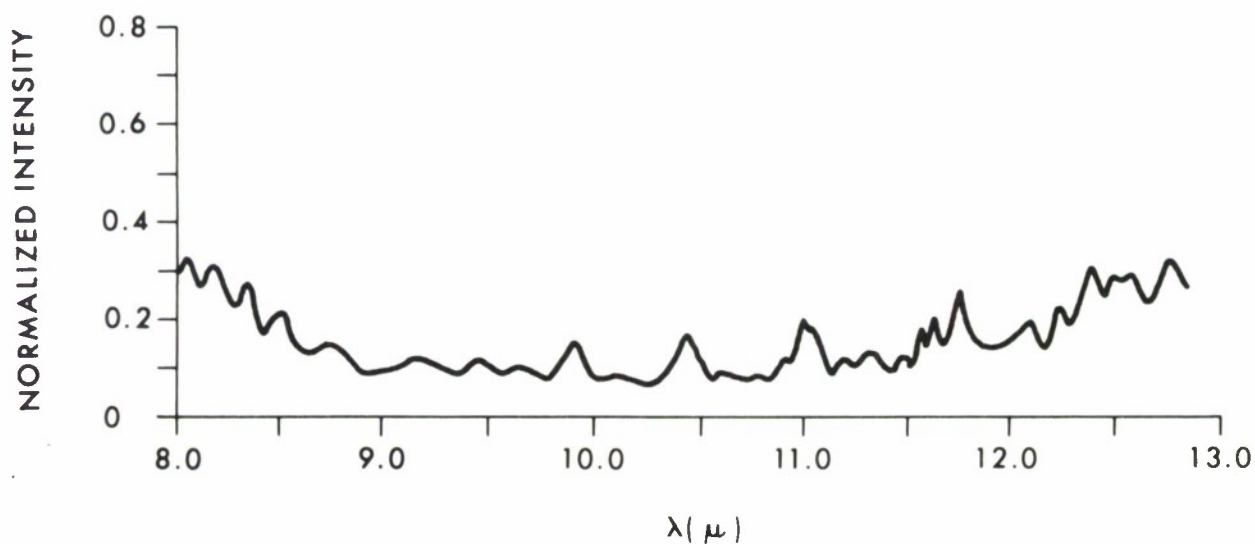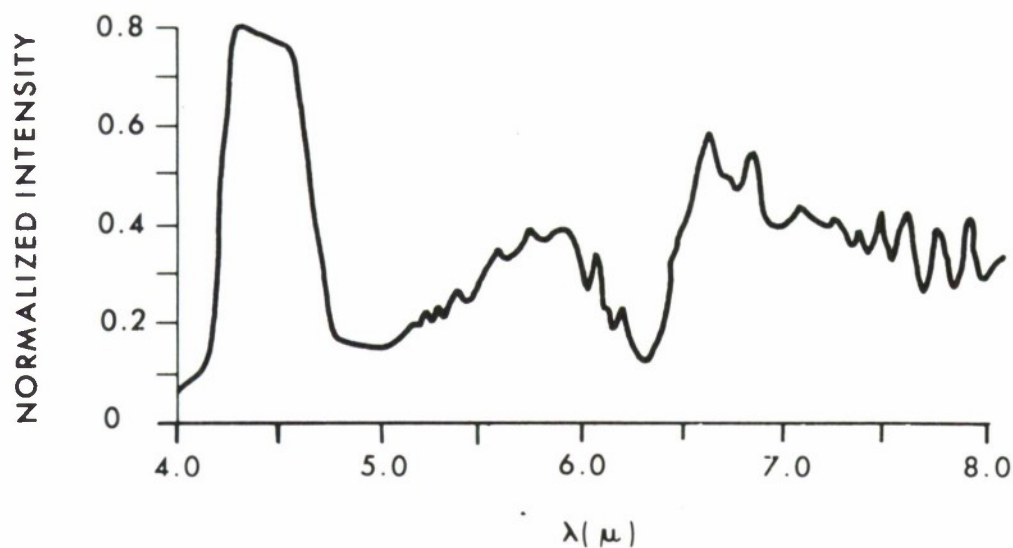
Figure C-3. 4μ to 13μ Flame Emission Spectra for Methanol in Oxygen*
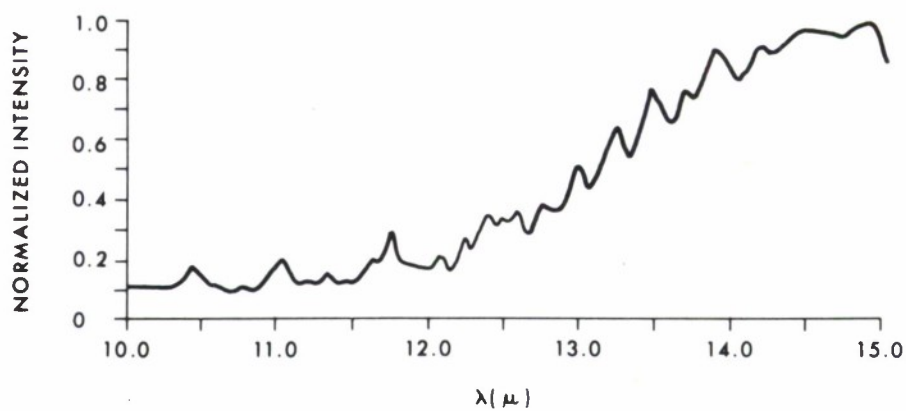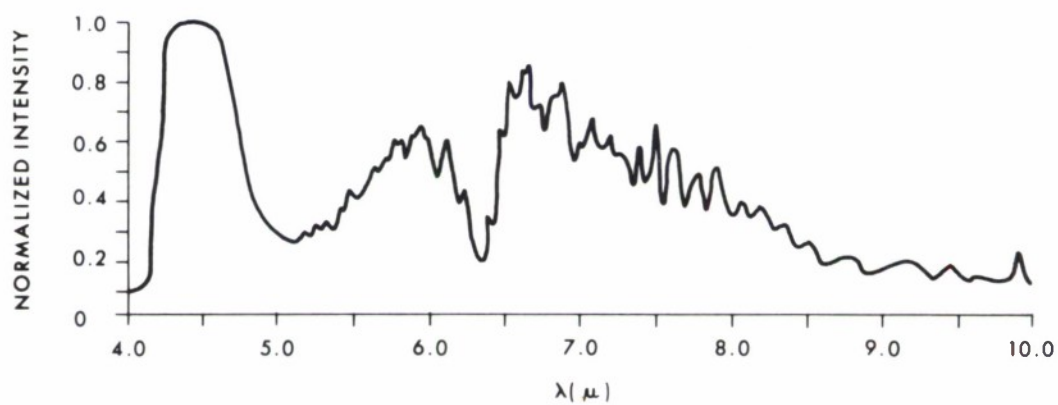
Figure C-4. 4μ to 15μ Flame Emission Spectrum of Hexane in Oxygen*

Ibid.

Figure C-5. 2μ to 15μ Flame Emission Spectrum of Ammonia in Oxygen*

*Ibid.

Figure C-6. 2μ to 15μ Flame Emission Spectrum of Hydrazine in Oxygen*

Ibid.
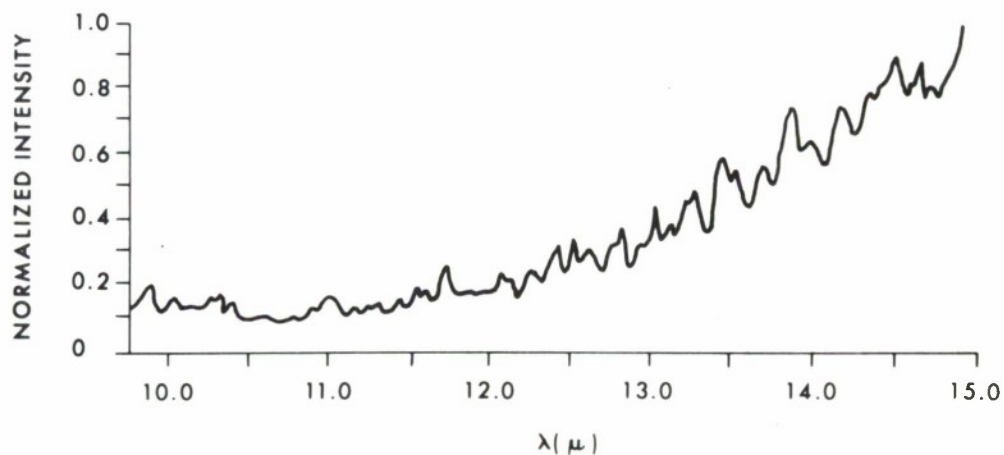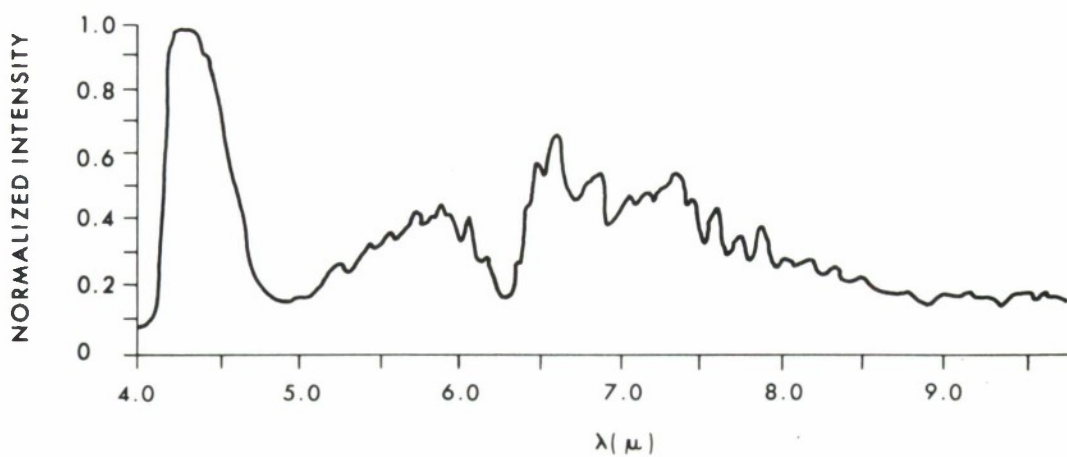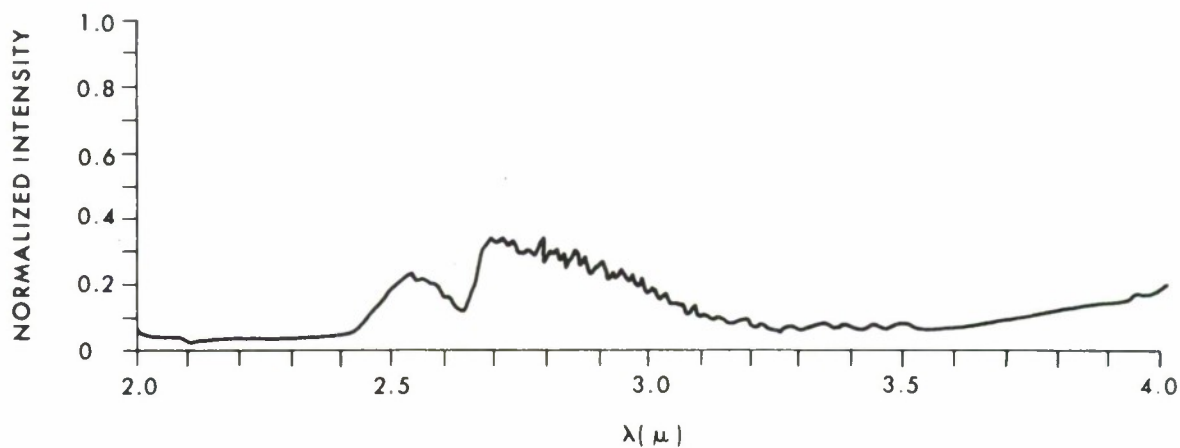
Figure C-7. 2μ to 15μ Flame Emission Spectrum of MMH in Oxygen*
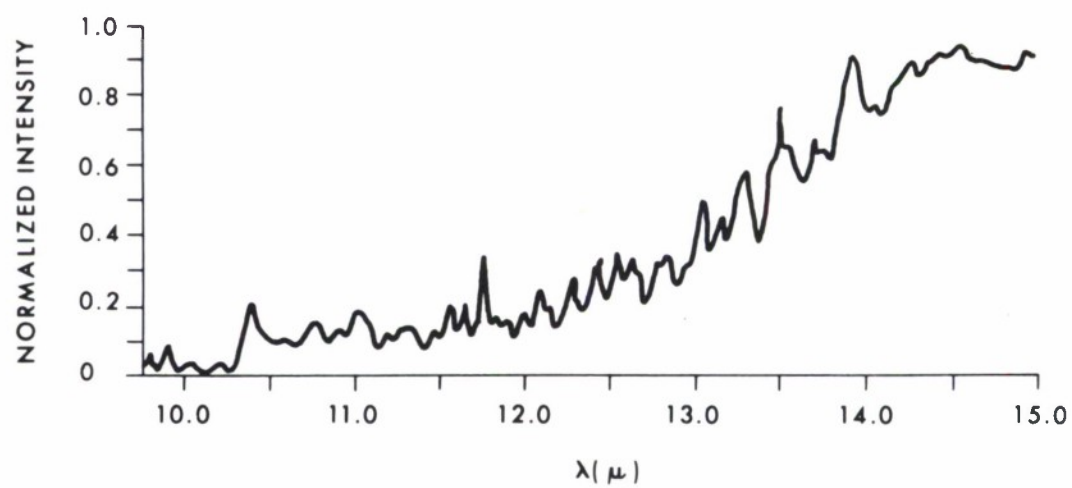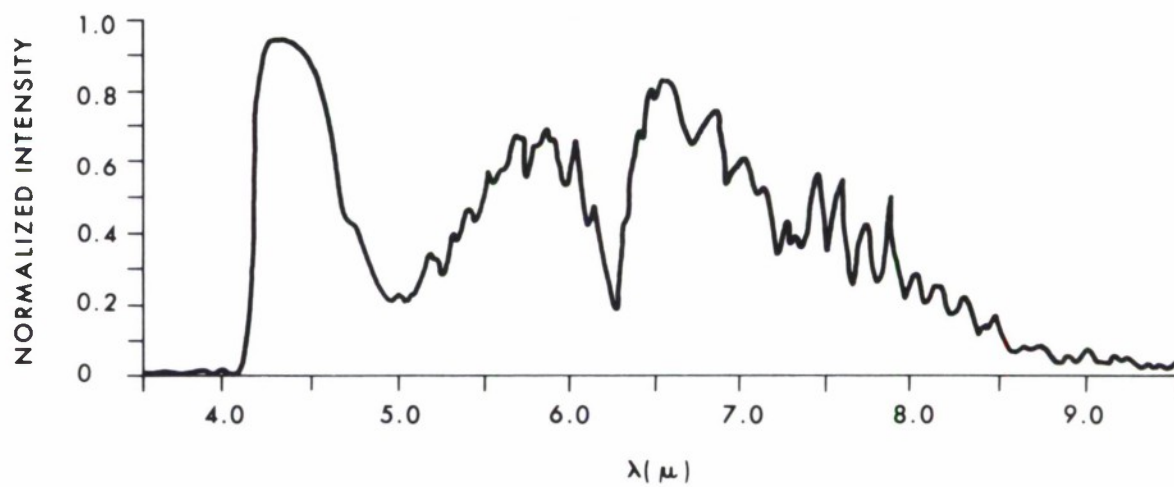
Figure C-8. 4μ to 15μ Flame Emission Spectrum of UDMH*

Ibid.

69
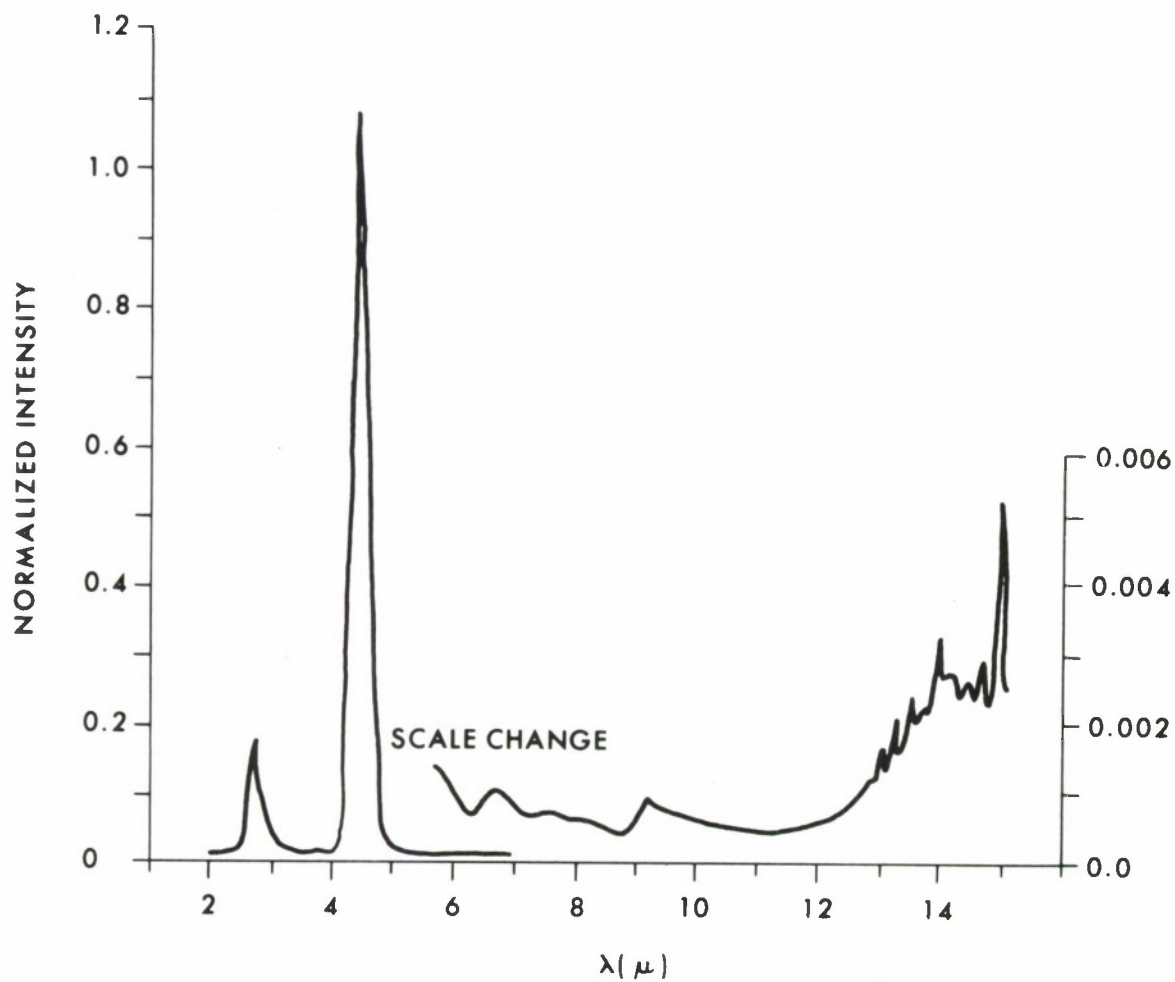
Figure C-9. 2μ to 15μ Flame Emission Spectrum of Carbon Monoxide in Oxygen*
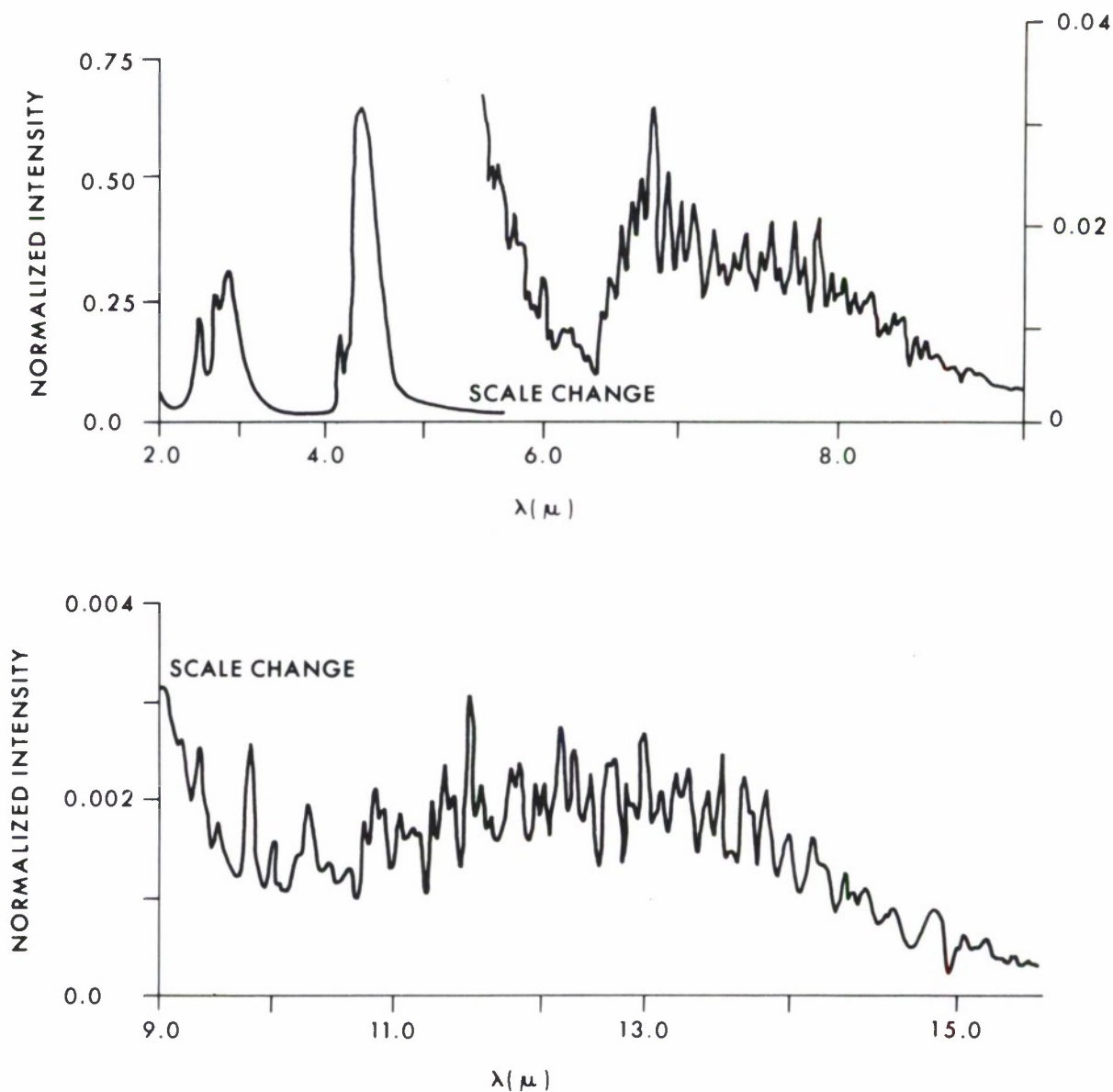
Figure C-10. 2μ to 15μ Flame Emission Spectrum of Methane in Air*
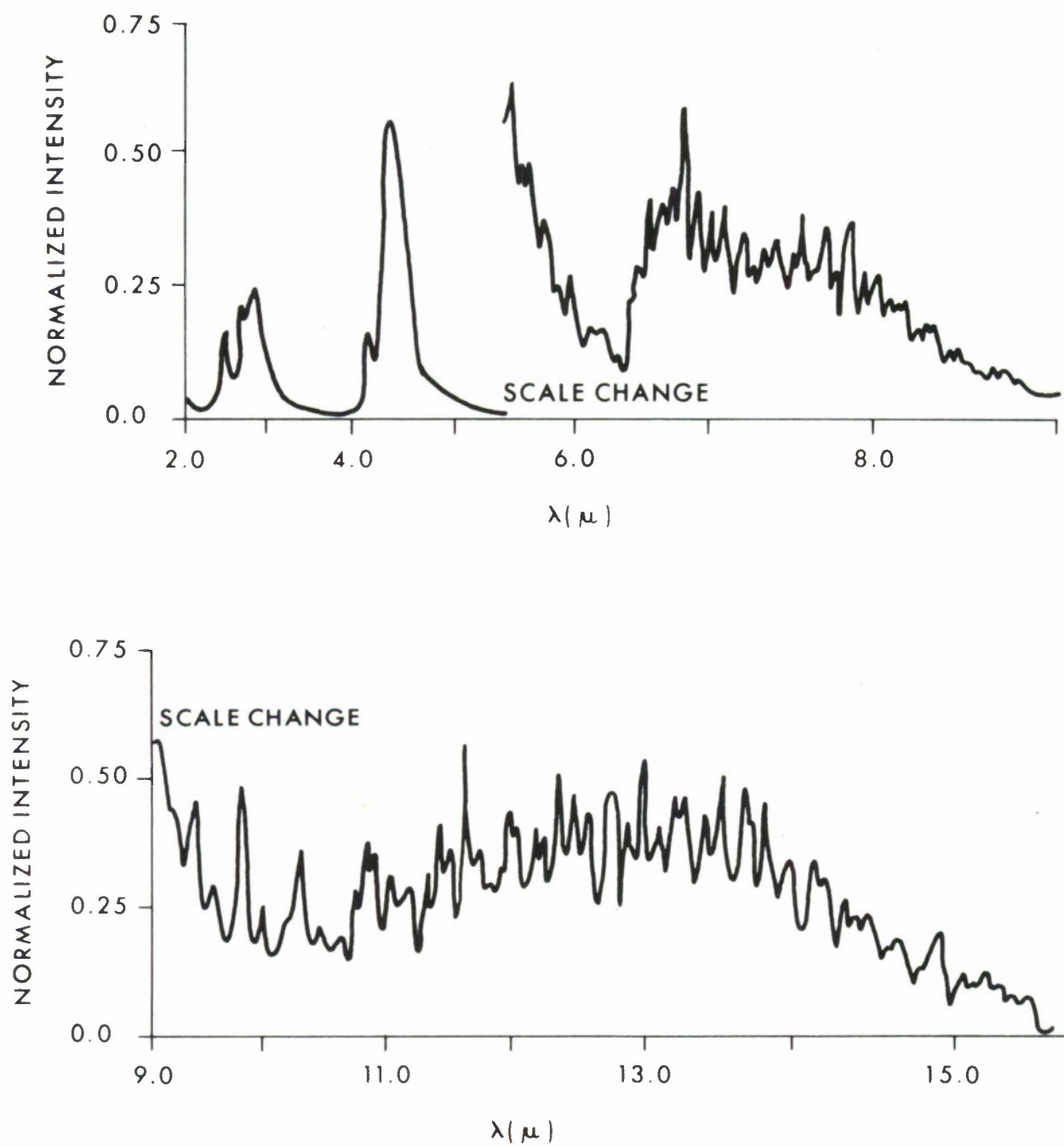
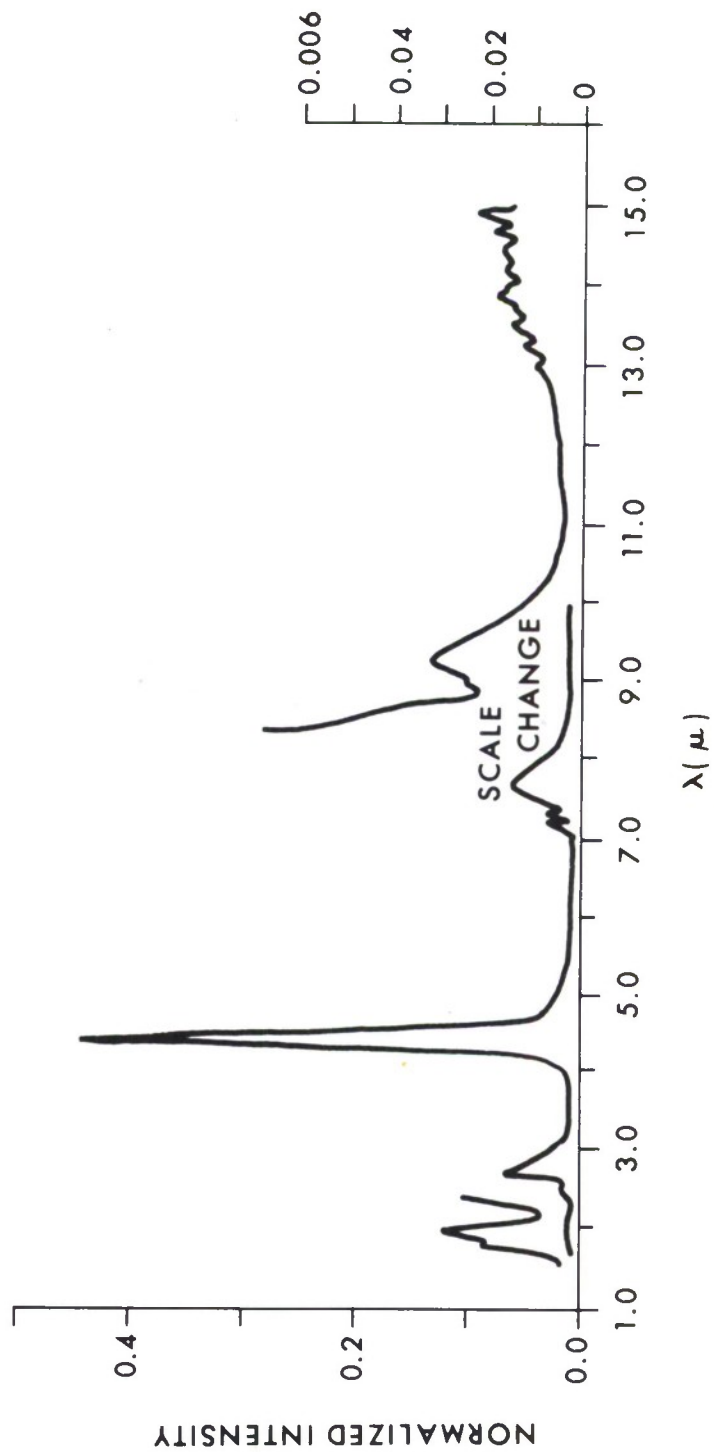Figure C-11. 2μ to 15μ Flame Emission Spectrum of Propane in Air*

*Ibid.

Figure C-12. 2μ to 15μ Flame Emission Spectrum of Carbonyl Sulfide in Oxygen*

*From Bell, Burnside, Dickey, Kopczynski, and Rowntree, *op. cit.*

BLANK

APPENDIX D

EXACT OVERLAP OF FUELS

The products of $f_\alpha(\lambda)$ and $f_\epsilon(\lambda)$ for various fuels are given in the following pages. Values of $f_\alpha(\lambda)$ and $f_\epsilon(\lambda)$ were taken from appendixes B and C. The area under the curves divided by the wavelength span is the overlap. The scale factors given in figures (for example, 4.17×10^{-4} for acetone, see figure D-1) are the factors by which the product of f_α and f_ϵ must be multiplied to give the unitless overlap values. These scale factors occur because of the non-uniformity of absorption cell thickness, pressure (for gas samples), etc.

The spectral regions of large overlap of absorption and emission spectra are (in decreasing order of importance): 4.5μ, 2.5μ, 3.5μ, 6μ, and 7μ.
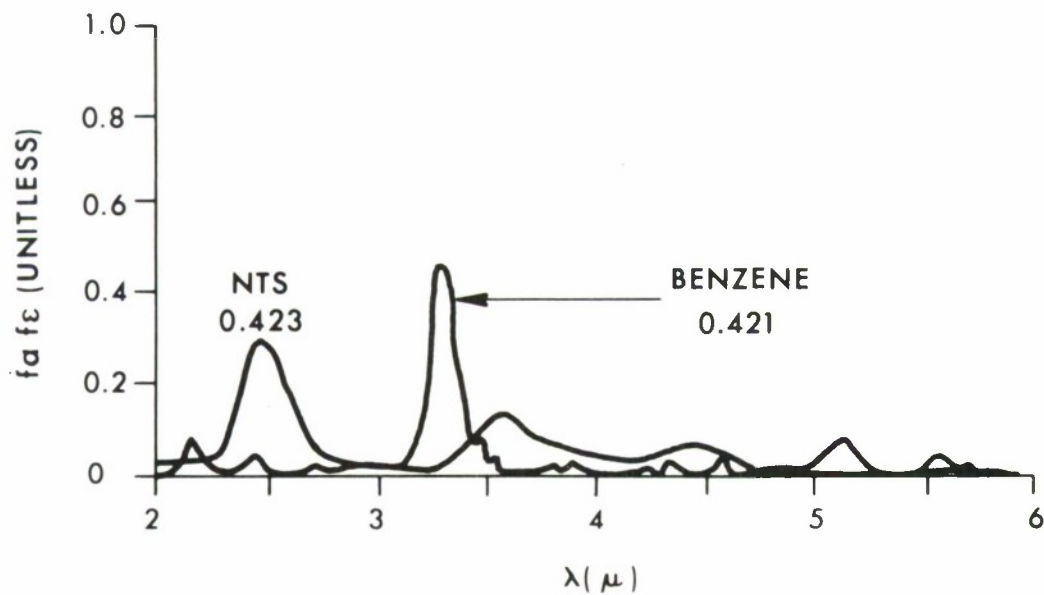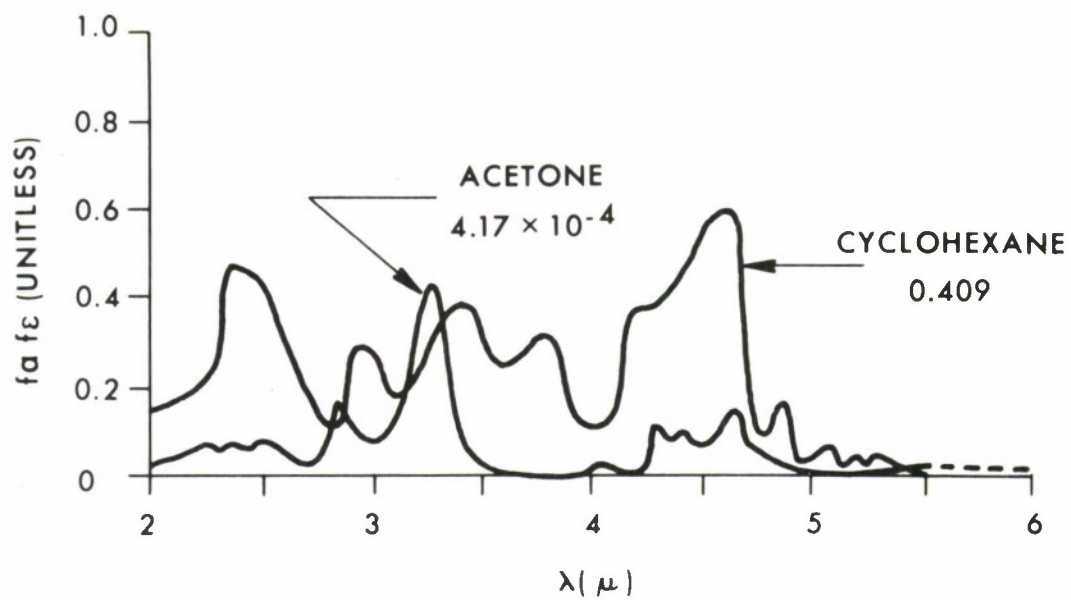
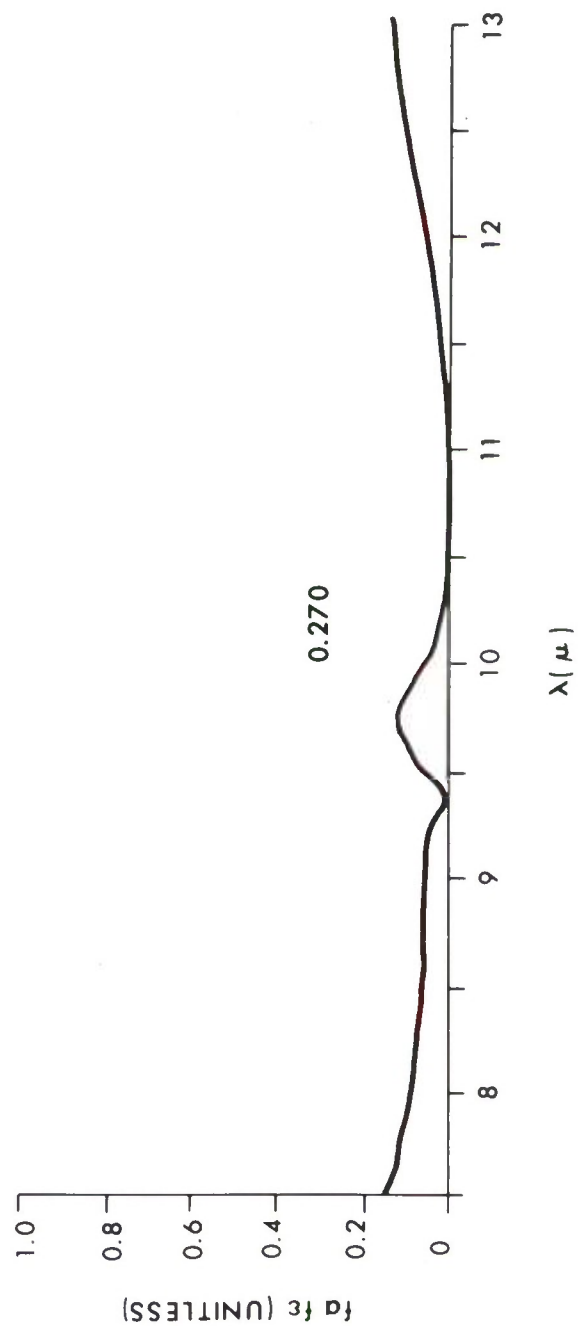Figure D-1. Exact Overlap of Acetone, Cyclohexane, Benzene, and NTS
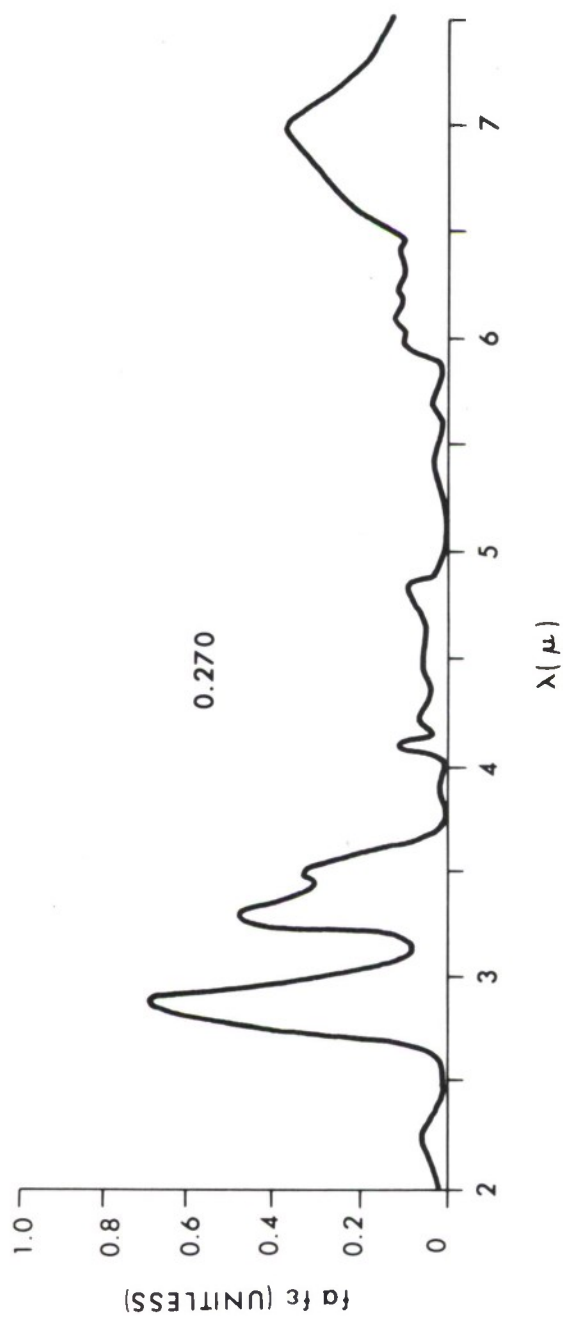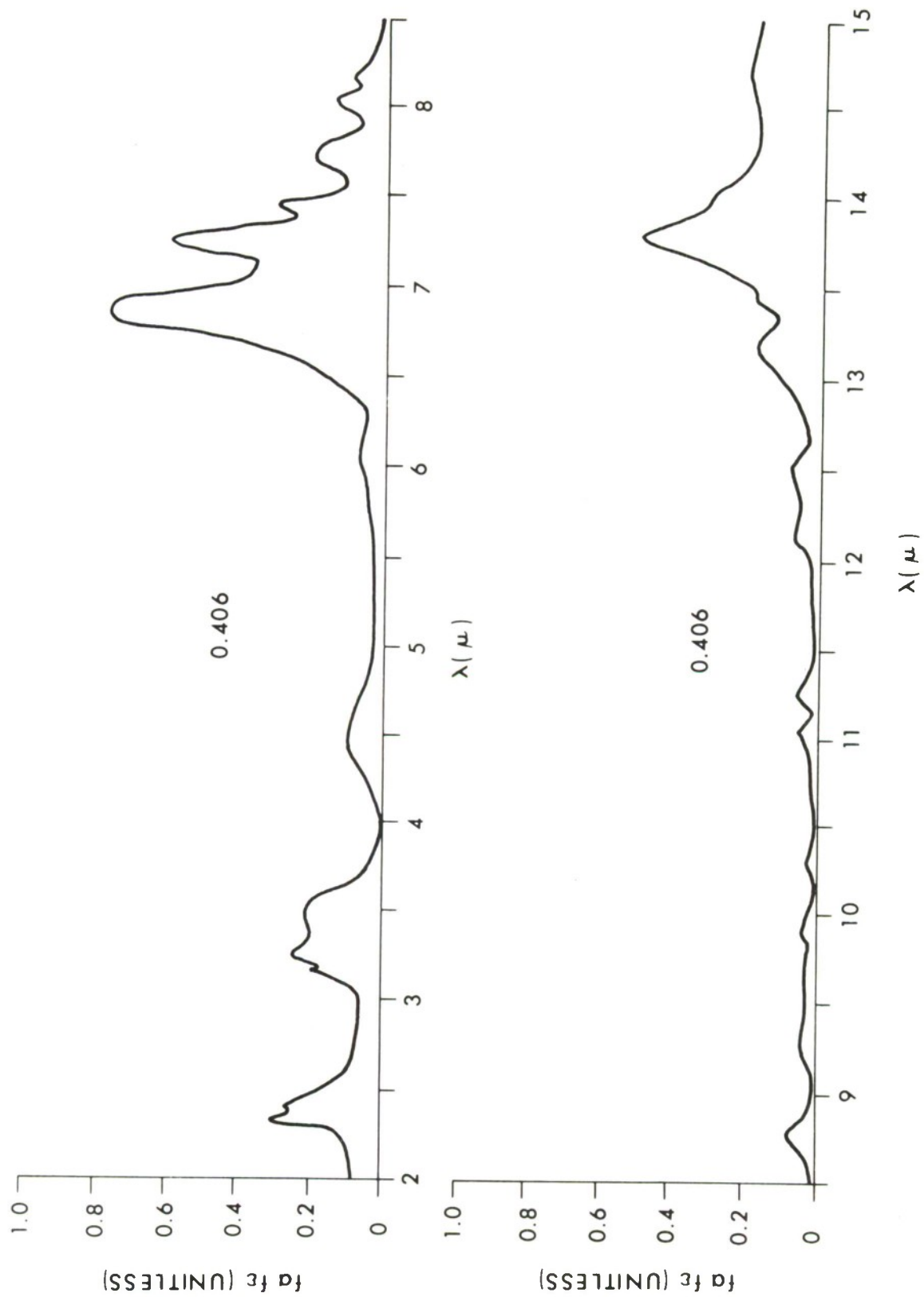
Figure D-2. Exact Overlap of Methanol
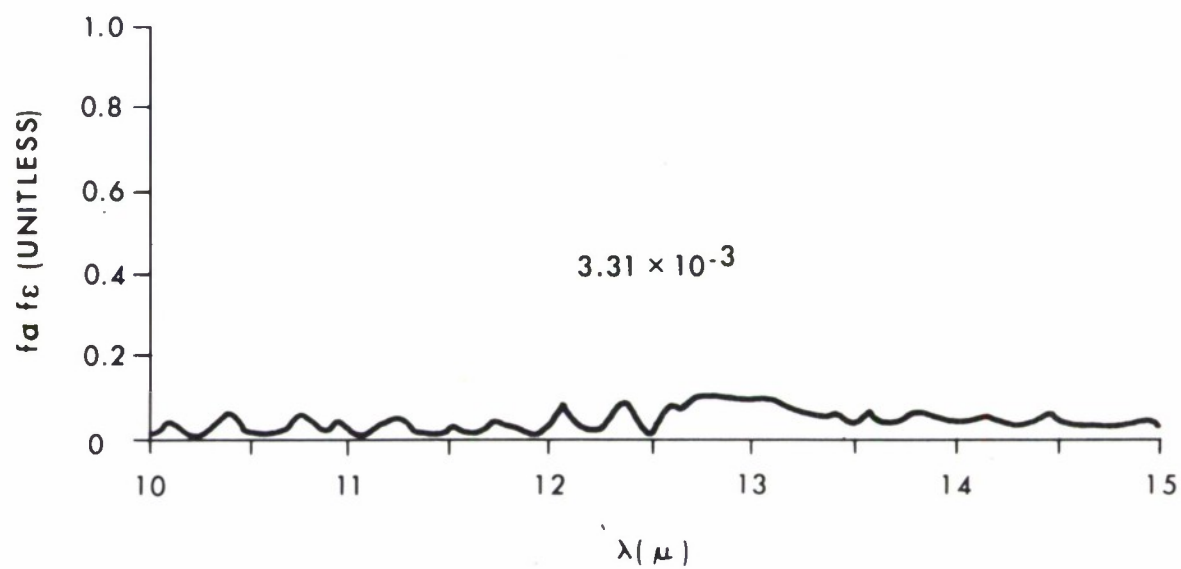
Figure D-3. Exact Overlap of Hexane

78
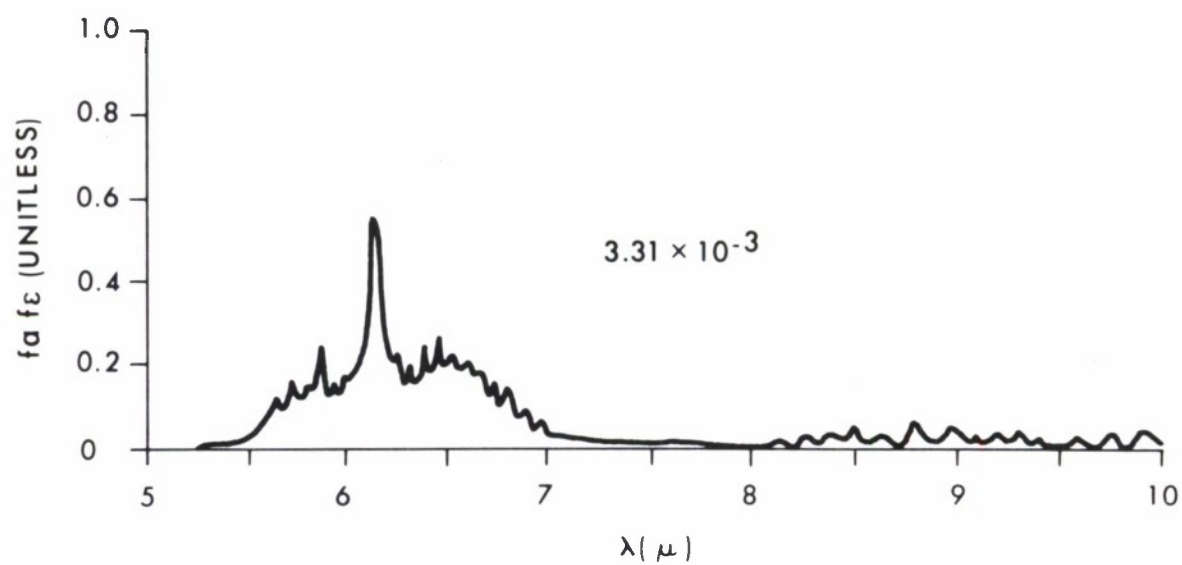
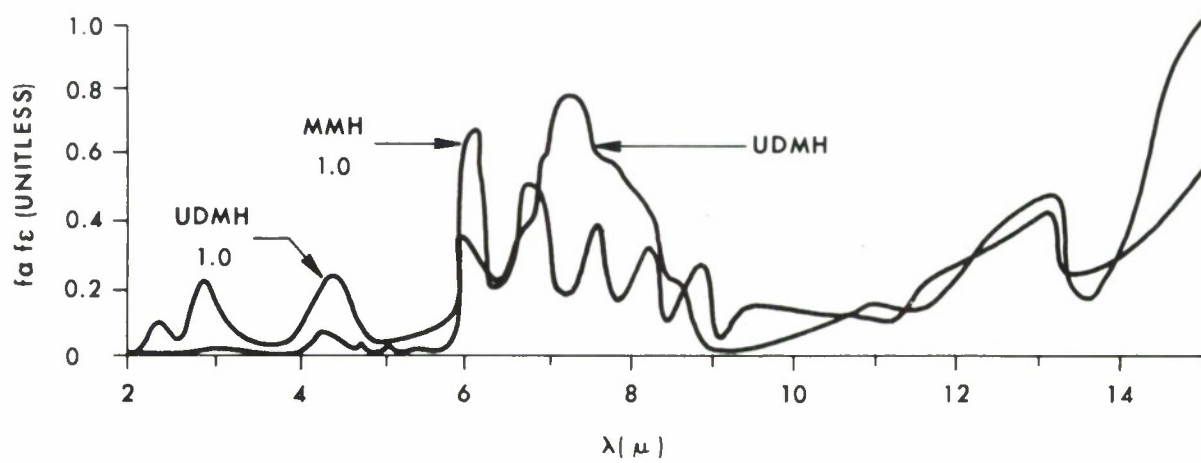Figure D-4. Exact Overlap of Ammonia
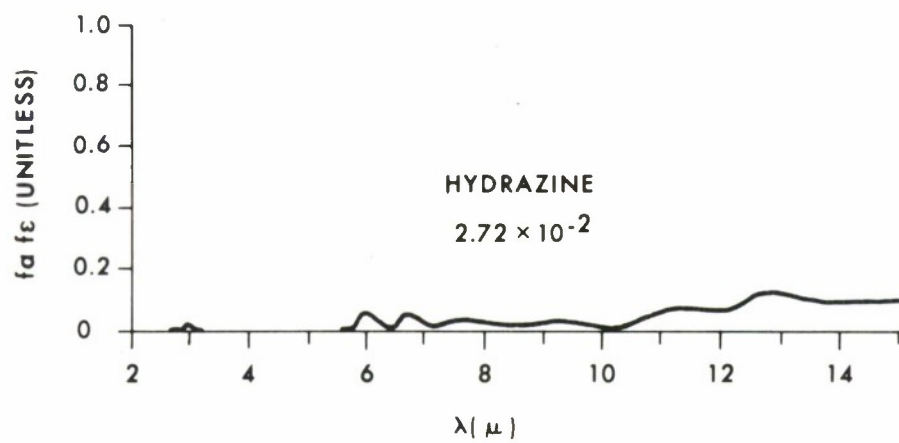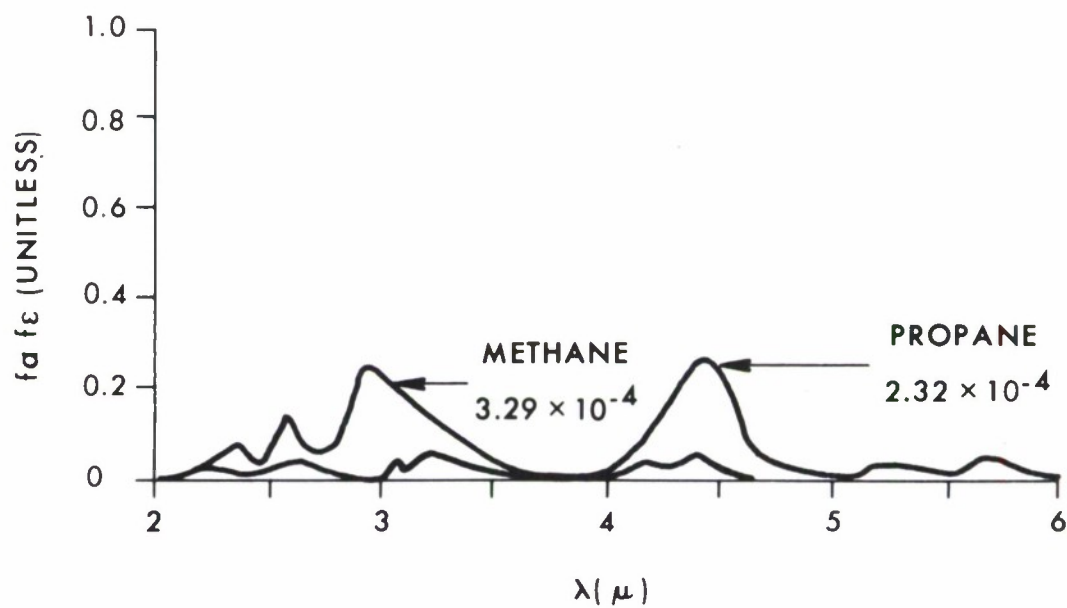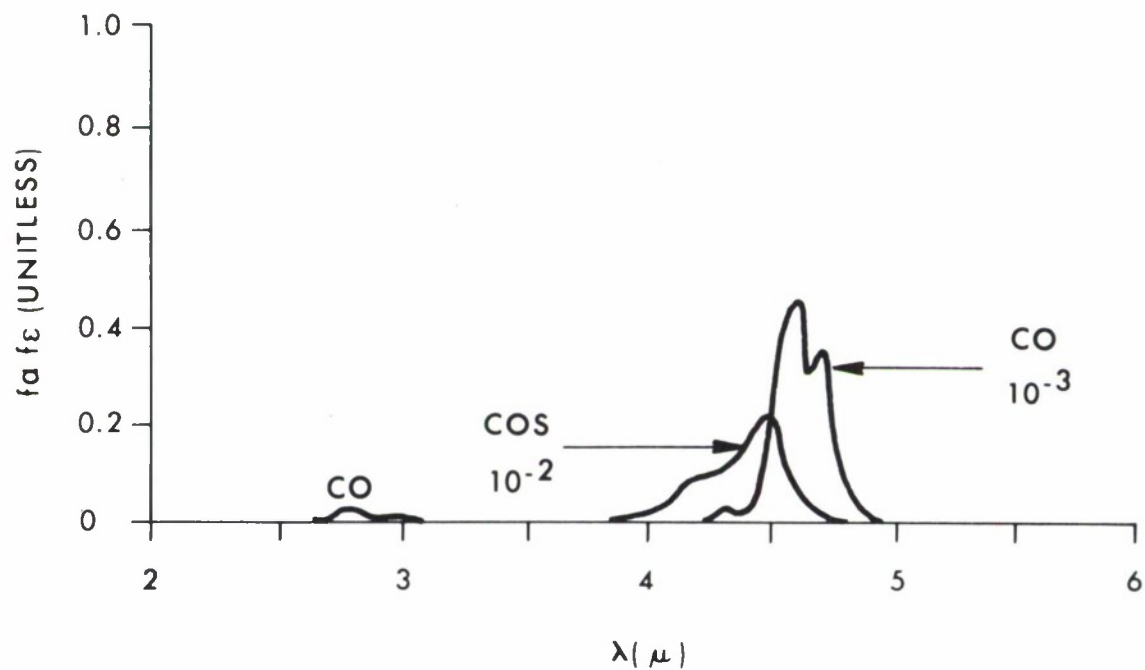
Figure D-5. Exact Overlap of Hydrazine, MMH, and UDMH

Figure D-6. Exact Overlap of CO, COS, Methane, and Propane

81

BLANK

Agency	Copies	Agency	Copies
EDGEWOOD ARSENAL		**DEPARTMENT OF THE ARMY**	

EDGEWOOD ARSENAL

Associate Technical Director
ATTN: SMUEA-TD-A — 1
Systems Analysis Office
ATTN: SMUEA-OS — 1
Patent Advisor, Office of Counsel — 1
Foreign Intelligence Office
ATTN: SMUEA-POF — 3
Director, USAMUCOM,
Operations Research Group — 1
CO, Quality Assurance Directorate
ATTN: SMUEA-QAE — 1
Record Copy, CO, APG, ATTN: STEAP-AD-R — 1
Authors Copy, Physical Research Laboratory — 1
— 1

Director, Research Laboratories — 1
Chief, Chemical Research Laboratory — 1
Chief, Analytical Chemistry Department — 1
Chief, Medical Research Laboratory — 1
ATTN: SMUEA-RM(3) — 7
Chief, Basic Medical Sciences Department
Chief, Clinical Medical Sciences Department — 1
Chief, Veterinary Medicine Department — 1
Chief, Physical Research Laboratory — 1
Chief, Defensive Research Department — 1
Chief, Dissemination Research Department — 1

Technical Support Directorate

ATTN: SMUEA-TS-T — 1

ATTN: SMUEA-TS-R — 1

ATTN: SMUEA-TS-L — 10

Director, DDEL
ATTN: SMUEA-DDW — 1
ATTN: SMUEA-DME(1) — 1
ATTN: SMUEA-DPP — 1
ATTN: SMUEA-DPP(2) — 1

Director, WDEL
ATTN: SMUEA-WMW — 1

Commanding Officer
Rocky Mountain Arsenal
ATTN: SMURM-F — 1
Denver, CO 80240

DEPARTMENT OF DEFENSE

Defense Documentation Center — 12
Cameron Station
Alexandria, VA 22314

Defense Intelligence Agency
ATTN: DIAAP-7E — 1
Washington, DC 20301

DEPARTMENT OF THE ARMY

Chief of Research & Development
ATTN: Life Sciences Division — 1
Department of the Army
Washington, DC 20310

Commanding Officer
Technical Library
ATTN: STEAP-TL — 1
Aberdeen Proving Ground, MD 21005

US Army Standardization Group — 1
Canada, Canadian Forces Hqs
Ottawa 4, Ontario, Canada

Senior Standardization Representative
US Army Standardization Group, UK
ATTN: CRDSGU-H — 1
Box 65, FPO, NY 09510

OFFICE OF THE SURGEON GENERAL

Commanding General
USA Medical Research & Development Command
ATTN: MEDDH-RPB — 1
Forrestal Building
Washington, DC 20314

Commander & Director
USAISR
Brooke Army Medical Center — 1
Fort Sam Houston, Texas 78234

Director
Armed Forces Institute of Pathology
ATTN: MEDEM-DR — 1
Washington, DC 20305

US ARMY MATERIEL COMMAND

Commanding General
US Army Materiel Command
ATTN: AMCRD-BC — 1
Washington, DC 20315

Director
Army Materiels & Mechanics Research Center
ATTN: AMXMR-STL — 1
Watertown, MA 02172

Commanding General
Deseret Test Center
ATTN: Technical Library — 1
Dugway, UT 84022

Commanding General
Deseret Test Center
ATTN: Technical Library — 1
Bldg 100, Soldier's Circle
Fort Douglas, UT 84113

Agency	Copies	Agency	Copies
Commanding General USA Test & Evaluation Command ATTN: AMSTE-NB Aberdeen Proving Ground, MD 21005	1	**DEPARTMENT OF THE NAVY** Department of the Navy Office of Naval Research ATTN: Code 443 800 N. Quincy Street Arlington, VA 22217	1
US Army Missile Command Redstone Scientific Information Center ATTN: Chief, Document Section Redstone Arsenal, AL 35809	1	Officer in Charge Naval Biomedical Research Laboratory, NSC Oakland, CA 94625	1
US ARMY MUNITIONS COMMAND Commanding General US Army Munitions Command ATTN: AMSMU-MS-CH ATTN: AMSMU-RE-CN ATTN: AMSMU-RE-RT ATTN: AMSMU-XM Dover, NJ 07801	1 1 1 1	Commander Naval Facilities Engineering Command ATTN: Code 0322 Washington, DC 20390	1
CONARC United States Army Infantry School Bde & Bn Dept, Cbt Spt Gp ATTN: Chmn, NBC Committee Fort Benning, GA 31905	1	Commanding Officer Naval Explosive Ordnance Disposal Facility ATTN: Army Chemical Office Indian Head, MD 20640	1
Commandant USA Chemical Center & School ATTN: ATSCM-A-D Fort McClellan, AL 36201	1	Commander US Naval Weapons Laboratory ATTN: FC Dahlgren, VA 22448	1
COMBAT DEVELOPMENTS COMMAND Commanding General US Army Combat Developments Command ATTN: CDCMR-U Fort Belvoir, VA 22060	1	Commanding Officer Nuclear Weapons Training Group, Atlantic ATTN: Nuclear Warfare Dept Norfolk, VA 23511	1
Commanding Officer USA CDC Medical Service Agency ATTN: CDCMSA-D Fort Sam Houston, TX 78234	1	**DEPARTMENT OF THE AIR FORCE** Headquarters Foreign Technology Division (AFSC) ATTN: PDTR-3 Wright-Patterson AFB, OH 45433	1
Commanding Officer USA CDC CBR Agency ATTN: CSGCB-P Fort McClellan, AL 36201	1	HQ USAF ATTN: RDPS ATTN: RDPA Washington, DC 20330	1 1
Commanding Officer USA CDC Infantry Agency ATTN: CAGIN-CM Fort Benning, GA 31905	1	Commander, USAFSAM ATTN: Aeromedical Library (SCL-4) Brooks AFB, Texas 78235	1
Commanding Officer USA CDC MP Agency ATTN: CSGMP-M Fort Gordon, GA 30905	1	HQ UFSC ATTN: DLTB Andrews AFB Washington, DC 20331	1
		AFTAL (DLNM) Eglin AFB, Florida 32542	1
		Commanding Officer OOAMA ATTN: MMECA ATTN: MMEOA Hill AFB, UT 84401	1 1

DISTRIBUTION LIST 1 (Cont'd)		DISTRIBUTION LIST FOR DD 1473's	
Agency	Copies	Agency	Copies
HQ USAF Directorate of Aerospace Safety ATTN: IGDSGE Norton AFB, CA 92409	1	Chief of Research and Development Headquarters, Department of the Army ATTN: Director of Army Technical Information Washington, DC 20310	3
US MARINE CORPS		Technical Support Directorate	
Marine Corps Development & Education Command Ground Operations Division Quantico, VA 22134	1	ATTN: SMUEA-TS-R	1
		ATTN: SMUEA-TS-L	2
OUTSIDE AGENCIES		Management Information Systems Directorate	
PHS/AMC Liaison Officer Fort Detrick Frederick, MD 21701	2	ATTN: SMUEA-MI	1
Director Toxicology National Research Council 2101 Constitution Ave., N.W. Washington, DC 20418	1		

BLANK

DOCUMENT CONTROL DATA - R & D

(Security classification of title, body of abstract and indexing annotation must be entered when the overall report is classified)

1. ORIGINATING ACTIVITY *(Corporate author)*	2a. REPORT SECURITY CLASSIFICATION
CO, Edgewood Arsenal ATTN: SMUEA-R-PRI(?) Edgewood Arsenal, Maryland 21010	UNCLASSIFIED
	2b. GROUP NA

3. REPORT TITLE

RADIATION TRANSFER BETWEEN FLAME BURNING ZONE AND UNBURNED FUEL

4. DESCRIPTIVE NOTES *(Type of report and inclusive dates)*

This work was started in June 1970 and completed in May 1971.

5. AUTHOR(S) *(First name, middle initial, last name)*

C. Stuart Kelley, Ph.D.

6. REPORT DATE	7a. TOTAL NO. OF PAGES	7b. NO. OF REFS
October, 1971	87	35

8a. CONTRACT OR GRANT NO.	9a. ORIGINATOR'S REPORT NUMBER(S)
b. PROJECT NO.	EATR 4555
c. Task No. 1T061101R91A15	9b. OTHER REPORT NO(S) *(Any other numbers that may be assigned this report)*
d.	

10. DISTRIBUTION STATEMENT

Approved for public release; distribution unlimited.

11. SUPPLEMENTARY NOTES	12. SPONSORING MILITARY ACTIVITY
	NA

13. ABSTRACT

A fuel continues to burn by the heat returned from the flame to the unburned fuel. The heat transferred by radiation is dependent upon the intensities of the flame emission spectrum, the fuel absorption spectrum, and especially on the overlap, or product, of the two spectra. The product of the two spectra was calculated point by point through the near infrared (2μ to 6μ) and integrated over wavelength for 14 fuels, primarily hydrocarbons. In general, maximum overlap occurs in the regions of CO_2 and H_2O emission bands. Overlap values vary from 3.19×10^{-6} for methane to 0.178 for unsymmetrical dimethylhydrazine. The overlap is shown to closely approximate the total radiation intensity absorbed by the fuel and is demonstrated to be linearly related to the fuel regression rate. Assumptions of graybody absorption and emission are found to be poor approximations for those heat transfer processes. Methods are discussed for enhancing overlap and thereby the rate of energy release by the flame.

14. KEYWORDS

    Flame
    Heat transfer
    Radiation transfer
    Flame emission spectra
    Fuel absorption spectra
    Fuel burning rates

DD FORM NOV 65 1473 REPLACES DD FORM 1473, 1 JAN 64, WHICH IS OBSOLETE FOR ARMY USE.